UNIVERSIDADE FEDERAL DO PARÁ
INSTITUTO DE CIÊNCIAS DA SÁUDE
PROGRAMA DE PÓS-GRADUAÇÃO EM CIÊNCIAS FARMACÊUTICAS

ATIVIDADE ANTILEISHMANIA E TOXICIDADE DO ÓLEO E FOLHAS DE *Carapa guianenses* Aubl. E SEUS METABÓLITOS

RENILSON CASTRO DE BARROS

BELÉM - PARÁ
2025

RENILSON CASTRO DE BARROS

ATIVIDADE ANTILEISHMANIA E TOXICIDADE DO ÓLEO E FOLHAS DE *Carapa guianenses* Aubl. E SEUS METABÓLITOS

Trabalho de dissertação do mestrado apresentado ao Programa de Pós-graduação em Ciências Farmacêuticas, da Universidade Federal do Pará, como requisito para obtenção do grau de mestre.
Orientador (a): Profa. Dra. Maria Fâni Dolabella
Coorientador (a): Dra. Marliane Batista Campos

BELÉM - PARÁ

2025

Dados Internacionais de Catalogação na Publicação (CIP) de acordo com ISBD
Sistema de Bibliotecas da Universidade Federal do Pará
Gerada automaticamente pelo módulo Ficat, mediante os dados fornecidos pelo(a) autor(a)

C355a Castro de Barros, Renilson.
ATIVIDADE ANTILEISHMANIA E TOXICIDADE DO ÓLEO E FOLHAS DE Carapa guianenses Aubl. E SEUS METABÓLITOS / Renilson Castro de Barros. — 2025.
122 f. : il. color.

Orientador(a): Profª. Dra. Maria Fâni Dolabela
Coorientação: Profª. Dra. Marliane Batista Campos
Dissertação (Mestrado) - Universidade Federal do Pará, Instituto de Ciências da Saúde, Programa de Pós-Graduação em Ciências Farmacêuticas, Belém, 2025.

1. Leishmaniose. 2. cicatrização. 3. limonóides. 4. ácidos graxos. 5. aldeídos.. I. Título.

CDD 615.4

RENILSON CASTRO DE BARROS

ATIVIDADE ANTILEISHMANIA E TOXICIDADE DO ÓLEO E FOLHAS DE *Carapa guianenses* Aubl. E SEUS METABÓLITOS

Trabalho de dissertação do mestrado apresentado ao Programa de Pós-graduação em Ciências Farmacêuticas, da Universidade Federal do Pará, como requisito para obtenção do título de Mestre.
Orientador (a): Profa. Dra. Maria Fâni Dolabela
Coorientador (a): Drª Marliane Batista Campos

Aprovado em: 17/03/2025

BANCA EXAMINADORA

gov.br Documento assinado digitalmente
MARIA FANI DOLABELA
Data: 04/04/2025 21:00:00-0300
Verifique em https://validar.iti.gov.br

_____
Profª. Dra. Maria Fâni Dolabela (Orientadora)

gov.br Documento assinado digitalmente
MARLIANE BATISTA CAMPOS
Data: 14/04/2025 15:03:26-0300
Verifique em https://validar.iti.gov.br

_____
Profª. Dra. Marliane Batista Campos (Coorientadora)

gov.br Documento assinado digitalmente
MOZANIEL SANTANA DE OLIVEIRA
Data: 11/04/2025 16:43:27-0300
Verifique em https://validar.iti.gov.br

_____
Prof.Dr. Mozaniel Santana de Oliveira (Membro Interno)

gov.br Documento assinado digitalmente
ANDREZA DO SOCORRO SILVA DA VEIGA
Data: 12/04/2025 11:54:30-0300
Verifique em https://validar.iti.gov.br

_____
Profª. Dra. Andreza do Socorro Silva da Veiga (Membro Externo)

BELÉM - PARÁ

2025

AGRADECIMENTOS

Agradeço primeiramente a Deus, por tudo que vem fazendo em minha vida.

À Universidade Federal do Pará e ao Programa de Pós-Graduação em Ciências Farmacêuticas (PPGCF) pela oportunidade de realizar o mestrado.

Agradecemos à FAPESPA/CAPES pelo programa "PDPG Parcerias Estratégicas nos Estados III (PDPG-FAPIII)", que fornece apoio ao autor como "Bolsista FAPESPA/CAPES - BRASIL", necessário para a condução desta pesquisa.

À minha orientadora Dra. Maria Fâni Dolabela pela oportunidade e por todos esses anos de ensinamento, dedicação e orientação na pesquisa.

À minha coorientadora Dra. Marliane Batista Campos pelas oportunidades, apoio e orientação.

À Doutora Kelly Cristina Oliveira de Albuquerque por ser minha segunda mãe de pesquisa, desde a graduação me acompanhando, me ajudando sempre em tudo o que solicitei.

Aos professores da banca, por aceitarem o convite de avaliar este trabalho e por todas as contribuições que somam o trabalho.

A minha família por todo apoio necessário, principalmente, meus pais: Renilson Sampaio de Barros, Ana Maria Castro de Barros e meu irmão: Renan Castro de Barros.

A minha noiva Suelem Daniella Pinho Farias por todo o suporte, companheirismo, porto seguro e amor.

A todas as minhas alunas, em especial, Lais, Fernanda e Samilly.

A Juliana e Heliton por todo apoio intelectual e pessoal nesta reta final de mestrado.

A todos colegas do mestrado, meus orientandos do PET e Laboratório de Farmacologia e Doenças Negligencias e Instituto Evandro chagas pela parceria.

A todos que contribuíram de alguma forma com este trabalho, meu muito obrigado!

EPÍGRAFE

“*Não temas, porque eu sou contigo; não te assombres, porque eu sou o teu Deus; eu te fortaleço, e te ajudo, e te sustento com a destra da minha justiça.”*
Isaías 41:10

RESUMO

ATIVIDADE ANTILEISHMANIA E TOXICIDADE DO ÓLEO E FOLHAS DE *Carapa guianenses* Aubl. E SEUS METABÓLITOS

Estudos anteriores com o óleo de *Carapa guianensis* demonstraram o potencial antileishmania de seus constituintes. O presente estudo avaliou a atividade antileishmania de *C. guianensis*. Neste sentido, foram realizados, revisão bibliográfica, estudos químicos com o óleo das sementes de *C. guianensis*, óleo essencial e de seu extrato etanólico e frações, sendo caracterizados por métodos cromatográficos e RMN. Verificou-se que a constituição química das folhas é diferente do óleo, sendo o extrato e frações caracterizados pela presença, principalmente, de flavonoides e terpenos. No óleo resina, temos a presença de limonóides e ácidos graxos. O óleo essencial de *C. guianensis*, detectou-se a presença de ácidos graxos, aldeídos e ésteres, principalmente. A atividade antipromastigota foi realizada em duas cepas de *L (L) amazonensis*, sendo determinadas as IC_{50}. O óleo resina (ORCG) foi considerado mais promissor, sendo neste óleo a ação antileishmania, a presença de limonóides. Nos estudos in silico foram selecionados as moléculas mais promissoras, limonóides, ácidos graxos e aldeidos foram submetidos aos estudos *in silico*. Investigou-se que a atividade do ORCG é devido efeito sinérgico resultante da inibição de vias envolvidas na resposta inflamatória (COX-2) pelos ácidos graxos, associada anti-parasitario, promovido catepsina-D pelos aldeídos e pela inibição do HIF-1-a pelos limonóides. Logo, para sugerir a segurança do uso de óleo resina de *C. guianensis* são necessários estudos se associação da inibição destas diferentes vias pode levar ao sinergismo para os efeitos tóxicos subletais em modelo de roedores.

Palavras-chave: leishmaniose, cicatrização, limonóides, ácidos graxos, aldeídos.

ABSTRACT

ANTILEISHMANIA ACTIVITY AND TOXICITY OF OIL AND LEAVES OF Carapa guianenses Aubl. AND ITS METABOLITES

Previous studies with *Carapa guianensis* oil have demonstrated the antileishmanial potential of its constituents. The present study evaluated the antileishmanial activity of *C. guianensis*. In this context, a literature review, chemical studies with the seed oil of *C. guianensis*, essential oil, and its ethanolic extract and fractions were conducted, characterized by chromatographic and NMR methods. It was found that the chemical composition of the leaves differs from that of the oil, with the extract and fractions being characterized mainly by the presence of flavonoids and terpenes. In the resin oil, limonoids and fatty acids were present. In the essential oil of *C. guianensis*, fatty acids, aldehydes, and esters were primarily detected. Antipromastigote activity was assessed in two strains of *L (L) amazonensis*, and IC50 values were determined. The resin oil (ORCG) was considered the most promising, with the antileishmanial action attributed to the presence of limonoids. *In silico* studies selected the most promising molecules, and limonoids, fatty acids, and aldehydes were subjected to in silico analysis. It was found that the activity of ORCG is due to a synergistic effect resulting from the inhibition of pathways involved in the inflammatory response (COX-2) by fatty acids, combined with the anti-parasitic action promoted by cathepsin-D through aldehydes and the inhibition of HIF-1-a by limonoids. Therefore, to suggest the safety of using C. guianensis resin oil, further studies are needed to determine whether the association of inhibiting these different pathways could lead to synergism in sublethal toxic effects in rodent models.

Keywords: leishmaniasis, wound healing, limonoids, fatty acids, aldehydes.

LISTA DE ILUSTRAÇÃO

Capítulo 3

LISTA DE TABELAS

Capítulo 3

LISTA DE ABREVIATURAS E SIGLAS

LogP	Coeficiente de partição óleo-água
TPSA	Área de superfície polarizada topológica
MM	Massa molecular
HBA	Aceptores de ligação de hidrogênio
HBD	Número de grupos doadores de ligação hidrogênio
MDCK	Madin-Darby Canine Kidney
Caco2	Células de Adenocarcinoma de Cólon Humano
HIA	Absorção Intestinal humana
PP	Proteína plasmática
BHE	Barreira hematoencefálica
CYP	Citocromo

LISTA DE SÍMBOLOS

ΔG.....Variação na energia livre devida à ligação

SUMÁRIO

1. INTRODUÇÃO

As doenças tropicais negligenciadas são prevalecentes em condições de pobreza, contribuindo para a manutenção de um quadro de desigualdade. Estas patologias representam um grande entrave ao desenvolvimento dos países, geralmente atingem populações empobrecidas que vivem em condições não privilegiadas, com acesso precário aos cuidados de saúde, educação e necessidades básicas (Dutra e Gollob, 2011). Dentre as doenças negligenciadas, leishmaniose merece bastante atenção.

As leishmanioses são causadas por protozoários do gênero *Leishmania* e são consideradas um grave problema de saúde pública (Vasconcelos, 2015). Segundo dados da Organização Mundial de Saúde (OMS), 350 milhões de pessoas estão expostas ao risco de contrair a doença, com registro aproximado de dois milhões de novos casos das diferentes formas clínicas; esta protoose está presente em 98 países do mundo, distribuída em cinco dos seis continentes e sua notificação é compulsória em apenas 30 deles (Alvar et al., 2012).

O tratamento farmacológico da leishmaniose é limitado, sendo realizado com os antimoniais pentavalentes (antimoniato de N-metil glucamina - glucantime®) e o estibogluconato de sódio - pentostan®), que possuem alto custo e geralmente requerem um longo período de administração. Estes fármacos são extremamente tóxicos, podendo causar alterações cardíacas, renais, pancreáticas e hepáticas. As alternativas terapêuticas (Anfotericina B, Miltefosina, Pentamidina, Imidazóis, Macrolídeos e Alopurinol), todos os fármacos possuem desvantagens e limitações (OPAS/OMS, 2022).

Neste contexto, torna-se importante a busca de novas possibilidades terapêuticas, sendo as plantas medicinais uma fonte promissora de fármacos. Uma espécie bastante promissora é a *Carapa guianensis* Aubl., que é utilizada pela comunidade amazônica para a cicatrização de feridas e como antiparasitário (BRASIL, 2015). O óleo obtido das sementes de *C. guianensis* também apresenta alegação de uso para a cicatrização de feridas (BRASIL, 2015).

Em termos químicos, o óleo obtido de semente de *C. guianensis* apresenta padrão de ácidos graxos semelhantes, o ácido oléico, ácido palmítico, ácido linoléico e ácido esteárico, láurico, mirístico, palmitoleico, araquídico, beênico, heptadecanóico e ácido lignocérico (Novello et al., 2015; Dos Santos Costa et al., 2014). Além disso,

este óleo possui os seguintes limonóides: 7-desacetoxi-7-hidroxigedunina, deacetildihidrogedunina, desoxigedunina, andirobina, gedunina, 11β-hidroxigedunina, 17-glicolildesoxigedunina, 6α-acetoxigedunina e 6α, 11β-diacetoxigedunina (Ambrozin et al., 2006; Tappin et al., 2008).

O óleo de *C. guianensis* foi submetido à avaliação de atividade contra promastigota e amastigota de *Leishmania amazonensis*, porém não foi ativo. Entretanto três frações ricas em limonóides foram ativas contra promastigotas (CI_{50} = 10,53 ± 0,050, 25,3 ± 0,057 e 56,9±0,043µg/mL) e duas foram à ativas contra amastigotas (CI_{50}= 27,31 ± 0,091, 78,42 ± 0,086). A atividade antileishmania foi relacionada a presença dos limonóides 11β-hidroxigedunina e 6α,11β-diacetoxigedunina (Oliveira et al., 2018). Visando identificar os possíveis danos ocasionados pelos limonóides ao Leishmania foram realizadas análises microscópicas, sendo observadas mudanças estruturais na mitocôndria e cinetoblasto. Adicionalmente, foram observados corpos lipídicos, vacuolização e vesículas na bolsa flagelar, indicando que podem ocorrer danos estruturais no parasito (Almeida-Souza et al., 2024).

No entanto, ainda faltam estudos de avaliação da atividade antileshmania destes limonóides de forma isolada, bem como seus potenciais tóxicos, aspectos farmacocinéticos e possíveis mecanismos de ação. Diante disso, é importante a realização de estudos complementares para melhor compreensão do potencial antileishmania de *C. guianensis*, justificando a realização do presente estudo.

2. REVISÃO DA LITERATURA

2.1. Leishmania e leishmaniose

O parasita *Leishmania* possui duas formas, a amastigota e promastigota. Esse protozoário é transmitido pelo mosquito fêmea do *Lutzomia* ou do *Psychodopygus*. A forma amastigota do parasita é encontrada no trato digestivo do vetor, que é infectado após o repasto sanguíneo de hospedeiro vertebrado infectado. A forma promastigota é encontrada após o mosquito regurgitar em um hospedeiro vertebrado não infectado, na corrente sanguínea, a forma promastigota é fagocitada por células do sistema imune, no entanto, por adaptação, o parasita não sofre a morte, mas se transforma em sua forma amastigota e se multiplica por divisão binária e rompendo as células fagocitárias, após isso, o ciclo se repete (Lazar e Abass, 2020) (Figura 1).

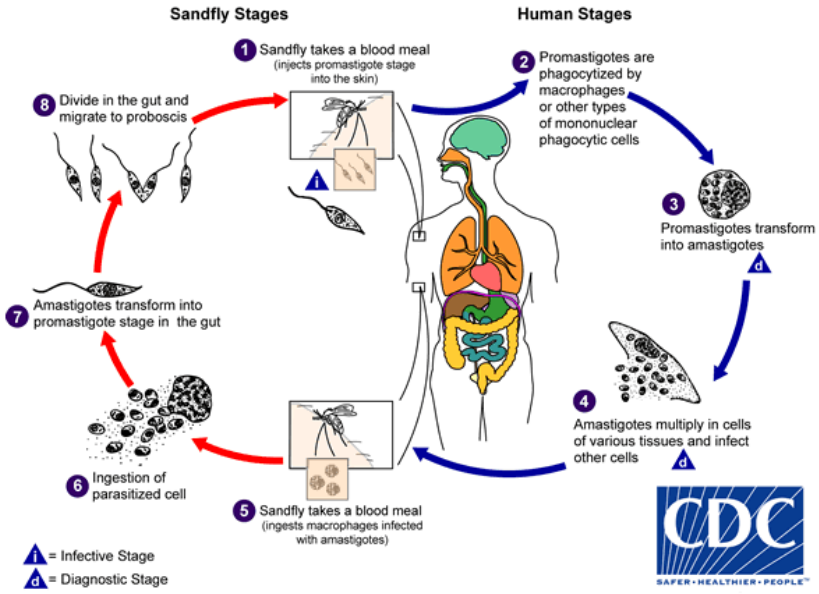

Figura 1 - Ciclo de vida Leishmania.
Fonte: Adaptado de CDC, 2017.

No Brasil são encontrados dois subgêneros (*Leishmania e Viannia*), que são classificadas de acordo com o desenvolvimento e a proliferação dos parasitos no trato digestivo do vetor, e cerca de 8 espécies, assim como as principais formas clínicas: a *L*.(L.) *infantum* (LV), *L.* (L.) *amazonensis* (LC e LCD), *L.* (V.) *braziliensis* (LC e LMC), *L.* (V.) *guyanensis* (LC e LMC), *L.* (V.) *lainsoni* (LC), *L.* (V.) *naiffi* (LC), *L.* (V.) *shawi* (LC) e a *L.* (V.) *lindenberg* (LC) (BRASIL, 2013).

O parasito da Leishmania causa uma doença denominada leishmaniose que pode cursar diferentes manifestações clínicas, classificadas em três formas: cutânea,

mucosa/mucocutânea e visceral. A leishmaniose cutânea (ou tegumentar) é a forma mais comum das leishmanioses, com tendência à cura espontânea e apresenta boa resposta ao tratamento, podendo ser única lesão ou múltiplas lesões. A leishmaniose mucocutânea caracteriza-se pelo acometimento de mucosas com lesões destrutivas, principalmente nas vias aéreas superiores, podendo levar à destruição parcial ou total das mucosas do nariz, boca e garganta (Chanda et al., 2021). A leishmaniose mucosa/mucocutânea também necessita de tratamento farmacológico, pois pode evoluir com a destruição parcial ou total das membranas mucosas do nariz e da boca, podendo causar grave incapacidade. A leishmaniose cutânea é a forma predominante (85% dos casos), caracterizada por lesões ulcerativas que deixam cicatrizes pelo resto da vida (OPAS/OMS, 2022).

A leishmaniose visceral (LV) é uma doença crônica e sistêmica que se não tratada e diagnosticada pode evoluir o paciente a óbito em 90% dos casos (BRASIL, 2017). A manifestação clínica da LV envolve o sistema endotelial e a infecção pode ser assintomática ou sintomas crônicos. Estes sintomas podem ser febre persistente, palidez na mucosa oral, perda de peso, fraqueza, falta de energia, associados a uma marcada hepatoesplenomegalia (BRASIL, 2015). A forma grave da doença é causada majoritariamente pelas espécies *Leishmania donovani* e *Leishmania chagasi*, nesta os parasitos promovem infecção em órgãos distantes como fígado, baço e medula óssea (Chanda et al., 2021). A LV tem sido reconhecida como uma infecção oportunista em indivíduos infectados pelo HIV (Pintado et al., 2001).

Ainda hoje, a leishmaniose é um importante problema de saúde em diferentes regiões do mundo: Américas, África Oriental, Norte da África e Oeste e Sudeste Asiático. Tendo uma relação direta da doença com fatores socioeconômicos, como a ocorrência de extrema pobreza, além dos ambientais e climáticos. Em nível global, a leishmaniose está entre as dez principais doenças tropicais negligenciadas, estima-se que 12 milhões de pessoas estejam infectadas (OPAS/OMS, 2022).

No Brasil, casos de leishmania é classificado como um problema de saúde pública uma vez que condições como clima tropical, presença de vetores adequados, a exemplo de flebotomíneos, bem como a vasta região amazônica colaboram para a criação de condições favoráveis para a transmissão do parasita causador da patologia. Esse cenário se associa ao crescimento das atividades antrópicas como ocupação desordenada e desmatamento colaboram para o aumento de casos de leishmaniose na região (Souza et al., 2021).

Em termos epidemiológicos, essa doença é endêmica em 99 países, sendo considerada a LC endêmica em 89 países e 9 países notificam 85%. Casos de LC são notificados desde o sul dos Estados Unidos, até o Norte de Argentina, com exceção do Caribe e Chile. A LV é endêmica em 80 países, e 68% dos casos ocorrem na Índia, Sudão, Brasil e Quênia. A associação LC+ LV é considerada endêmica em 71 países, ainda a coinfecção Leishmania- HIV já foi registrada em 42 países. Entre 2001 a 2021, 1.105.545 casos de leishmaniose cutânea (LC) e mucosa (LM) foram notificados à OPAS (Média de casos por ano= 52.645). Neste período, foram registrados 69.665 novos casos de LV (2.488 casos/ ano; taxa de letalidade= 8%), estes números notificados nas Américas são considerados elevados quando comparada a outros continentes (OPAS/OMS, 2022).

O tratamento da leishmaniose é realizado, principalmente, com os antimoniais pentavalentes (SB5+; Antimoniato de N-Metil glucamina-Glucantime® e o Estibogluconato de sódio-Pentostan®), que são quimioterápicos de alto custo. Outra questão importante é seu potencial cardiotoxico, sendo obeservadas alterações nelo eletrocardiograma e arritmias cardíacas. Ainda foram toxicidades para o pâncreas e fígado, mialgias ou artralgias e anorexia. Além disso, o tratamento é demorado contribuindo para a baixa adesão ao tratamento (Oliveira et al., 2018). Diante dos efeitos tóxicos, o paciente precisa ser supervisionado por profissionais qualificados e realizar uma série de exames, dependendo da região de moradia não é possível o acompanhamento clínico laboratorial de forma plena.

O tratamento alternativo aos antimoniais pentavalentes utiliza a Anfotericina B (Aguiar, 2017), que após a ligação ao ergosterol criam-se poros na membrana celular do protozoário, levando a liberação de íons e outras moléculas essenciais (Baginski, 2006). Infelizmente, o uso deste fármaco pode ocasionar diferentes eventos adversos como: nefrotoxicidade, calafrios, febre, náuseas e vômitos e perda da função hepática (Mcgwire, 2014; Falci, 2015). Visando reduzir a toxicidade da Anfotericina B, recomenda-se o uso da forma lipossomal que eleva ainda mais o preço do tratamento medicamentos. Devidos os problemas relacionados a administração da Anfotericina B, o paciente requer uma internação e acompanhamento de uma equipe, tornando ainda mais oneroso o tratamento da leishmaniose (Aguiar, 2017).

A miltefosina (hexadecilfosfocolina) é um análogo da fosfatidilcolina, com registro em diferentes países para o tratamento da leishmaniose e seu uso é por via oral (Berman, 2008). O estudo indiano de Fase III mostrou uma taxa de cura de 97%

em ~ 300 pacientes > 12 anos (2,5mg/kg/dia- 100mg/dia/40kg, 6 meses de acompanhamento) (Sundar et al., 2000).

O estudo de Fase IV da miltefosina de braço único, em pacientes ambulatoriais com diagnóstico de LV não grave ou grave não pré-morbido (2 a 65 anos) atendidos em 13 clínicas em Bihar, Índia. Os pacientes foram avaliados semanalmente durante o tratamento, no final do tratamento e nas consultas de acompanhamento 2 meses e 6 meses após o tratamento. Foram avaliados parâmetros laboratoriais (hemogramas, exames hepáticos enzimas, bilirrubina, nitrogênio ureico no sangue e creatinina). A cura inicial foi definida como a erradicação dos parasitas em aspirados esplênicos realizados no final do tratamento, aos 6 meses de seguimento, pela ausência de sinais e sintomas clínicos atribuíveis a leishmaniose visceral ou aspirado esplênico negativo se estavam presentes sinais e sintomas individuais que levaram a repetir a aspiração esplênica para descartar recidiva da doença. Dos 1.132 pacientes que receberam tratamento, 1.084 pacientes que completaram as 4 semanas de tratamento, 1.055 demonstraram cura inicial. No final do acompanhamento pós-tratamento de 6 meses, 717 pacientes foram determinados com cura final. Duzentos e cinquenta e quatro pacientes tiveram alguma indicação de possível leishmaniose visceral, e por isso foi submetido aspiração esplênica. Em síntese, a taxa de cura final foi de 82% e 95% pela análise por protocolo. A miltefosina foi bem tolerada em geral, sendo as principais reações adversas (RAM) a diarreia, vômito e outras queixas gastrointestinais (Bhattacharya et al., 2007).

A pentamidina é considerada tratamento de segunda linha para leishmaniose, vem sendo usada em países da América do Sul e África. A pentamidina possui RAMs menos severas que a Anfotericina B (Pimentel et al., 2011) e não necessitando de internação para sua administração. Em média, o tratamento e leva 3 semanas (Lai et al., 2002). As principais reações adversas são: dor, enduração e abscessos estéreis no local da aplicação, náuseas, vômitos, tontura, adinamia, mialgia, cefaleia, hipotensão, síncope, hipoglicemia e hiperglicemia transitórias (Neves et al., 2011).

A paromicina para o tratamento e apresenta como vantagens baixo custo, eficácia no tratamento, não sendo menos eficaz do que o tratamento com anfotericina B e compostos de antimônio e pode ser associada a outros tratamentos (Sundar et al., 2010). As principais RAM associadas a este fármaco são: náuseas, dor abdominal e hepatotoxicidade. Durante o tratamento deve-se monitorar a função hepática através da realização de exames das enzimas hepáticas (Wiwanitkit, 2012).

Um sério problema do tratamento da leishmaniose visceral é a falha dos antimoniais pentavalentes em leishmaniose, que é atribuída ao surgimento de cepas de Leishmania resistentes aos antimoniais, resultando em recaídas frequentes após o tratamento (Kafetzis, Maltezou, 2002; Murray, 2001). Na Índia, o antimônio não é mais usado, pois 65% dos casos de LV não respondem ou recaem imediatamente (Sundar et al., 2000). Tratamentos quimioterápicos alternativos com anfotericina B e sua formulação lipídica apresentam severas limitações devido ao seu efeito tóxico e ao alto custo proibitivo do tratamento (Murray, 2001). Estudo *in vitro* já mostrou que a Leishmania também desenvolveu resistência contra a miltefosina (Perez-Victoria et al., 2001). As crescentes limitações nas estratégias quimioterápicas disponíveis devido às cepas resistentes emergentes e à falta de uma estratégia de vacina eficaz contra a LV aprofundam a crise.

Na análise da resistência de Leishmania aos fármacos deve-se considerar a facilidade com que os parasitos resistentes podem ser selecionados para um determinado medicamento; e propagação da resistência numa população, sendo este o principal fator (Croft, 2002). Esta propagação pode ser mensurável pelos seguintes parâmetros: volume de medicamento utilizado; probabilidade do parasito sensível se tornar resistente; duração da infecção em indivíduos; custos de aptidão incorridos por ser resistente na ausência de medicamentos, grau em que se desenvolvem mecanismos compensatórios que compensam esses custos de aptidão (Bjorkman et al., 2000; Levin et al., 2000).

A propagação da resistência adquirida aos fármacos não é um fator a ser considerado na leishmaniose cutânea, exceto quando causada por *L. tropica*, é um fator de grande importância em *L. donovani* no estado de Bihar, Índia (Croft, 2002). Isto não exclui uma série de estudos que descrevem o desenvolvimento de resistência em parasitas associados a infecções em animais (Gramiccia et al., 1992) ou em humanos durante longos períodos de tratamento, especialmente em pacientes imunocomprometidos (Faraut-gambarelli et al., 1997).

Além da crescente resistência do parasito aos fármacos disponíveis, outro fator que interfere na resposta ao tratamento medicamentoso da leishmaniose é o estado imunológico, sendo muito importante em relação ao tratamento antimonial pentavalente e coinfecções HIV/LV (Croft, 2002). Neste caso se observa ausência da resposta imune específica mediada por células T, podendo estar relacionado a deficiências de respostas mediadas por células Th1 e de macrófagos (Murray et al.,

1989; Escobar et al., 2001). Modelos experimentais demostraram que as atividades antileishmania da anfotericina B e da miltefosina são independentes das células T, enquanto a pentamidina é dependente das células T (Murray et al., 1993; Murray e Delph-Etienne, 2000; Escobar et al., 2001).

Nesse contexto, outro problema relacionado ao tratamento das leishmanioses é a resistência parasitária à múltiplos fármacos, a principal causa dessa resistência é ocasionada devido a variabilidade genética e mutações da *Leishmania*. Já está descrito na literatura casos de falha terapêutica ou recidiva em pacientes tratados com o Estibogluconato de Sódio (Sundar et al., 2000), assim como resistência ao tratamento com Miltefosina (Srivastava et al., 2017; Carnielliet al., 2019). Devido isso, surge a necessidade de desenvolvimento de novos fármacos menos tóxicos, mais baratos e que ajam contra os parasitos resistentes. A busca por compostos naturais presentes em plantas medicinais é muito forte, tendo em vista seu uso no tratamento de diversas enfermidades por cerca de 80% da população (Oliveira et al., 2009).

Várias espécies possuem alegação de uso para o tratamento de feridas de difíceis cicatrizações ou doenças parasitárias. Uma espécie de grande impotância amazônica que se enquadra neste grupo é a *Carapa guianensis* Aubl.

2.2. Carapa guianensis Aulb

A *C. guianensis,* conhecida como andiroba, pertence à classe Equisetopsida C. Agardh, subclasse Magnoliidae Novák ex Takht., superordem Rosanae Takht., ordem Sapindales Juss. ex Bercht. & J. Presl, família Meliaceae Juss., gênero Carapa Aubl. e possui as seguintes sinonímias: Carapa latifolia Willd. ex C. DC., *Carapa macrocarpa* Ducke, *Carapa nicaraguensis* C. DC., *Carapa slateri* Standl., *Granatum guianense* (Aubl.) Kuntze, *Granatum nicaraguense* (C. DC.) Kuntze, *Guarea mucronulata* C. DC., *Persoonia guareoides* Willd. e *Xylocarpus carapa* Spreng (Pennington, 1981).

Essa espécie possui altura que pode variar entre 25-35 m, sendo monoica, com flores que duram no máximo um dia, florescem duas vezes ao ano (De Souza, 2006; Maués, 2008) (Figura 2). Além disso, possui a presença de frutos que para amadurecerem, necessitando temperaturas que variam entre 17°C a 30°C, umidade entre 70% a 90% e precipitações entre 1800 mm e 3500 mm anuais com solos argilosos e barrentos (Revilla, 2001). Espécies pertencentes a este gênero ocorrem em locais de clima tropical úmido e equatorial, presente em toda região Amazônica e em alguns estados do Nordeste como Bahia e Maranhão (Lorenzi, 2002), podendo ser cultivada em áreas de vegetação de terra firme e várzea (Lima e Azevedo, 1996).

Esta tem papel importante na economia da região, a massa que sobra da extração do óleo, serve para fazer sabão, vela e sabonete, o que viabilizou uma industrialização desse óleo no Pará, marcando *a década dos anos 70, neste período mais de 300 toneladas do óleo foi exportado para a Europa e Estados Unidos (Moraes et al., 2019).

Figura 2 - *Carapa guianensis*.
Fonte: Adaptado de David J. Stang, 2006.

O uso popular da espécie é variado, principalmente do óleo, os povos nativos da Amazônia utilizam de forma tópica para o tratamento de picada de cobras, escorpiões e abelhas (Pio Correa, 1931; Prance & Silva, 1975; Orellana, 2004), acelerar o processo de cicatrização de feridas (Pinto, 1963; Shanley, 1998). Também é utilizado como anti-helmíntico, tanto pela população indígena, como na área urbana das cidades da Região Norte (Shanley, 1998). As folhas são utilizadas popularmente em forma cataplasma como analgésico e anti-inflamatório sobre a pele, o chá também é consumido para tratar gripe (Pinto, 1963; Shanley, 1998; Ambrozin et al., 2006; Chicaro, 2009; Berg, 2010; Nayak et al., 2011; Santos et al., 2012; Da Silva, 2014).

O uso do óleo de andiroba como inseticida é verificado através da queima direta em lamparinas ou no uso de velas preparadas com o óleo isolado ou misturados com outras plantas como cacau, citronela ou eucalipto (Pinto, 1963; Shanley, 1998; Ferrari et al., 2007; Monteiro et al., 2011; Klauck et al., 2015).

O óleo de andiroba (AO) possui em sua composição química dos ácidos graxos (Moraes et al., 2012; Novello et al., 2015), já tendo sido descritos doze ésteres metílicos e cerca de 60,5% representam a composição dos ácidos graxos insaturados. Os principais ácidos encontrados foram: ácido oleico (48,67%), ácido palmítico (26,89%;), ácido linoléico (10,79%;) e ácido esteárico (8,80%;). Entretanto, alguns ácidos estão menor percentual, dentre estes: láurico (0,89%), mirístico (0,68%), palmitoleico (0,81%), araquídico (1,30%;), beênico (0,25), heptadecanóico (0,29%) e ácido lignocérico (0,20%). Esses ácidos desempenham papel importante para o

tratamento de feridas, com ação emoliente e propriedades biológicas (Novello et al., 2015; Dos santos costa et al., 2014).

O ácido linoléico integra o estrato córneo e evita a perda transepidérmica de água, garantindo sua integridade, se utilizado como curativo cutâneo pode atuar como barreira bacteriana e prevenir a desidratação da pele (Manhezi et al., 2008; Ferreira et al., 2012). Além disso, este composto favorece o desbridamento autolítico da ferida e acelera o processo de cicatrização (Silva et al., 2021).

Além disso, o ácido oleico (Ômega 9) e o ácido linoléico (Ômega 6) são ácidos graxos essenciais (AGE), que induz o processo de granulação tecidual, facilita a proliferação celular e aumenta a permeabilidade celular da membrana, protegendo a lesão (Ferreira et al., 2012). A presença de componentes não ácidos graxos (tocoferóis, caroteno e tetranortriterpenóides) também atribui outras propriedades medicinais e efeitos anti-inflamatórios ao AO (Tappin et al., 2008; Novello et al., 2015; Kiruma et al., 2016; Pardauil et al., 2017). Os principais ácidos graxos encontrados de acordo com a composição no óleo das sementes de *C. guianensis* (Figura 3) (Filho e Chaves, 2013; Salgado et al., 2015; Farias & Silva, 2018).

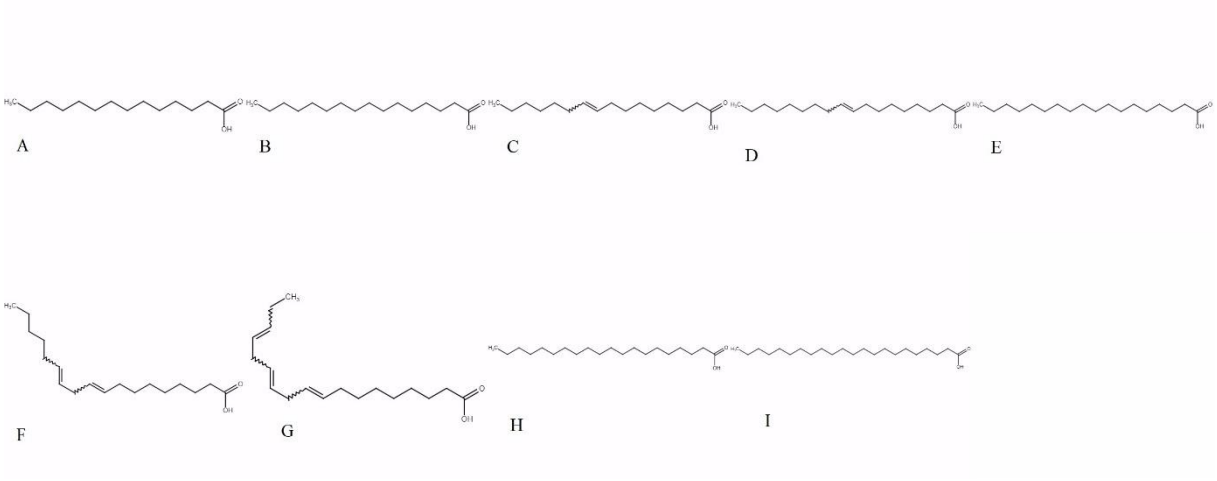

Figura 3 - Principais ácidos graxos identificados no óleo de *C. guianensis*

Legenda: A=Ácido mirístico; B= Ácido palmítico; C= Ácido palmitoleico; D= Ácido oléico; E= Ácido esteárico; F= Ácido linoléico; G= Ácido linolênico; H= Ácido Araquidico; I= Ácido beenico.
Fonte: Salgado et al., 2015; Farias; Filho e Chaves, 2013; Silva, 2018.

Os limonóides mais encontrados no óleo de *C. guianensis* são: gedunina, 6α-acetoxigedunina, angolensato de metila, 7-desacetoxi-7-oxogedunina, andirobina, 6-hidroxi-angolensato de metila, 17β-hidroxiazadiradiona, 1,2-dihidro- 3β- hidroxi-7-

desacetoxi-7-oxogedunina e xiloccensina k (Figura 4) (Ambrozin et al., 2006; Tappin et al., 2008).

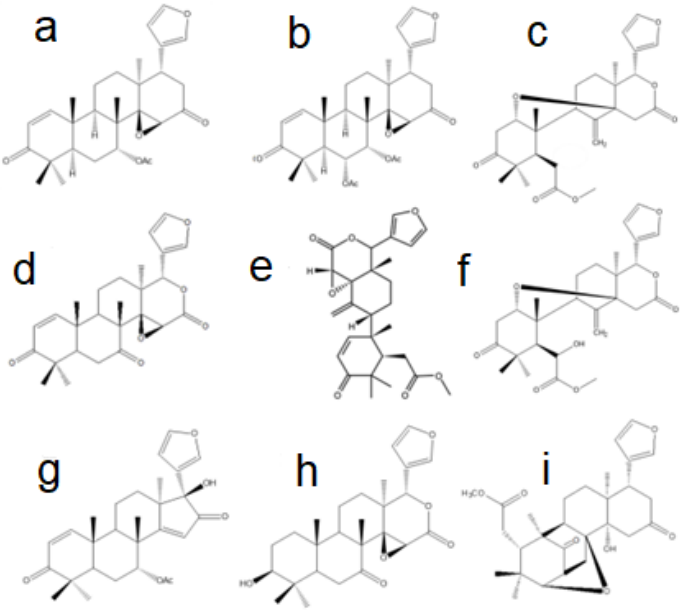

Figura 4 - Principais limonóides identificados em *C. guianensis*

Legenda: a= gedunina; b = 6α-acetoxigedunina; c= angolensato de metila; d = 7-desacetoxi-7-oxogedunina; e = andirobina; f = 6-hidroxi-angolensato de metila; g= 17β-hidroxiazadiradione; h= 1,2-dihidro- 3β-hidroxi-7-desacetoxi-7-oxogedunina; i= xiloccensina k.

Fonte: Ambrozin et al., 2006; Tappin et al., 2008.

Estudo anterior avaliou a atividade antileishmania do óleo das sementes e frações ricas em limonóides de *C. guianensis,* sendo utilizadas formas de promastigotas e amastigotas intracelulares de *Leishmania amazonensis*. Antes da avaliação da atividade antiamastigota foi realizada a avaliação da citotoxicidade em macrófagos peritoneais. O óleo não se mostrou promissor para a leishmania, porém duas frações contendo limonóides foram ativas em promastigota (CI_{50}= 10,53 ± 0,050, 25,3 ± 0,057 µg/mL) e amastigotas (CI_{50}= 27,31 ± 0,091, 78,42 ± 0,086 µg/mL). Além disso, estas frações foram seletivas para o parasito, visto que a citotoxicidade foi superior a 1000 µg/mL. A atividade antileishmania das frações ricas em limonóides pode ser atribuído aos compostos 11β-hidroxigedunina e 6α,11βdiacetoxigedunina detectados na análise química (Oliveira, 2018).

Além do efeito antiparasitário, é importante avaliar a capacidade de induzir a cicatrização da ferida. A ação cicatrizante foi testada pela aplicação tópica em ratos de emulsão à base do óleo de andiroba. As feridas tratadas apresentavam-se menores, contraíam mais cedo, tiveram aumento da angiogênese, menos macrófagos $CD68^{+}$ e M2 em 15 dias de tratamento, os miofibroblastos, em feridas não tratadas

apareceram no período de 3-7 dias, em comparação com o grupo tratado, o período foi ampliado para 7-15 dias, demonstra evidências de que a emulsão à base de andiroba é eficaz em melhorar a cicatrização de feridas cutâneas, sugestivo de ter papel anti-inflamatório e modulação associada a macrófagos, miofibroblastos e níveis de TGFβ3 (Chia, 2018).

A atividade anti-inflamatória e antialérgica de tetranortriterpenoides (TNTPs) contendo 6(alfa)- acetoxigedunina (Figura 4b), 7- deacetoxi-7-oxogedunina (Figura 4d), anglolensato de metila (Figura 4f) e gedunina (Figura 4a) têm sido descritas. A incubação de esplenócitos com o conjunto de TNTPs e TNTPS isolados foram capazes de inibir a ativação, proliferação e a produção de IL-2, CCL11/Eotaxina e CCL5/RANTES em linfócitos T após o bloqueio da translocação do fator NfkB. A incubação com eosinófilos tratos com o conjunto e isolados inibiu a adesão e quimiotaxia. A avaliação destes dados sugere que a gedunina apresenta uma importante atividade antialérgica (Ferraris, 2012).

No modelo de pleurisia alégica induzida por ovalbumina (OVA) emcamundongos, houve uma redução do processo com o pré-tratamento com gedunina, devido bloqueio do influxo de eosinófilos e de linfócitos T, diminuição dos níveis de CCL2, CCL3, CCL5, CCL11, IL-5 e LTB4. O tratamento in vitro de linfócitos T com gedunina inibiu a ativação, proliferação, produção de IL2 e translocação de NfkB e de NFAT induzido por (alfa)-CD3 mAb. Na análise do pós-tratamento com gedunina reverteu a inflamação aguda pulmonar alérgica induzida por OVA, diminuindo linfócitos T e eosinófilos e os níveis de mediadores eosinofilotáticos (Ferraris, 2011).

Estudo avaliou efeitos anti-inflamatório e -nociceptivos induzida pelo zymosan da gedunina e seu efeito biológico na expressão de ET-1. O pré e pós-tratamento diminuíram o acúmulo de neutrófilos, inchaço na articulação do joelho, expressão de RNAm para preproET-1 e produção de mediadores inflamatórios. O pré-tratamento inibiu a ativação e quimiotaxia de neutrófilos induzida por ET-1. Todos os resultados obtidos por Ferraris (2011) demonstram o potencial anti-inflamatório dos TNTPS.

A citotoxicidade do óleo de andiroba foi avaliada em linhagem celular de câncer gástrico (ACP02), através do teste de viabilidade celular (MTT) e mutagenicidade pelo teste de micronúcleo. Uma redução significativa foi detectada na viabilidade celular para culturas expostas à maior concentração (1 mg/mL) por 48 horas, com aumento significativo ($P < 0,05$) na apoptose, observado em tempos de 24 h (45.4 ± 3.93) e 48

h (78.03 ± 3.77). Também não houve diferença no índice de proliferação de bloqueio de citocinese com relação à frequência de micronúcleos, mostrando que o óleo da andiroba, é capaz de induzir a morte celular por apoptose em células de linhagem de adenocarcinoma gástrico humano (ACP02) sem exercer efeitos mutagênicos, sugerindo ser promissor para terapia contra câncer primário no estômago (Porfírio-Dias et al.,2020).

A administração via oral do óleo de andiroba em ratas Wistar, nas doses de 0,375, 0,75, 1,5 ou 3,0g/kg, nos primeiros 14 dias de gestação, não produziu nenhuma morte ou sinais clínicos de toxicidade, não observando malformações congênitas (Costa-Silva, 2008).

2.3 Estudos *in silico*

Nos últimos anos, com o avanço computacional, houve o surgimento do estudo *in silico* o qual envolve estudos simulações computacionais de compostos para predizer diversas propriedades como propriedades físico-químicas, farmacocinéticas e toxicidades. A origem da técnica de estudo teve início ainda no ano de 1989 nos Estados Unidos, desde então sua utilização vem sendo aprimorada nos últimos anos e permitiu avanços significativos nos processos de triagem molecular, com diminuição de custos e uso de animais (Sotomayor & Schulten, 2007; Brogi et al., 2020).Deve-se ressaltar que a modelagem molecular permite avaliar a afinidade e seletividade da molecula com seu alvo biológico específico e, ferramentas como docking molecular**,** ajudam a prever a interação entre moléculas e seus alvos (Barreiro et al.,1997; Santos et al, 2013). A dinâmica molecular representa a simulação do comportamento de moléculas ao longo do tempo, levando em consideração interações físicas e químicas dentro de um ambiente específico (Namba et al., 2008). Desta forma, pode-se entender a estabilidade, flexibilidade e afinidade de biomoléculas e compostos químicos com seu alvo (Pietralonga et al, 2015).

Computadores e softwares cada vez mais avançados permitem a modelagem molecular de diversas formas, como modelos de valência, representações gráficas, nuvens eletrônicas e estruturas tridimensionais. Esses softwares utilizam algoritmos para calcular descritores moleculares, que são representações matemáticas derivadas da informação estrutural da molécula, podendo variar desde propriedades físico-químicas simples, como a massa molecular, até impressões digitais moleculares complexas. Esses descritores ajudam a prever interações entre moléculas e organismos vivos, correlacionando propriedades químicas com medidas de

toxicidade, como a carcinogenicidade. Os algoritmos buscam relações entre a estrutura química de um composto e sua atividade biológica, gerando um resultado chamado de endpoint. Modelos *in silico* são amplamente utilizados para estudar fenômenos de toxicidade, como mutagenicidade, carcinogenicidade e biodegradabilidade, sendo os dois primeiros os mais investigados devido à sua complexidade (Pietralonga et al., 2015; Rocha et al., 2015).

A inclusão dos estudos *in silico* no protocolo experimental que visa identificar o possível marcador farmacológico de uma espécie vegetal utilizada com fins medicinais apresenta várias vantagens, tais como: óleos vegetais ou extratos apresentam inúmeros metabolitos secundários, o isolamento e identificação destes metabolitos demandam um tempo relativamente elevado e um custo, sendo que a triagem destes compostos por ferramenta *in silico* pode permitir identificar o(s) metabolito(s) envolvido na atividade, redução dos estudos fitoquímicos, menor numero de moleculas serão submetidas aos estudos in vitro- redução do tempo de estudo e dos custos com solventes (Cruz et al., 2019). Estudos recentes trazem reflexões críticas sobre a filosofia moral tradicional relacionada ao uso de animais em pesquisas experimentais (Sganzerla e Xavier, 2020). As abordagens *in silico* têm se mostrado uma ferramenta importante para reduzir o número de animais utilizados em experimentos in vivo. Nesse contexto, essas metodologias contribuem para os "princípios da técnica experimental humanitária", propostos por William Russel e Rex Burch em 1959, que se baseiam nos princípios dos 3R's: redução, substituição e refinamento.

3. OBJETIVOS

3.1. Objetivo Geral

Avaliar a atividade antileishmania *in vitro* e *in silico* de *Carapa guianensis e* toxicidade *in silico* das folhas e óleo.

3.2. Objetivos específicos

- Realizar estudos químicos de *C. guianensis* para verificar os metabolitos presentes*;*
- Avaliar o potêncial de atividade antileishmania das amostras de *C. guianensis*;
- Realizar estudos *in sílico* das moléculas presentes no óleo;
- Investigar o possível mecanismo de ação envolvido na atividade antileishmania para contribuir com futuros tratamentos.

4. RESULTADOS

CAPÍTULO 1

toxics

MDPI

Review

The Role of Oxidative Stress in the Pathogenesis and Treatment of Leishmaniasis: Impact on Drug Toxicity and Therapeutic Potential of Natural Products

Heliton Patrick Cordovil Brígido [1,2,*], Laís Gabrielly Abreu dos Santos [3], Renilson Castro de Barros [4], Juliana Correa-Barbosa [5], Paulo Victor Barbosa dos Santos [3], Rayana Franciele Lopes Paz [3], Amanda Ramos Pereira [2], Kelly Cristina Oliveira de Albuquerque [2], Marliane Batista Campos [6], Fernando Tobias Silveira [6], Sandro Percário [2] and Maria Fâni Dolabela [2,4,5,*]

1 National Council for Scientific and Technological Development (CNPq), Federal University of Pará (UFPA), Belém 66075-110, PA, Brazil
2 Biotechnology and Biodiversity Postgraduate Program (BIONORTE), Federal University of Pará, Belém 66075-110, PA, Brazil; ams.ramos@outlook.com (A.R.P.); kellyoalbuquerque@gmail.com (K.C.O.d.A.); percario@ufpa.br (S.P.)
3 Faculty of Pharmacy, Federal University of Pará, Belém 66075-110, PA, Brazil; laisgabriellyas@gmail.com (L.G.A.d.S.); paulo.victor@ics.ufpa.br (P.V.B.d.S.); rayanaapaz@gmail.com (R.F.L.P.)
4 Pharmaceutical Sciences Postgraduate Program, Federal University of Pará, Belém 66075-110, PA, Brazil; renilsonbarros0988@gmail.com
5 Postgraduate Pharmaceutical Innovation Program, Institute of Health Sciences, Federal University of Pará, Belém 66075-110, PA, Brazil; correabjuliana@gmail.com
6 Parasitology Department, Evandro Chagas Institute, Ananindeua 67030-000, PA, Brazil; marlianecampos@iec.gov.br (M.B.C.); fernandotobias@iec.pa.gov.br (F.T.S.)
* Correspondence: helitombrigido@gmail.com (H.P.C.B.); fani@ufpa.br (M.F.D.)

check for updates

Academic Editor: Chongshan Dai

Received: 15 February 2025
Revised: 2 March 2025
Accepted: 3 March 2025
Published: 7 March 2025

Citation: Brígido, H.P.C.; dos Santos, L.G.A.; de Barros, R.C.; Correa-Barbosa, J.; Santos, P.V.B.d.; Paz, R.F.L.; Pereira, A.R.; Albuquerque, K.C.O.d.; Campos, M.B.; Silveira, F.T.; et al. The Role of Oxidative Stress in the Pathogenesis and Treatment of Leishmaniasis: Impact on Drug Toxicity and Therapeutic Potential of Natural Products. *Toxics* **2025**, *13*, 190. https://doi.org/10.3390/toxics13030190

Abstract: The treatment of leishmaniasis has limitations due to drug toxicity and the increasing resistance of the parasite. In this study, we analyze the role of oxidative stress in the pathogenesis and treatment of leishmaniasis, as well as in new therapeutic alternatives of natural origin. The evasion mechanisms against the host immune response involve surface molecules present in the parasite, which modulate oxidative stress to ensure its survival. Drug treatment requires strict monitoring to minimize adverse reactions and ensure patient safety, as mechanisms such as lipid peroxidation, mitochondrial dysfunction, and depletion of antioxidant defenses are associated with drug toxicity. Plant-derived products with antileishmanial activity impact the parasite's redox balance, inducing apoptosis and reducing its parasitic load. Most studies are still in preliminary stages, making in vivo assays and clinical studies essential, along with the development of accessible formulations. Oxidative stress is involved in the pathogenesis of leishmaniasis, as *Leishmania* manipulates the host's redox balance to survive. It also contributes to drug toxicity, as antimonials and amphotericin B increase reactive oxygen species, causing cellular damage. Several plant-derived compounds have demonstrated antileishmanial activity by modulating oxidative stress and promoting parasite apoptosis. Examples include alkaloids from *Aspidosperma nitidum*, lignans from *Virola surinamensis*, flavonoids from *Geissospermum vellosii*, and triterpenoids such as β-sitosterol. Although these compounds show promising selectivity, most studies remain in preliminary stages, requiring in vivo assays and clinical studies to confirm efficacy and safety, as well as the development of affordable formulations.

Keywords: leishmaniasis; oxidative stress; natural products

1. Introduction

Leishmaniasis is one of the ten leading neglected tropical diseases, representing a serious global public health problem. The disease is present in various regions of the world, including the Americas, East Africa, North Africa, and West and Southeast Asia. It is estimated that over 12 million people are infected, with the disease being endemic in 99 countries. Specifically, cutaneous leishmaniasis (CL) is endemic in 89 countries, while visceral leishmaniasis (VL) occurs in 80 countries. Additionally, 71 countries have both clinical forms of the disease as endemic, highlighting its wide geographical distribution and impact on public health [1].

The etiological agent of leishmaniasis is a parasite of the genus *Leishmania*, belonging to the family *Trypanosomatidae*, which includes approximately 22 species pathogenic to humans. These species are classified into the subgenera *Leishmania* and *Viannia*. The parasite has a digenetic life cycle, alternating between two morphological forms: the promastigote form, found in the phlebotomine vector, and the amastigote form, which develops inside the cells of the vertebrate host [2].

Clinically, leishmaniasis manifests in different forms and is classified into three main categories: cutaneous, mucosal/mucocutaneous, and visceral. Visceral leishmaniasis, the most severe form of the disease, is characterized by weight loss, hepatosplenomegaly, and anemia, which can lead to death in over 90% of untreated cases. Mucosal/mucocutaneous leishmaniasis affects the mucous membranes of the nose and mouth, potentially causing severe tissue destruction and disability. Cutaneous leishmaniasis, the most common form, causes ulcerative skin lesions, leaving permanent scars and impacting patients' quality of life [3].

Given the complexity of the disease and the associated therapeutic challenges, this study analyzes the infection mechanisms of the parasite in vertebrate hosts, exploring the role of oxidative stress in the pathogenesis and treatment of leishmaniasis. Additionally, new therapeutic approaches of natural origin are discussed, with emphasis on plant-derived compounds, such as *Aspidosperma nitidum*, *Virola surinamensis*, *Geissospermum vellosii*, and *Corchorus capsularis*, which have demonstrated antileishmanial activity. These natural products modulate oxidative stress, promoting parasite apoptosis and exhibiting low cytotoxicity to host cells. The study evaluates the role of oxidative stress in both the efficacy and toxicity of these alternatives, aiming to contribute to the development of safer and more effective strategies to combat the disease.

2. Human Infection by the *Leishmania* Parasite, Immune Response, and Oxidative Stress

Parasites of the genus *Leishmania* have developed various adaptation mechanisms to ensure their survival in hostile environments throughout their life cycle [4]. In the vertebrate host, the first barrier faced by the parasite is the complement system, which plays a role in defending against foreign agents. However, *Leishmania* uses mechanisms to avoid its destruction by the complement system. Lipophosphoglycan (LPG), a glycoconjugate present on the surface of the parasite, prevents the insertion of the membrane attack complex (C5b-9), protecting the cell against lysis. In addition, the glycoprotein gp63 plays an important role in immune evasion by cleaving the C3b molecule into C3bi. This would prevent the formation of C5 convertase, activating the complement cascade and allowing the parasite to avoid elimination by the immune system [5].

Once they escape extracellular destruction, the parasites are phagocytosed by macrophages, specialized cells of the immune system. This process occurs mainly through the interaction of C3b and C3bi molecules with specific receptors, such as CR1 and CR3, present on the surface of macrophages. The internalization of the parasite via CR3 repre-

sents an efficient immune evasion strategy, as it prevents the activation of the microbicidal respiratory burst and reduces the production of IL-12, a cytokine essential for the immune response against infections [5].

In addition to interacting with complement receptors, metacyclic promastigotes can be opsonized by immunoglobulins and internalized via Fc receptors. Another phagocytosis pathway involves an interaction between LPG molecules and the mannose receptor on macrophages [4]. GPL also binds to C-reactive protein (CRP), one of the first molecules involved in the inflammatory response, promoting the parasite's entry through CRP receptors [6]. Furthermore, both gp63 and GLP can interact with fibronectin and complement receptor 4 (CR4), expanding the possibilities of Leishmania internalization [7].

Once inside macrophages, the parasite is endocytosed into a phagosome, which subsequently undergoes a series of fusions to form the phagolysosome. In this environment, the amastigote form becomes susceptible to acidic and hydrolytic degradation promoted by the phagolysosome. However, *Leishmania* can modulate this process by influencing intracellular calcium levels and inhibiting protein kinase C (PKC) activity, thereby preventing the activation of the destruction mechanism [8,9].

In addition to macrophages, other phagocytic cells in the skin can be targeted for infection, including Langerhans cells (LCs), which express receptors for the C3 component of the complement system [10]. LCs play a crucial role in American cutaneous leishmaniasis (ACL), as they are responsible for presenting parasitic antigens to T lymphocytes in regional lymph nodes [11–13]. The surface of these cells contains essential molecules for the immune response, including MHC II, Fc and C3b receptors, ICAM-1, ICAM-3, and CD1, as well as IL-2 receptors and membrane ATPase activity [12]. Thus, LCs are essential in initiating the immune response against *Leishmania*, promoting the differential activation of CD4 T cells, Th1, and Th2. The balance between these different response profiles directly influences the host's ability to eliminate or tolerate the parasite, with the Th1 response stimulating leishmanicidal mechanisms through the production of IL-2, IFN-γ, and TNF-α, while the Th2 response promotes parasite persistence by inducing immunosuppressive cytokines such as IL-4, IL-5, IL-6, IL-10, and IL-13 [14].

Leishmania infection can modulate the innate immune response, leading to a state of immunosuppression. Langerhans cells, for example, when presenting parasitic antigens via MHC II to CD4 T cells, can inhibit inflammatory events and favor parasite evasion [15]. Clinical studies have found that in patients infected with *L.* (*L.*) *amazonensis*, there is a progressive increase in the density of Langerhans cells compared to the reduction of CD4 and CD8 cells, indicating a modulation of the immune response in favor of the parasite [16].

The immune response mediated by CD4 Th1 T cells plays a crucial role in activating macrophages for parasite elimination. This process occurs through the production of nitric oxide (NO) by the enzyme nitric oxide synthase type 2 (NOS2), one of the main leishmanicidal mechanisms in murine macrophages and canine infections [17,18]. Additionally, in monocytes of infected dogs and in polymorphonuclear cells from peripheral blood, the production of the superoxide anion also significantly contributes to parasite killing [19].

Figure 1 illustrates the effects of reactive oxygen species (ROS) generated during an immune response, highlighting their impact on various cellular structures. The activation of NADPH oxidase in cell membranes leads to the production of superoxide anions (O_2^-) and hydrogen peroxide (H_2O_2), which are crucial for parasite killing. These free radicals induce significant damage, such as lipid peroxidation, protein oxidation, and DNA strand breaks, in addition to activating apoptotic pathways and the p53 protein, triggering programmed cell death.

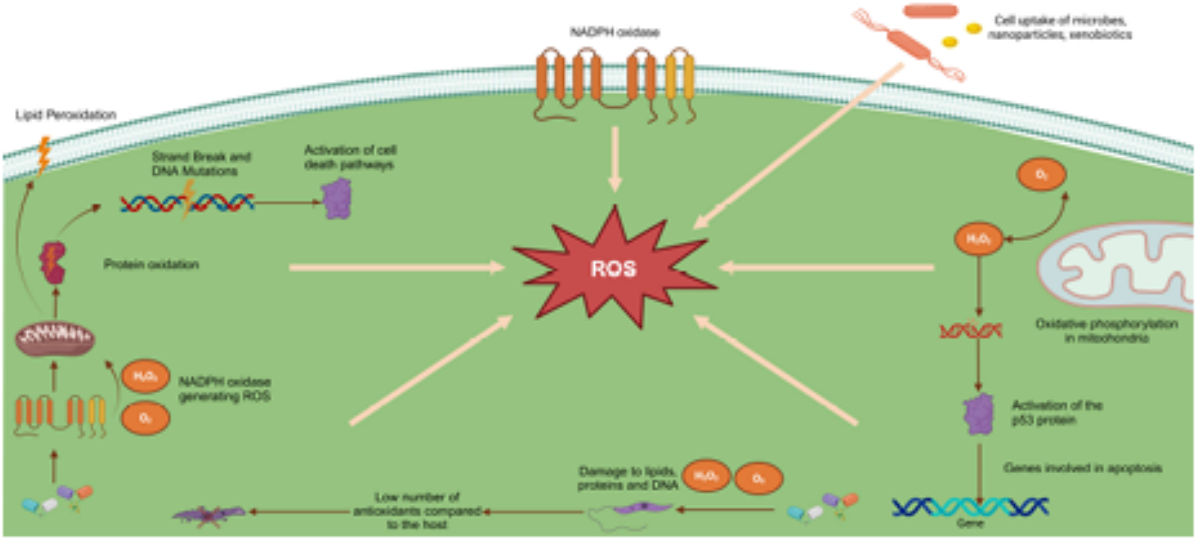

Figure 1. Representation of the impact of reactive oxygen species (ROS) on the host cell and the *Leishmania* parasite.

However, *Leishmania* has developed various strategies to resist the oxidative stress generated by macrophages. The parasite can interfere with iNOS induction and reduce the response to IFN-γ, as well as inhibit the oxidative burst by modulating PKC activity [20,21]. To protect itself from ROS and reactive nitrogen species (RNS), *Leishmania* utilizes molecules such as glutathione, trypanothione, and ovothiol A, which act as non-enzymatic scavengers of free radicals [22–24].

Tryparedoxin, for example, transfers reducing equivalents from trypanothione to tryparedoxin peroxidase (TXNPx) or to a glutathione peroxidase homolog, aiding in the neutralization of oxidative stress. Interestingly, *Leishmania* lacks catalase or a classical glutathione peroxidase, making other antioxidant mechanisms essential for its survival [25,26]. Additionally, iron superoxide dismutase (FeSOD) plays a crucial role in eliminating superoxide toxicity [27,28]. GLP also contributes to oxidative stress resistance by scavenging oxygen radicals [29], as well as by preventing the assembly of NADPH oxidase in the phagolysosome [30]. Additionally, a cellular chaperone HSP70 has been identified as a protective factor against oxidative stress [31].

In this way, *Leishmania* demonstrates a remarkable ability to adapt, escaping the immune response and modulating the intracellular environment to favor its survival. The balance between the host's immune mechanisms and the parasite's evasion strategies defines the progression of the disease and the effectiveness of potential therapeutic approaches. In this context, oxidative stress plays a crucial role, both in the elimination of the parasite by the immune system and in its resistance and persistence in the host. While macrophages trigger ROS and RNS to destroy the parasite, *Leishmania* develops efficient antioxidant mechanisms to neutralize these compounds and ensure its survival. Furthermore, the redox imbalance induced by antileishmanial drugs can be explored as a therapeutic strategy, enhancing the parasite's vulnerability and promoting its cell death. Therefore, understanding the impacts of oxidative stress on the parasite–host interaction is essential for the development of new, more effective, and selective therapies.

3. Treatment of Leishmaniasis and Possible Involvement of Oxidative Stress

The treatment of leishmaniasis is complex and depends on multiple factors, including the clinical form of the disease, the presence of comorbidities, the species of the parasite involved, and the geographical location of the patient. Although it is a treatable and curable disease, the effectiveness of therapy is directly related to the competence of the immune system, as the available drugs do not completely eradicate the parasite. Therefore, immunocompromised patients have an increased risk of relapses and complications [32].

Among the first-line therapeutic options, pentavalent antimonials stand out, represented by meglumine antimoniate (Glucantime®) and sodium stibogluconate. These compounds have similar mechanisms of action, with their efficacy and toxicity being directly influenced by the antimony content in their formulation. The most common side effects include gastrointestinal symptoms, such as anorexia, vomiting, nausea, and abdominal pain, as well as systemic manifestations like malaise, myalgia, arthralgia, headache, metallic taste, and lethargy [33].

In addition to these symptoms, antimonials can induce electrocardiographic changes, with the most common being T wave inversion, QT interval prolongation, and the occurrence of arrhythmias. Elevated levels of pancreatic and hepatic enzymes are also common, as well as blood dyscrasias such as leukopenia, anemia, and thrombocytopenia [1].

Meglumine antimoniate (MA) caused significant protein carbonylation in the heart, spleen, and brain tissue. Increased lipoperoxidation was found in the liver and brain tissue. An imbalance between the activities of superoxide dismutase and catalase can be observed in the heart, liver, spleen, and brain tissue, suggesting that MA induces oxidative stress in several vital organs. This indicates that the production of highly reactive oxygen and nitrogen species induced by MA may be involved in some of its toxic effects [34].

Given the challenges posed by the toxicity of conventional treatments, new approaches have been explored. Recent studies investigated the potential of green-synthesized zinc nanoparticles (ZnNPs) in combating *Leishmania major*, either alone or in combination with meglumine antimoniate (MA). The combination of ZnNPs + MA resulted in a significant synergistic effect, reducing the 50% inhibitory concentration (IC_{50}) to 12.6 µg/mL, compared to 43.2 µg/mL for ZnNPs alone and 26.3 µg/mL for MA [35].

Treatment with ZnNPs modulated the immune response in a favorable manner, promoting the increased expression of iNOS, TNF-α, and IFN-γ while reducing levels of IL-10, a cytokine associated with the parasite's immune evasion. Additionally, significant activation of caspase-3 was observed, indicating a potential role in inducing apoptosis in parasitized cells without causing significant toxicity to normal cells [35].

Another drug widely used in the treatment of leishmaniasis is amphotericin B, which can be administered in its conventional or liposomal form. Although effective, its administration is associated with significant adverse reactions, such as high fever, stiffness, chills, and thrombophlebitis. Moreover, more severe effects include nephrotoxicity, hypokalemia, and myocarditis [36].

The mechanism of action of amphotericin B involves binding to ergosterol present in the cell membrane of fungi and protozoa, leading to destabilization and cell lysis [37]. However, this interaction is not completely selective and can also occur with cholesterol in human cells, which contributes to its toxicity [36]. The nephrotoxicity induced by the drug has been associated with the excessive generation of reactive oxygen species (ROS), which cause mitochondrial damage and promote the activation of exaggerated inflammatory responses, intensifying tissue injury [38].

Paromomycin, another antileishmanial agent, when administered, can cause mild pain at the injection site, as well as ototoxicity, renal toxicity, and hepatotoxicity [39]. Auditory

toxicity, in particular, has been associated with the accumulation of reactive oxygen species (ROS), which promote apoptosis and irreversible damage to the cells of the inner ear [40]. Additionally, mechanisms such as lipid peroxidation, mitochondrial dysfunction, and the depletion of cellular antioxidant defenses contribute to the toxicity of this drug [41].

Another drug used, pentamidine isetionate, is related to oxidative stress, the inhibition of nucleic acid synthesis, and mitochondrial dysfunction [42]. The accumulation of ROS in parasite cells can lead to mitochondrial dysfunction, ATP depletion, and programmed cell death [43]. In the host, pentamidine can cause nephrotoxicity, and it may also potentially contribute to the development of diabetes by inducing the destruction of pancreatic beta cells [44]. Additionally, its cardiac toxicity, characterized by arrhythmias and QT interval prolongation, may be related to oxidative damage in myocardial cells [45].

Miltefosine, one of the few orally available drugs, is associated with gastrointestinal adverse events, including anorexia, nausea, vomiting (38%), and diarrhea (20%). Additionally, it has teratogenic potential, being contraindicated for pregnant women and women with reproductive potential [46,47]. Its mechanism of action appears to involve the induction of oxidative stress both in the parasite and in the host cells, which may contribute to its therapeutic effects but also to its toxicity [48].

Mitochondria are one of the main targets of miltefosine toxicity. The excessive accumulation of ROS in these organelles can lead to mitochondrial dysfunction and cell apoptosis, particularly in susceptible tissues such as the kidneys and liver. Furthermore, there is evidence that the oxidative stress induced by the drug can cause DNA damage, resulting in strand breaks, mutations, and cell death, which may be related to its teratogenic and embryotoxic effects [49].

The parenteral administration of antileishmanial drugs requires strict monitoring to minimize adverse events and ensure the safety of the treatment. However, this need significantly increases therapeutic costs and complicates patient adherence, especially for those living in remote areas. Moreover, the growing resistance of the parasite to conventional drugs highlights the urgency of finding new effective therapeutic alternatives against resistant strains [50].

Finally, it is important to highlight the dual role of oxidative stress in leishmaniasis. While it plays an essential role in the destruction of the parasite by host cells, the same phenomenon, when induced by available drugs, can be directly associated with their toxic effects. Given this scenario, a central question arises: do natural products with leishmanicidal activity act through the induction of oxidative stress, or alternatively, do they follow a distinct pathway, thereby reducing the risk of toxicity?

4. New Therapeutic Alternatives for the Treatment of Leishmaniasis and Their Toxic Potential

The search for new therapeutic approaches against leishmaniasis has led to the investigation of plant extracts, fractions, and isolated compounds with antileishmanial potential. While some studies have been limited to in vitro assays, others have progressed to in vivo models, allowing for a more comprehensive evaluation of the efficacy and safety of these substances. However, the mechanisms of action of these compounds, particularly regarding the induction of oxidative stress, are not yet fully understood, nor are the data on their toxicity.

One study evaluated the antileishmanial activity of extracts obtained from the leaves of *Virola surinamensis* against *L. chagasi* and *L. amazonensis*. The ethyl acetate, methanol extracts, and fractions C1–C6 did not show activity against promastigotes and did not have a significant effect on *L. amazonensis* amastigotes. The hexane extract (HEVS) was the only one to exhibit activity against *L. chagasi* promastigotes (IC_{50} = 86.40 µg/mL) and

L. amazonensis (IC_{50} = 79.7 ± 1.3 µg/mL), and it was considered active. However, the fraction and surinamesine did not show a significant increase in antipromastigote activity compared to the crude extract [51].

Moreover, cytotoxicity tests demonstrated that all the samples tested exhibited low cellular toxicity (CC_{50} > 500 µg/mL), resulting in selectivity indices (SI) greater than 5.8 for *L. chagasi* and 6.2 for *L. amazonensis*, indicating a favorable safety profile. However, the extracts did not show any effect on intracellular amastigote forms of *L. amazonensis*, suggesting the need for structural modifications or formulations that could improve their in vivo efficacy (Table 1) [51].

Table 1. Therapeutic and toxicological profile of alternatives in the treatment of leishmaniasis.

Samples	Antileishmania Activity		Toxicity Profile	SI	Mechanism of Action
	Promastigote	Amastigote			
Virola surinamensis (hexanic extract)	IC_{50} = 86.40 µg/mL (*L. chagasi*), 79.7 ± 1.3 µg/mL (*L. amazonensis*)	Inactive	(CC_{50} > 500 µg/mL) Low toxicity	>5.78 >6.27	Modulation of oxidative stress and apoptosis in the parasite
(-)-5-Demethoxygrandisin B	IC_{50} = 7.0 µM	IC_{50} = 26.04 µM	(CC_{50} = 26.04 µM) High selectivity, low toxicity	3.7	Mitochondrial damage, interaction with TryR
β-Sitosterol	IC_{50} = 17.7 ± 0.43 µg/mL	Induction of apoptosis	(>500 µg/mL) Low toxicity	>28.2	Increased ROS and mitochondrial depolarization
Sterculia villosa (methanolic extract)	IC_{50} = 17.5 µg/mL	DNA fragmentation	Low toxicity	ND	ROS overproduction and oxidative stress
Flavopereirine (*Geissospermum vellosii*)	IC_{50} = 0.23 µg/mL (24 h)	IC_{50} = 0.15 µg/mL (72 h)	(CC_{50} = 499.3 µg/mL) High selectivity	3328.7	Inhibition of oligopeptidase B
Aspidosperma nitidum (ethanol extract)	IC_{50} = 23.87 µg/mL	Reduction of parasite load in vivo	(CC_{50} = 500 µg/mL) in vitro No toxicity in vivo	21	Inhibition of trypanothione reductase, apoptosis
Aspidosperma nitidum (alkaloidal fraction)	IC_{50} = 18.5 µg/mL	Reduction of parasite load in vivo	(CC_{50} = 200 µg/mL) in vitro No toxicity in vivo	11	Inhibition of trypanothione reductase, apoptosis
Artemether (ART)	IC_{50} = 16.43 µg/mL	IC_{50} = 37.12 µg/mL	Reduced toxicity	ND	Interference in mitochondrial phosphorylation
Artemether (NLC-ART)	IC_{50} = 15.42 µg/mL	IC_{50} = 32.1 µg/mL	Reduced toxicity	ND	Interference in mitochondrial phosphorylation
Salidroside (*Rhodiola* spp.)	Reduction of promastigote growth	Reduction of parasite load	Low liver and kidney toxicity	ND	Modulation of the immune response, increased NO and ROS
Iridoid glycosides (*Nyctanthes arbortristis*)	Induction of apoptosis via oxidative stress	ROS-induced cell death	Low cytotoxicity in normal cells	ND	Mitochondrial oxidative damage, apoptosis
HO-3867 (Curcumin analogue)	Cell cycle arrest	Interruption of intracellular charge	Low cytotoxicity to macrophages	ND	Disruption of the STAT3 pathway and activation of apoptotic pathways

Legend: IC_{50}: 50% inhibitory concentration; CC_{50}: 50% cytotoxic concentration; ND: not determined; NO: nitric oxide; PARP1: Poly (ADP-ribose) Polymerase 1; ROS: reactive oxygen species; SI: selectivity index; STAT3: transcription factor involved in cell growth and survival regulation; TryR: trypanothione reductase.

Another investigation analyzed the action of (-)-5-desmethoxygrandisine B, a compound isolated from *V. surinamensis*, against promastigotes and intracellular amastigotes of *L. amazonensis*. Treatment with this lignan induced ultrastructural alterations in promastigotes, such as mitochondrial swelling, kDNA disorganization, vacuole formation, vesicular

structures, and an increase in flagellar pockets. Additionally, it reduced mitochondrial membrane potential and interacted with critical residues of the trypanothione reductase enzyme (TryR), suggesting that its leishmanicidal action may be related to the induction of oxidative stress (Table 1) [52].

The antiparasitic activity of β-sitosterol, a compound isolated from the chloroform extract of *Corchorus capsularis* L. and present in various plant species, showed efficacy against *L. donovani* promastigotes (IC_{50} = 17.7 ± 0.43 µg/mL) and induced oxidative stress in the parasite, leading to intracellular ROS production. As a consequence, cell apoptosis was observed, characterized by mitochondrial membrane depolarization, phosphatidylserine externalization, and DNA fragmentation. Molecular docking studies indicated that β-sitosterol inhibited trypanothione reductase (LdTryR), an essential enzyme for the parasite's redox balance (Table 1) [53].

Similarly, the methanolic extract obtained from the bark of *Sterculia villosa* Roxb. (SVE) exhibited concentration-dependent antipromastigote activity against *L. donovani* (IC_{50} = 17.5 µg/mL). Treatment resulted in increased levels of ROS, superoxide, and lipid peroxidation, as well as DNA fragmentation, suggesting a mechanism of action based on oxidative stress induction. It is important to note that the extract did not show significant cytotoxicity, indicating a favorable safety profile (Table 1) [54].

Another study investigated the effect of flavopeirerine, an alkaloid isolated from *Geissospermum vellosii*, against *L. amazonensis*. Fractionation of the extract contributed to increased antipromastigote activity, with flavopeirerine showing high leishmanicidal potency, with IC_{50} values of 0.23 µg/mL (24 h) and 0.15 µg/mL (72 h). Selectivity was also specific, presenting a selectivity index (SI) of 976.2 (24 h) and 4993.2 (72 h), demonstrating greater safety compared to amphotericin B, the therapeutic reference for leishmaniasis (Table 1) [55].

Molecular dynamics studies revealed beneficial and selective interactions with the parasite's oligopeptidase B (OpB), an enzyme associated with *Leishmania* virulence and adaptation to oxidative stress. Flavopeirerine interacted with the Tyr-499 residue of OpB, indicating an inhibitory effect on this enzyme. Since OpB is involved in regulating proteins essential for the parasite's antioxidant defense, its inhibition may impair *Leishmania*'s ability to neutralize ROS generated by the host immune system. This mechanism may enhance the leishmanicidal effect of flavopeirerine, making the parasite more susceptible to oxidative stress and reducing its ability to replicate and survive (Table 1) [55].

Among the investigated species, *Aspidosperma nitidum* has emerged as a promising candidate for leishmaniasis treatment. Four recent studies have evaluated its efficacy and toxicity in vitro and in vivo [56–59]. The first study evaluated the in vitro leishmanicidal activity of extracts and fractions of *A. nitidum* against *L. amazonensis*. The results showed that the ethanolic extract (EE) exhibited significant activity against intracellular amastigotes with an IC_{50} of 23.87 µg/mL, while the alkaloid fraction (AF) displayed a lower IC_{50} of 18.5 µg/mL, indicating greater antileishmanial potency. The dichloromethane fraction (FrDCL) demonstrated moderate activity against promastigotes (IC_{50} = 105.7 µg/mL), revealing higher selectivity for the intracellular form of the parasite. The relationship between leishmanicidal activity and cytotoxicity showed that EE had a SI of 21, while AF had an SI of 11, reinforcing the therapeutic potential of this species (Table 1) [57].

The difference in selectivity indices (SIs) between extracts may be related to the chemical composition of each fraction [56]. While the ethanolic extract (EE) presents a greater diversity of bioactive compounds, the alkaloid fraction (AF) may contain substances with more potent action but with greater cytotoxicity. This variation reinforces the importance of specific chemical characterization for the selection of compounds with a better therapeutic profile.

The second study identified that alkaloids isolated from this plant induced morphological alterations in *L. amazonensis*, including flagellum shortening, cell rounding, and the formation of cytoplasmic vacuoles, suggesting a mechanism of action related to mitochondrial dysfunction and oxidative stress (Table 1) [58].

Another study evaluated the acute and subacute toxicity of *A. nitidum* extracts in BALB/c mice. No clinical, metabolic, or histopathological alterations were observed after the administration of 2000 mg/kg in the acute phase and 1000 mg/kg over 28 days in the subacute phase, indicating a favorable safety profile compared to conventional drugs that often induce oxidative stress and hepatorenal toxicity (Table 1) [56].

The in vivo efficacy of *A. nitidum* extracts was also evaluated in mice infected with *L. amazonensis*. The treatment significantly reduced the splenic parasite load and modulated the immune response by promoting an increase in IFN-γ production and a decrease in IL-10 levels, a cytokine associated with immunosuppression. Additionally, histopathological analysis revealed an accelerated healing process, with reduced parasitic infiltration and increased collagen fiber deposition, indicating a regenerative effect associated with the treatment (Table 1) [59].

The investigation of the mechanism of action of *A. nitidum* alkaloids indicated that corynantheol, yohimbine, and dihydrocorynantheol act as potential inhibitors of trypanothione reductase (TR), a critical enzyme for *Leishmania*'s antioxidant defense. Molecular docking experiments demonstrated favorable interactions, and molecular dynamics simulations confirmed the stability of these interactions, suggesting strong enzymatic inhibition. Since *Leishmania* lacks glutathione reductase, TR inhibition compromises ROS neutralization, leading to cellular dysfunction and parasite death. This mechanism represents a significant advantage over conventional drugs, such as antimonials and amphotericin B, which induce oxidative stress nonspecifically and may cause systemic toxicity (Table 1) [59].

Studies indicate that anthracene endoperoxides (AcEPs) AcEP1117, AcEP1118, AcEP1129, and AcEP1130, derived from *Artemisia annua*, exhibit significant activity against *Leishmania*, with IC_{50} values in the low micromolar range. AcEP1118 and AcEP1129 were the most potent compounds, showing IC_{50} values of 1.00 ± 0.73 µM and 0.61 ± 0.21 µM against *L. tarentolae* promastigotes, respectively. For *L. donovani* promastigotes, AcEP1117 exhibited an IC_{50} of 2.65 ± 0.34 µM, while AcEP1129 and AcEP1130 showed IC_{50} values of 4.21 ± 0.36 µM and 39.48 ± 3.48 µM, respectively [60].

The investigation of the interaction kinetics between these compounds and iron revealed the formation of oxygen- and carbon-centered radicals, which trigger the secondary production of superoxide radicals, compromising the parasite's mitochondrial functions and leading to its cell death. Since iron is essential for *Leishmania* replication, participating in metabolic processes and DNA biosynthesis, the parasite's dependence on this metal becomes a strategic target for new therapies. However, it was observed that AcEPs also exhibit toxicity toward J774 macrophages, with IC_{50} values ranging from 0.90 ± 0.28 µM (AcEP1129) to 43.80 ± 36.12 µM (AcEP1117), which may limit their therapeutic use without structural modifications to enhance selectivity [60].

Aiming to optimize efficacy and reduce toxicity, one of the artemisinin analogs, artemether (ART), was incorporated into a lipid-based nanostructure (NLC-ART) and tested against *Leishmania infantum*. Both ART and NLC-ART were active against promastigote forms (IC_{50} ART = 37.12 µg/mL; NLC-ART = 32.1 µg/mL) and amastigote forms (IC_{50} ART = 16.43 µg/mL; NLC-ART = 15.42 µg/mL), with a slight reduction in IC_{50} values for the nanostructured formulation. This strategy may represent a significant advancement in drug targeting to the parasite, reducing systemic toxicity and increasing efficacy (Table 1) [61].

In addition to endoperoxides, phenylpropanoid glycosides, such as salidroside (SAL), have been studied for their immunomodulatory and antileishmanial properties. Isolated from species of the *Rhodiola* genus, SAL is known for its protective activity in various physiological systems, including the liver [62], heart [63], and nervous system [64]. In addition, it has shown therapeutic potential for inflammatory skin diseases [65].

The leishmanicidal activity of SAL was evidenced by its ability to interrupt the cell cycle of *L. donovani*, halting the promastigotes at the sub-G0/G1 stage [66]. In a murine model of visceral leishmaniasis, treatment with SAL significantly reduced the parasitic load. In addition to modulating the immune response and promoting a greater polarization toward the Th1 profile, the compound stimulated the production of CD4+ and CD8+ T cells, favoring a more effective response against the parasite. Molecular analysis showed increased expression of genes related to oxidative stress, such as NF-κB, iNOS, NO, and ROS. It is important to note that SAL showed minimal toxicity to human THP-1 cells and did not reveal toxic effects on the liver and kidneys (Table 1) [66].

Another group of promising compounds are the iridoid glycosides isolated from *Nyctanthes arbortristis*, which have the ability to induce oxidative stress in the parasite. Among the compounds evaluated, arbortristoside A, arbortristoside B, and arbortristoside C showed significant leishmanicidal activity against *L. donovani*, promoting an increase in ROS production and an imbalance in the parasite's redox homeostasis. These compounds act by inhibiting TR, an enzyme crucial for the antioxidant defense of *Leishmania*. The reduction in reduced thiol levels limits the parasite's ability to neutralize oxidative stress, causing progressive cellular damage and apoptosis. In vitro tests showed that the iridoid glycosides demonstrated high potency against intracellular amastigotes, even at low concentrations. Furthermore, toxicity evaluation in human embryonic kidney cells (HEK 293) and mouse macrophages (J774A.1) indicated that these compounds have low cytotoxicity, revealing a favorable safety profile (Table 1) [67].

HO-3867, a curcumin analog belonging to the class of diarylidenylpiperidones (DAPs), is a promising inhibitor of *Leishmania* metabolism. This compound is a potent inhibitor of the STAT3 signaling pathway, acting in the modulation of inflammation and cellular apoptosis. Furthermore, it has the ability to induce ROS production, activate caspase-3, and promote PARP1-mediated apoptosis, a mechanism previously observed in cancer cells (Table 1) [68–72].

Despite their therapeutic potential, curcuminoids face challenges related to their low bioavailability, which limits their clinical efficacy [73,74]. To overcome this limitation, a liposomal formulation of HO-3867 (PC-SA/HO-3867) was developed, which was shown to increase the stability and absorption of the drug [75].

In vitro assays revealed that PC-SA/HO-3867 induced apoptosis in *L. donovani*, evidenced by changes in cell morphology, the externalization of phosphatidylserine, mitochondrial depolarization, and the accumulation of intracellular lipids. Additionally, the compound caused cell cycle arrest in promastigotes and significantly reduced the load of intracellular amastigotes. Regarding safety, it exhibited low cytotoxicity to murine macrophages [75].

Additionally, treatment with PC-SA/HO-3867 induced the activation of metacaspase and PARP1 in *L. donovani*, as well as negatively regulating the expression of the Sir2 gene, involved in the parasite's longevity. This formulation also reduced the intracellular load of *L. donovani* amastigotes in in vitro assays. The results suggest that this compound exerts its action through the induction of oxidative stress and increased NO production, enhancing the parasite's susceptibility to immune-mediated destruction (Table 1) [75]. Among the

compounds developed, flavopeirine, β-sitosterol, and alkaloids from *A. nitidum* stood out due to their high selectivity index. These compounds represent promising candidates for the development of new antileishmanial therapies, as they showed significant leishmanicidal activity with low toxicity to host cells.

Thus, different natural and synthetic compounds have shown therapeutic potential against leishmaniasis in various studies, many of them exploring the selective induction of oxidative stress as a mechanism of action. However, the transition of these candidates to clinical use requires additional studies on pharmacokinetics, chronic toxicity, and clinical trials to confirm their safety and efficacy in humans.

5. Conclusions

Oxidative stress plays a crucial role in the immune response and *Leishmania* infection. During immune activation, macrophages present various ROS and NO to eliminate the parasite. However, *Leishmania* has developed mechanisms to neutralize this oxidative stress, ensuring its intracellular survival. The imbalance between ROS production and neutralization can influence the progression of the infection and the effectiveness of the host's immune response.

Furthermore, oxidative stress is strongly associated with the toxicity of drugs used in the treatment of leishmaniasis. Drugs such as antimonials, amphotericin B, and miltefosine induce excessive ROS generation, resulting in mitochondrial damage, cellular apoptosis, and tissue inflammation. These adverse effects compromise the safety of the treatment and limit its applicability, requiring rigorous monitoring to minimize systemic toxicity.

This research highlights that most studies on new therapeutic alternatives for leishmaniasis are still in the preliminary stage and are predominantly conducted in vitro. Although these studies provide important insights into the mechanisms of action and toxicity of the compounds investigated, there is still a significant gap in understanding the benefits and risks of oxidative stress induced by plant-derived substances and their derivatives. Additionally, the development of specific formulations, while promising, presents challenges related to high costs, which may limit patient access to these treatments.

In light of these findings, it is essential to establish strict guidelines for the research and development of new leishmanicidal drugs. In oral toxicity studies, it is necessary to evaluate whether the substances under testing induce oxidative changes and possess immunomodulatory properties in healthy animals. Then, in experimental models of *Leishmania* infection, it is important to investigate whether oxidative modifications occur and how these interactions influence the immune response, comparing these effects with positive and healthy control groups.

In addition to antiparasitic efficacy, the development of accessible formulations should be prioritized. Strategies to enable low-cost oral formulations are crucial to expanding the availability of these treatments, especially in endemic regions where leishmaniasis represents a serious public health problem.

Finally, the continuation of studies should encompass an integrated approach, considering not only the leishmanicidal activity of the compounds but also their safety, economic forecast, and potential for clinical use. Only through this multidimensional approach will it be possible to develop innovative therapies that are effective, safe, and accessible, contributing to the control and treatment of leishmaniasis in a sustainable and equitable manner.

Author Contributions: Conceptualization, H.P.C.B. and M.F.D.; methodology, H.P.C.B. and R.C.d.B.; software, R.C.d.B.; validation, H.P.C.B., S.P. and M.F.D.; formal analysis, H.P.C.B., S.P. and J.C.-B.; investigation, H.P.C.B., L.G.A.d.S., R.C.d.B., P.V.B.d.S., R.F.L.P., A.R.P., K.C.O.d.A., M.B.C. and F.T.S.; resources, M.F.D. and S.P.; data curation, H.P.C.B. and J.C.-B.; writing—original draft preparation, H.P.C.B.; writing—review and editing, S.P. and M.F.D.; visualization, H.P.C.B.; supervision, M.F.D.;

project administration, M.F.D.; funding acquisition, M.F.D. All authors have read and agreed to the published version of the manuscript.

Funding: This research was funded by the National Council for Scientific and Technological Development (CNPq), Brazil, through the Senior Postdoctoral Fellowship (Process No. 172225/2023-0), and by the Qualified Publication Support Program (PAPQ) of the Federal University of Pará (UFPA).

Institutional Review Board Statement: Not applicable.

Informed Consent Statement: Not applicable.

Data Availability Statement: This review article did not use new data. The data related to this study are not available due to privacy restrictions or ethical considerations.

Acknowledgments: FAPESPA/CAPES provided support through the program "PDPG Strategic Partnerships in the States III (PDPG-FAPIII)", which supports one of the authors as a FAPESPA/CAPES-BRASIL Fellow.

Conflicts of Interest: The authors declare no conflicts of interest.

Abbreviations

LC	Cutaneous leishmaniasis
LV	Visceral leishmaniasis
GLP	Glycosylphosphatidylinositol
CRP	C-reactive protein
CR4	Complement receptor 4
PKC	Protein kinase C
CL	Langerhans cells
LTA	American tegumentary leishmaniasis
NO	Nitric oxide
NOS2	Nitric oxide synthase type 2
ROS	Reactive oxygen species
O_2^-	Superoxide anions
H_2O_2	Hydrogen peroxide
NADPH oxidase	Nicotinamide Adenine Dinucleotide Phosphate Oxidase
O_2	Molecular oxygen
RNS	Reactive nitrogen species
TXNPx	Thioredoxin peroxidase
FeSOD	Iron superoxide dismutase
MA	Meglumine antimoniate
ZnNPs	Zinc nanoparticles synthesized by green synthesis
CC_{50}	50% cytotoxic concentration
HEVS	Hexane extract
SI	Selectivity index
IC_{50}	50% inhibitory concentration

References

1. WHO World Health Organization. Leishmaniasis. 2023. Available online: https://www.who.int/news-room/fact-sheets/detail/leishmaniasis (accessed on 2 February 2025).
2. Gontijo, C.M.F.; Melo, M.N. Leishmaniose Visceral No Brasil: Quadro Atual, Desafios e Perspectivas. *Rev. Bras. Epidemiol.* **2004**, *7*, 338–349. [CrossRef]
3. Ornellas-Garcia, U.; Cuervo, P.; Ribeiro-Gomes, F.L. Malaria and Leishmaniasis: Updates on Co-Infection. *Front. Immunol.* **2023**, *14*, 1122411. [CrossRef] [PubMed]
4. Cunningham, A.C. Parasitic Adaptive Mechanisms in Infection by Leishmania. *Exp. Mol. Pathol.* **2002**, *72*, 132–141. [CrossRef] [PubMed]

5. Dos-Santos, A.L.A.; Carvalho-Kelly, L.F.; Dick, C.F.; Meyer-Fernandes, J.R. Innate Immunomodulation to Trypanosomatid Parasite Infections. *Exp. Parasitol.* **2016**, *167*, 67–75. [CrossRef]
6. Culley, F.J.; Harris, R.A.; Kaye, P.M.; McAdam, K.P.; Raynes, J.G. C-Reactive Protein Binds to a Novel Ligand on *Leishmania donovani* and Increases Uptake into Human Macrophages. *J. Immunol.* **1996**, *156*, 4691–4696. [CrossRef]
7. Brittingham, A.; Chen, G.; Mcgwire, B.S.; Chang, K.-P.; Mosser, D.M. Interaction of Leishmania Gp63 with Cellular Receptors for Fibronectin. *Infect. Immun.* **1999**, *67*, 4477–4484. [CrossRef]
8. Tejle, K.; Magnusson, K.-E.; Rasmusson, B. Phagocytosis and Phagosome Maturation Are Regulated by Calcium in J774 Macrophages Interacting with Unopsonized Prey. *Biosci. Rep.* **2002**, *22*, 529–540. [CrossRef]
9. Holm, Å.; Tejle, K.; Gunnarsson, T.; Magnusson, K.-E.; Descoteaux, A.; Rasmusson, B. Role of Protein Kinase C α for Uptake of Unopsonized Prey and Phagosomal Maturation in Macrophages. *Biochem. Biophys. Res. Commun.* **2003**, *302*, 653–658. [CrossRef]
10. Blank, C.; Fuchs, H.; Rappersberger, K.; Rollinghoff, M.; Moll, H. Parasitism of Epidermal Langerhans Cells in Experimental Cutaneous Leishmaniasis with Leishmania Major. *J. Infect. Dis.* **1993**, *167*, 418–425. [CrossRef]
11. Moll, H. Epidermal Langerhans Cells Are Critical for Immunoregulation of Cutaneous Leishmaniasis. *Immunol. Today* **1993**, *14*, 383–387. [CrossRef]
12. Axelrod, O.; Klaus, S.; Frankenburg, S. Antigen Presentation by Epidermal Langerhans Cells in Experimental Cutaneous Leishmaniasis. *Parasite Immunol.* **1994**, *16*, 593–598. [CrossRef]
13. Moll, H.; Flohé, S.; Röllinghoff, M. Dendritic Cells in Leishmania Major-Immune Mice Harbor Persistent Parasites and Mediate an Antigen-Specific T Cell Immune Response. *Eur. J. Immunol.* **1995**, *25*, 693–699. [CrossRef]
14. Silveira, F.T.; Müller, S.R.; de Souza, A.A.A.; Lainson, R.; Gomes, C.; Laurenti, M.D.; Corbett, C.E.P. Revisão Sobre a Patogenia Da Leishmaniose Tegumentar Americana Na Amazônia, Com Ênfase à Doença Causada Por *Leishmania* (V.) *Braziliensis* e *Leishmania* (L.) *amazonensis*. *Rev. Para. Med.* **2008**, *22*, 9–20.
15. Machado, P.R.L.; Araújo, M.I.A.S.; Carvalho, L.; Carvalho, E.M. Mecanismos de Resposta Imune Às Infecções. *An. Bras. Dermatol.* **2004**, *79*, 647–662. [CrossRef]
16. Silveira, F.T. What Makes Mucosal and Anergic Diffuse Cutaneous Leishmaniases So Clinically and Immunopathogically Different? A Review in Brazil. *Trans. R. Soc. Trop. Med. Hyg.* **2019**, *113*, 505–516. [CrossRef]
17. Bogdan, C.; Röllinghoff, M.; Diefenbach, A. The Role of Nitric Oxide in Innate Immunity. *Immunol. Rev.* **2000**, *173*, 17–26. [CrossRef] [PubMed]
18. Vouldoukis, I.; Drapier, J.C.; Nüssler, A.K.; Tselentis, Y.; Da Silva, O.A.; Gentilini, M.; Mossalayi, D.M.; Monjour, L.; Dugas, B. Canine Visceral Leishmaniasis: Successful Chemotherapy Induces Macrophage Antileishmanial Activity via the L-Arginine Nitric Oxide Pathway. *Antimicrob. Agents Chemother.* **1996**, *40*, 253–256. [CrossRef] [PubMed]
19. Panaro, M.A.; Lisi, S.; Mitolo, V.; Acquafredda, A.; Fasanella, A.; Carelli, M.G.; Brandonisio, O. Evaluation of Killing, Superoxide Anion and Nitric Oxide Production by Leishmania Infantum-Infected Dog Monocytes. *Cytobios* **1998**, *95*, 151–160.
20. Olivier, M.; Gregory, D.J.; Forget, G. Subversion Mechanisms by Which Leishmania Parasites Can Escape the Host Immune Response: A Signaling Point of View. *Clin. Microbiol. Rev.* **2005**, *18*, 293–305. [CrossRef]
21. Olivier, M.; Brownsey, R.W.; Reiner, N.E. Defective Stimulus-Response Coupling in Human Monocytes Infected with *Leishmania donovani* Is Associated with Altered Activation and Translocation of Protein Kinase C. *Proc. Natl. Acad. Sci. USA* **1992**, *89*, 7481–7485. [CrossRef]
22. Fairlamb, A.H.; Blackburn, P.; Ulrich, P.; Chait, B.T.; Cerami, A. Trypanothione: A Novel Bis (Glutathionyl) Spermidine Cofactor for Glutathione Reductase in Trypanosomatids. *Science (1979)* **1985**, *227*, 1485–1487. [CrossRef] [PubMed]
23. Spies, H.S.C.; Steenkamp, D.J. Thiols of Intracellular Pathogens: Identification of Ovothiol A in *Leishmania donovani* and Structural Analysis of a Novel Thiol from Mycobacterium Bovis. *Eur. J. Biochem.* **1994**, *224*, 203–213. [CrossRef] [PubMed]
24. Ariyanayagam, M.R.; Fairlamb, A.H. Ovothiol and Trypanothione as Antioxidants in Trypanosomatids. *Mol. Biochem. Parasitol.* **2001**, *115*, 189–198. [CrossRef] [PubMed]
25. Krauth-Siegel, L.R.; Comini, M.A.; Schlecker, T. The Trypanothione System. In *Peroxiredoxin Systems*; Structures and Functions; Springer: Dordrecht, The Netherlands, 2007; pp. 231–251.
26. Irigoín, F.; Cibils, L.; Comini, M.A.; Wilkinson, S.R.; Flohé, L.; Radi, R. Insights into the Redox Biology of Trypanosoma Cruzi: Trypanothione Metabolism and Oxidant Detoxification. *Free Radic. Biol. Med.* **2008**, *45*, 733–742. [CrossRef]
27. Plewes, K.A.; Barr, S.D.; Gedamu, L. Iron Superoxide Dismutases Targeted to the Glycosomes of Leishmania Chagasi Are Important for Survival. *Infect. Immun.* **2003**, *71*, 5910–5920. [CrossRef]
28. Wilkinson, S.R.; Prathalingam, S.R.; Taylor, M.C.; Ahmed, A.; Horn, D.; Kelly, J.M. Functional Characterisation of the Iron Superoxide Dismutase Gene Repertoire in Trypanosoma Brucei. *Free Radic. Biol. Med.* **2006**, *40*, 198–209. [CrossRef]
29. Chan, J.; Fujiwara, T.; Brennan, P.; McNeil, M.; Turco, S.J.; Sibille, J.-C.; Snapper, M.; Aisen, P.; Bloom, B.R. Microbial Glycolipids: Possible Virulence Factors That Scavenge Oxygen Radicals. *Proc. Natl. Acad. Sci. USA* **1989**, *86*, 2453–2457. [CrossRef]

30. Lodge, R.; Diallo, T.O.; Descoteaux, A. *Leishmania donovani* Lipophosphoglycan Blocks NADPH Oxidase Assembly at the Phagosome Membrane. *Cell. Microbiol.* **2006**, *8*, 1922–1931. [CrossRef]
31. Miller, M.A.; McGowan, S.E.; Gantt, K.R.; Champion, M.; Novick, S.L.; Andersen, K.A.; Bacchi, C.J.; Yarlett, N.; Britigan, B.E.; Wilson, M.E. Inducible Resistance to Oxidant Stress in the Protozoan Leishmania Chagasi. *J. Biol. Chem.* **2000**, *275*, 33883–33889. [CrossRef]
32. Madusanka, R.K.; Silva, H.; Karunaweera, N.D. Treatment of Cutaneous Leishmaniasis and Insights into Species-Specific Responses: A Narrative Review. *Infect. Dis. Ther.* **2022**, *11*, 695–711. [CrossRef]
33. Solomon, M.; Ollech, A.; Pavlotsky, F.; Barzilai, A.; Schwartz, E.; Sharon, B.; Astman, N. Comparison of Intralesional Sodium Stibogluconate versus Intralesional Meglumine Antimoniate for the Treatment of Leishmania Major Cutaneous Leishmaniasis. *Acta Derm. Venereol.* **2024**, *104*, adv35089. [CrossRef] [PubMed]
34. Bento, D.B.; De Souza, B.; Steckert, A.V.; Dias, R.O.; Leffa, D.D.; Moreno, S.E.; Petronilho, F.; de Andrade, V.M.; Dal-Pizzol, F.; Romão, P.R. Oxidative Stress in Mice Treated with Antileishmanial Meglumine Antimoniate. *Res. Vet. Sci.* **2013**, *95*, 1134–1141. [CrossRef] [PubMed]
35. Yadegari, J.G.; Khalaf, A.K.; Ezzatkhah, F.; Shakibaie, M.; Mohammadi, H.R.; Mahmoudvand, H. Antileishmanial, Cellular Mechanisms, and Cytotoxic Effects of Green Synthesized Zinc Nanoparticles Alone and in Combined with Glucantime against Leishmania Major Infection. *Biomed. Pharmacother.* **2023**, *164*, 114984.
36. Laniado-Laborín, R.; Cabrales-Vargas, M.N. Amphotericin B: Side Effects and Toxicity. *Rev. Iberoam. Micol.* **2009**, *26*, 223–227. [CrossRef] [PubMed]
37. Baginski, M.; Czub, J.; Sternal, K. Interaction of Amphotericin B and Its Selected Derivatives with Membranes: Molecular Modeling Studies. *Chem. Rec.* **2006**, *6*, 320–332. [CrossRef]
38. Rahal, A.; Kumar, A.; Singh, V.; Yadav, B.; Tiwari, R.; Chakraborty, S.; Dhama, K. Oxidative Stress, Prooxidants, and Antioxidants: The Interplay. *Biomed. Res. Int.* **2014**, *2014*, 761264. [CrossRef]
39. Pokharel, P.; Ghimire, R.; Lamichhane, P. Efficacy and Safety of Paromomycin for Visceral Leishmaniasis: A Systematic Review. *J. Trop. Med.* **2021**, *2021*, 8629039. [CrossRef]
40. Henderson, D.; Salvi, R.J.; Quaranta, A.; McFadden, S.L.; Burkard, R.F. *Ototoxicity: Basic Science and Clinical Applications*; New York Academy of Sciences: New York, NY, USA, 1999.
41. Armstrong, D.; Stratton, R.D. (Eds.) *Oxidative Stress and Antioxidant Protection: The Science of Free Radical Biology and Disease*; John Wiley & Sons: Hoboken, NJ, USA, 2016.
42. Berra, C.M. Estudos de Reparo de DNA Por Excisão de Nucleotídeos Em Lesões Oxidativas Em Células de Mamíferos. Ph.D. Thesis, Universidade de São Paulo, São Paulo, Brazil, 2008.
43. Grivicich, I.; Regner, A.; Brondani Da Rocha, A. Morte Celular Por Apoptose. *Rev. Bras. Cancerol.* **2007**, *53*, 335–343. [CrossRef]
44. Kajimoto, Y.; Kaneto, H. Role of Oxidative Stress in Pancreatic β-Cell Dysfunction. *Mitochondrial Pathog. Genes. Apoptosis Aging Dis.* **2004**, *1011*, 168–176.
45. Kalil Filho, R.; Hajjar, L.A.; Bacal, F.; Hoff, P.M.; Diz, M.d.P.; Galas, F. I Diretriz Brasileira de Cardio-Oncologia Da Sociedade Brasileira de Cardiologia. *Arq. Bras. Cardiol.* **2011**, *96*, 1–52. [CrossRef]
46. Teixeira, V.C.; Amorim, A.C.O.; Rodrigues, C.R.; Sampaio Filho, H.C.; Cambuy, M.R.T.; Machado, R.D.; De Cayres, T.B.; Dos Santos, Y.R.A. Miltefosina No Tratamento Da Leishmaniose Tegumentar: Eficácia e Limitações Da Primeira Terapia Oral Autorizada No Brasil. *Braz. J. Health Rev.* **2023**, *6*, 17261–17272. [CrossRef]
47. Pinheiro, B.M.K.; Granzoto, A.C.G. Uma Visão Biomédica Sobre a Leishmaniose Tegumentar Americana:: Revisão de Literatura. *Rev. Mato-Grossense Saúde* **2023**, *1*, 143–157.
48. Silva, L.R.S.d.; Silva, L.R.S.d.; Silva, F.P.B.d.; Rocha, F.H.B.P.d.; Costa, Y.K.d.S.; Bezerra, D.C.B.; Lima, L.d.L.S.; Chiacchio, A.D. Análise Dos Benefícios Do Desenvolvimento de Vacinas Contra Leishmaniose Em Relação Ao Tratamento Clássico. *Contrib. A Las Cienc. Soc.* **2024**, *17*, e7407. [CrossRef]
49. Pinto-Martinez, A.K.; Rodriguez-Durán, J.; Serrano-Martin, X.; Hernandez-Rodriguez, V.; Benaim, G. Mechanism of Action of Miltefosine on *Leishmania donovani* Involves the Impairment of Acidocalcisome Function and the Activation of the Sphingosine-Dependent Plasma Membrane Ca^{2+} Channel. *Antimicrob. Agents Chemother.* **2018**, *62*, 10–1128. [CrossRef] [PubMed]
50. Sundar, S.; Chakravarty, J. An Update on Pharmacotherapy for Leishmaniasis. *Expert. Opin. Pharmacother.* **2015**, *16*, 237–252. [CrossRef]
51. Veiga, A.; Albuquerque, K.; Corrêa, M.E.; Brigido, H.; Silva e Silva, J.; Campos, M.; Silveira, F.; Santos, L.; Dolabela, M. *Leishmania amazonensis* and *Leishmania chagasi*: In Vitro Leishmanicide Activity of *Virola surinamensis* (Rol.) Warb. *Exp. Parasitol.* **2017**, *175*, 68–73. [CrossRef]
52. Paes, S.S.; Silva-Silva, J.V.; Portal Gomes, P.W.; Silva, L.O.d.; Costa, A.P.L.d.; Lopes Júnior, M.L.; Hardoim, D.d.J.; Moragas-Tellis, C.J.; Taniwaki, N.N.; Bertho, A.L. (-)-5-Demethoxygrandisin B a New Lignan from *Virola surinamensis* (Rol.) Warb. Leaves: Evaluation of the Leishmanicidal Activity by In Vitro and In Silico Approaches. *Pharmaceutics* **2023**, *15*, 2292. [CrossRef]

53. Pramanik, P.K.; Chakraborti, S.; Bagchi, A.; Chakraborti, T. Bioassay-Based Corchorus Capsularis L. Leaf-Derived β-Sitosterol Exerts Antileishmanial Effects against *Leishmania donovani* by Targeting Trypanothione Reductase. *Sci. Rep.* **2020**, *10*, 20440. [CrossRef]
54. Das, A.; Das, M.C.; Das, N.; Bhattacharjee, S. Evaluation of the Antileishmanial Potency, Toxicity and Phytochemical Constituents of Methanol Bark Extract of Sterculia Villosa. *Pharm. Biol.* **2017**, *55*, 998–1009. [CrossRef]
55. da Silva e Silva, J.V.; Cordovil Brigido, H.P.; Oliveira de Albuquerque, K.C.; Miranda Carvalho, J.; Ferreira Reis, J.; Vinhal Faria, L.; Coelho-Ferreira, M.R.; Silveira, F.T.; da Silva Carneiro, A.; Percário, S. Flavopereirine—An Alkaloid Derived from *Geissospermum vellosii*—Presents Leishmanicidal Activity In Vitro. *Molecules* **2019**, *24*, 785. [CrossRef]
56. Brígido, H.P.C.; Varela, E.L.P.; Gomes, A.R.Q.; Bastos, M.L.C.; de Oliveira Feitosa, A.; do Rosário Marinho, A.M.; Carneiro, L.A.; Coelho-Ferreira, M.R.; Dolabela, M.F.; Percário, S. Evaluation of Acute and Subacute Toxicity of Ethanolic Extract and Fraction of Alkaloids from Bark of *Aspidosperma nitidum* in Mice. *Sci. Rep.* **2021**, *11*, 18283. [CrossRef] [PubMed]
57. da Veiga, A.d.S.S.; Silveira, F.T.; do Rosario Marinho, A.M.; da Trindade, R.C.d.S.; Campos, M.B.; Dolabela, M.F. Atividade *Leishmanicida de Aspidosperma nitidum* Benth. Ex Müll. Arg. *Res. Soc. Dev.* **2021**, *10*, e50210212646. [CrossRef]
58. do Socorro Silva da Veiga, A.; Silveira, F.T.; da Silva, E.O.; Júnior, J.A.P.D.; Araújo, S.C.; Campos, M.B.; do Rosário Marinho, A.M.; Brandão, G.C.; Vale, V.V.; Percário, S. Activity of Alkaloids from *Aspidosperma nitidum* against *Leishmania* (*Leishmania*) *amazonensis*. *Sci. Rep.* **2022**, *12*, 8662. [CrossRef] [PubMed]
59. Brígido, H.P.C.; Varela, E.L.P.; Quadros Gomes, A.R.; Neves Cruz, J.; Correa-Barbosa, J.; Siqueira, J.E.d.S.; Chagas, C.K.S.; Marinho, A.M.d.R.; Almeida Carneiro, L.; Coelho-Ferreira, M.R. *Aspidosperma nitidum* Reduces Parasite Load and Modulates Cytokines in BALB/c Mice Infected with *Leishmania (Leishmania) amazonensis*. *Front. Chem.* **2024**, *12*, 1492770. [CrossRef]
60. Geroldinger, G.; Tonner, M.; Fudickar, W.; De Sarkar, S.; Dighal, A.; Monzote, L.; Staniek, K.; Linker, T.; Chatterjee, M.; Gille, L. Activation of Anthracene Endoperoxides in Leishmania and Impairment of Mitochondrial Functions. *Molecules* **2018**, *23*, 1680. [CrossRef]
61. Khazaei, M.; Rahnama, V.; Motazedian, M.H.; Samani, S.M.; Hatam, G. In Vitro Effect of Artemether-Loaded Nanostructured Lipid Carrier (NLC) on Leishmania Infantum. *J. Parasit. Dis.* **2021**, *45*, 964–971. [CrossRef]
62. Wu, Y.-L.; Feng, X.-C.; Lian, L.-H.; Jiang, Y.-Z.; Nan, J.-X. The Protective Effects of Total Saponins from Ornithogalum Saundersiae (Liliaceae) on Acute Hepatic Failure Induced by Lipopolysaccharide and D-Galactosamine in Mice. *J. Ethnopharmacol.* **2010**, *132*, 450–455.
63. Wang, Y.; Xu, P.; Wang, Y.; Liu, H.; Zhou, Y.; Cao, X. The Protection of Salidroside of the Heart against Acute Exhaustive Injury and Molecular Mechanism in Rat. *Oxid. Med. Cell Longev.* **2013**, *2013*, 507832. [CrossRef]
64. Xie, H.; Zhu, D.H. Advance in Studies on Pharmacological Effect of Salidroside on Nervous System Diseases. *Zhongguo Zhong Yao Za Zhi* **2012**, *37*, 2505–2509.
65. Wu, D.; Yuan, P.; Ke, C.; Xiong, H.; Chen, J.; Guo, J.; Lu, M.; Ding, Y.; Fan, X.; Duan, Q. Salidroside Suppresses Solar Ultraviolet-Induced Skin Inflammation by Targeting Cyclooxygenase-2. *Oncotarget* **2016**, *7*, 25971. [CrossRef]
66. Chauhan, K.; Kaur, G.; Kaur, S. Evaluation of Antileishmanial Efficacy of Salidroside against the SSG-Sensitive and Resistant Strain of *Leishmania donovani*. *Parasitol. Int.* **2019**, *72*, 101928. [CrossRef] [PubMed]
67. Shukla, A.K.; Patra, S.; Dubey, V.K. Iridoid Glucosides from Nyctanthes Arbortristis Result in Increased Reactive Oxygen Species and Cellular Redox Homeostasis Imbalance in Leishmania Parasite. *Eur. J. Med. Chem.* **2012**, *54*, 49–58. [CrossRef]
68. Selvendiran, K.; Tong, L.; Bratasz, A.; Kuppusamy, M.L.; Ahmed, S.; Ravi, Y.; Trigg, N.J.; Rivera, B.K.; Kálai, T.; Hideg, K. Anticancer Efficacy of a Difluorodiarylidenyl Piperidone (HO-3867) in Human Ovarian Cancer Cells and Tumor Xenografts. *Mol. Cancer Ther.* **2010**, *9*, 1169–1179. [CrossRef] [PubMed]
69. Tierney, B.J.; McCann, G.A.; Cohn, D.E.; Eisenhauer, E.; Sudhakar, M.; Kuppusamy, P.; Hideg, K.; Selvendiran, K. HO-3867, a STAT3 Inhibitor Induces Apoptosis by Inactivation of STAT3 Activity in BRCA1-Mutated Ovarian Cancer Cells. *Cancer Biol. Ther.* **2012**, *13*, 766–775. [CrossRef] [PubMed]
70. Rath, K.S.; Naidu, S.K.; Lata, P.; Bid, H.K.; Rivera, B.K.; McCann, G.A.; Tierney, B.J.; ElNaggar, A.C.; Bravo, V.; Leone, G. HO-3867, a Safe STAT3 Inhibitor, Is Selectively Cytotoxic to Ovarian Cancer. *Cancer Res.* **2014**, *74*, 2316–2327. [CrossRef]
71. Madan, E.; Parker, T.M.; Bauer, M.R.; Dhiman, A.; Pelham, C.J.; Nagane, M.; Kuppusamy, M.L.; Holmes, M.; Holmes, T.R.; Shaik, K. The Curcumin Analog HO-3867 Selectively Kills Cancer Cells by Converting Mutant P53 Protein to Transcriptionally Active Wildtype P53. *J. Biol. Chem.* **2018**, *293*, 4262–4276. [CrossRef]
72. Mast, J.M.; Tse, D.; Shee, K.; Lakshmi Kuppusamy, M.; Kmiec, M.M.; Kálai, T.; Kuppusamy, P. Diarylidenylpiperidones, H-4073 and HO-3867, Induce G2/M Cell-Cycle Arrest, Apoptosis and Inhibit STAT3 Phosphorylation in Human Pancreatic Cancer Cells. *Cell Biochem. Biophys.* **2019**, *77*, 109–119. [CrossRef]
73. Anand, P.; Kunnumakkara, A.B.; Newman, R.A.; Aggarwal, B.B. Bioavailability of Curcumin: Problems and Promises. *Mol. Pharm.* **2007**, *4*, 807–818. [CrossRef]

74. Sinjari, B.; Pizzicannella, J.; D'Aurora, M.; Zappacosta, R.; Gatta, V.; Fontana, A.; Trubiani, O.; Diomede, F. Curcumin/Liposome Nanotechnology as Delivery Platform for Anti-Inflammatory Activities via NFkB/ERK/PERK Pathway in Human Dental Pulp Treated with 2-Hydroxyethyl Methacrylate (HEMA). *Front. Physiol.* **2019**, *10*, 633. [CrossRef]
75. Das, A.; Kamran, M.; Ali, N. HO-3867 Induces ROS-Dependent Stress Response and Apoptotic Cell Death in *Leishmania donovani*. *Front. Cell. Infect. Microbiol.* **2021**, *11*, 774899. [CrossRef]

CAPÍTULO 2

frontiers | Frontiers in Chemistry

TYPE Original Research
PUBLISHED 30 July 2024
DOI 10.3389/fchem.2024.1394126

OPEN ACCESS

EDITED BY
Anakuthil Anoop,
Indian Institute of Technology Kharagpur, India

REVIEWED BY
Rosa E. Del Rio,
Michoacana University of San Nicolás de Hidalgo, Mexico
Marcus Scotti,
Federal University of Paraíba, Brazil

*CORRESPONDENCE
Maria Fani Dolabela,
faridolabela03@gmail.com

RECEIVED 01 March 2024
ACCEPTED 01 July 2024
PUBLISHED 30 July 2024

CITATION
de Barros RC, Araujo da Costa R, Farias SDP, de Albuquerque KCO, Marinho AMR, Campos MB, Marinho PSB and Dolabela MF (2024), *In silico* studies on leishmanicide activity of limonoids and fatty acids from *Carapa guianensis* Aubl. *Front. Chem.* 12:1394126. doi: 10.3389/fchem.2024.1394126

In silico studies on leishmanicide activity of limonoids and fatty acids from *Carapa guianensis* Aubl

Renilson Castro de Barros[1], Renato Araujo da Costa[2], Suelem Daniella Pinho Farias[3], Kelly Cristina Oliveira de Albuquerque[4], Andrey Moacir R. Marinho[5], Marliane Batista Campos[6], Patricia Santana Barbosa Marinho[5] and Maria Fani Dolabela[1,3,4]*

[1]Pharmaceutical Sciences Postgraduate Program, Federal University of Pará, Belém, PA, Brazil, [2]Federal Institute of Education Sciences of the State of Pará, Abaetetuba, PA, Brazil, [3]Faculty of Pharmacy, Federal University of Pará, Belém, PA, Brazil, [4]Biotechnology and Biodiversity Postgraduate Program (BIONORTE), Federal University of Pará, Belém, PA, Brazil, [5]Post-Graduation in Chemistry, Federal University of Pará, Belém, PA, Brazil, [6]Leishmaniasis Laboratory, Evandro Chagas Institute, Ananindeua, PA, Brazil

The oil of *Carapa guianensis* showed leishmanicidal activity, with its activity being related to limonoids, but fatty acids are the major constituents of this oil. The present study evaluated the physicochemical, pharmacokinetic, and toxicity profiles of limonoids and fatty acids already identified in the species. Based on these results, 2 limonoids (methyl angosinlate, 6-OH-methyl angosinlate) and 2 fatty acids (arachidic acid; myristic acid) were selected for the prediction of possible targets and molecular docking. Included in this study were: Gedunin, 6α-acetoxygedunin, Methyl angosenlato, 7-deacetoxy-7-oxogedunin, Andirobin, 6-hydroxy-angolensate methyl, 17β-hydroxyazadiradione, 1,2-dihydro-3β-hydroxy-7-deacetoxy-7-oxogedunin, xyllocensin k, 11beta-Hydroxygedunin, 6α,11-11β-diacetoxygedunin, Oleic Acid, Palmitic Acid, Stearic Acid, Arachidic Acid, Myristic Acid, Palmitoleic Acid, Linoleic Acid, Linolenic Acid, and Beenic Acid. Regarding physicochemical aspects, fatty acids violated LogP, and only limonoid 11 violated Lipinski's rule. A common pharmacokinetic aspect was that all molecules were well absorbed in the intestine and inhibited CYP. All compounds showed toxicity in some model, with fatty acids being mutagenic and carcinogenic, and limonoids not being mutagenic and carcinogenic at least for rats. In in vivo models, fatty acids were less toxic. Molecular dockings were performed on COX-2 steroids (15 and 16) and hypoxia-inducible factor 1 alpha for limonoids (3,6), with this target being essential for the intracellular development of leishmania. Limonoids 3 and 6 appear to be promising as leishmanicidal agents, and fatty acids are promising as wound healers.

KEYWORDS

methyl angolensate, 6-hydroxy-methyl angolensate, arachidic acid, myristic acid, COX-2, hypoxia-inducible factor 1 alpha

1 Introduction

The treatment of leishmaniasis is carried out using pentavalent antimonials, which are chemotherapeutic agents of high cost, requiring long-term treatment and capable of causing strong adverse reactions that negatively interfere with treatment adherence (Mann et al., 2021). Another drug is Amphotericin B (Aguiar and Rodrigues, 2017), which also presents

10.3389/fchem.2024.1394126

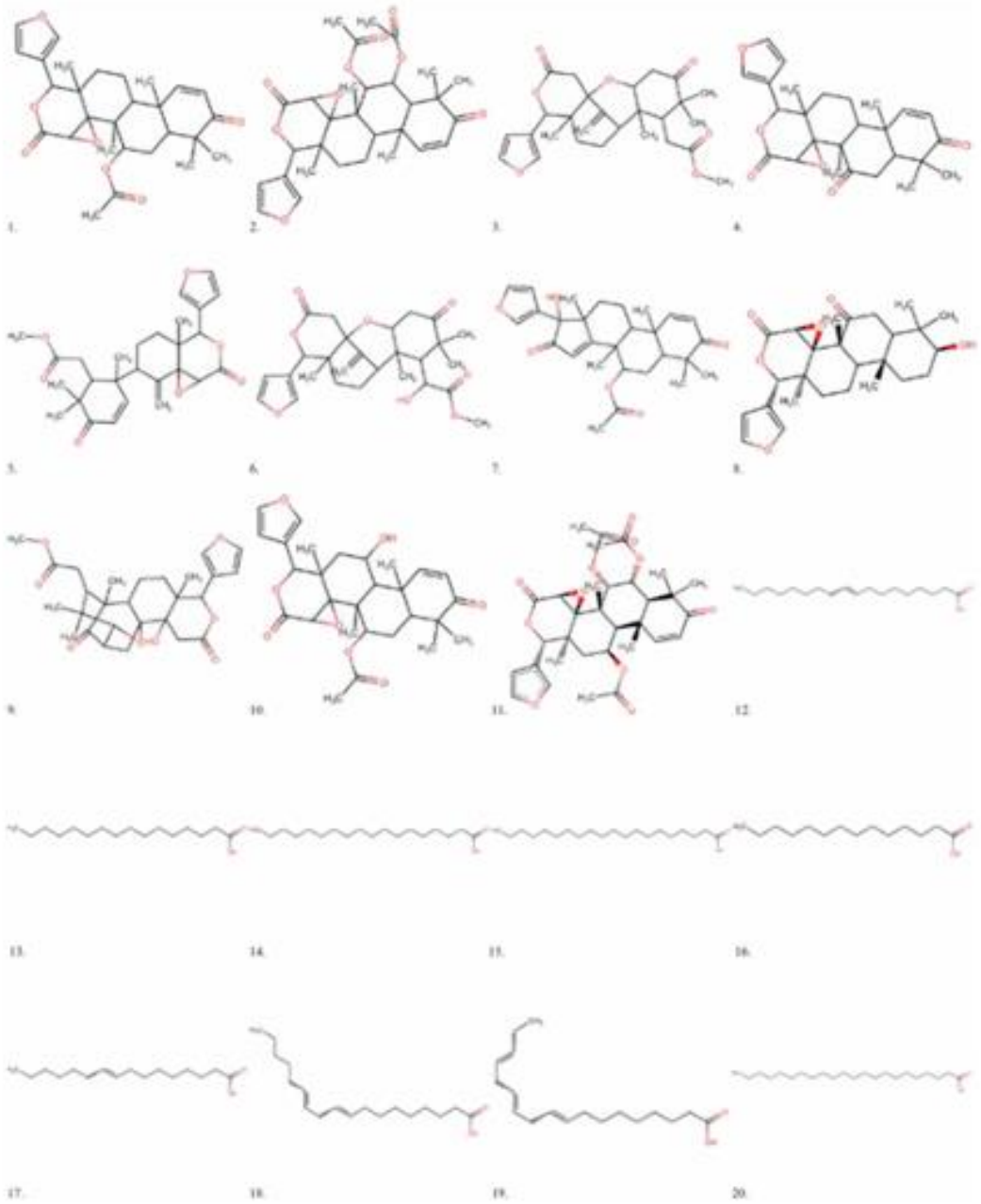

FIGURE 1
Main Limonoids and fatty acids isolated from *Carapa guianensis* oil. 1 - Gedunin; 2 - 6α-acetoxygedunin; 3 - Methyl angolensate; 4 - 7-deacetoxy-7-oxogedunin; 5 - Andirobin; 6 - 6-hydroxy-methyl angolensate; 7 - 17β-hydroxyazadiradione; 8 - 1,2-dihydro-3β-hydroxy-7-deacetoxy-7-oxogedunin; 9 - Xylocensin K; 10 - 12beta-Hydroxygedunin; 6 α, 11 - 11β-diacetoxygedunin; 12 - Oleic acid; 13 - Palmitic acid; 14 - Stearic acid; 15 - Arachidic acid; 16 - Myristic acid; 17 - Palmitoleic acid; 18 - Linoleic acid; 19 - Linolenic acid; 20 - Behenic acid.

10.3389/fchem.2024.1394126

TABLE 1 Prediction of physicochemical properties.

Molecules	MM	LogP	TPSA	nHBA	nHBD
1	482.57	4.56	95.34	7	0
2	540.00	4.10	121.64	9	0
3	470.56	4.56	92.04	7	0
4	438.52	4.19	86.11	6	0
5	468.54	4.33	95.34	7	0
6	486.56	3.35	112.27	8	1
7	466.57	4.52	93.81	6	1
8	442.55	4.21	89.27	6	1
9	486.56	3.36	112.27	8	1
10	498.52	3.53	115.57	8	1
11	598.64	3.64	147.94	11	0
12	282.46	6.10	37.30	1	1
13	256.43	5.55	37.30	1	1
14	284.48	6.33	37.30	1	1
15	312.53	7.11	37.30	1	1
16	228.37	4.77	37.30	1	1
17	254.41	5.32	37.30	1	1
18	280.45	5.88	37.30	1	1
19	278.43	5.66	37.30	1	1
20	340.59	7.89	37.30	1	1

Lipinski's rule: LogP - oil-water partition coefficient ≤5; TPSA: topological polar surface area ≤140 Å; nHBA: number of hydrogen bond acceptors ≤10; nHBD: number of hydrogen bond donor groups ≤5; MM, molecular mass ≤500D (Lipinski, 2004). 1 - Gedunin, 2 - 6α-acetoxygedunin, 3 - Methyl angolensate, 4 - 7-deacetoxy-7-oxogedunin, 5 - Andirobin, 6 - 6-hydroxy-methyl angolensate, 7–17β-hydroxyazadiradione, 8–1,2-dihydro-3β-hydroxy-7-deacetoxy-7-oxogedunin, 9 - Xylocensin K, 10–11beta-Hydroxygedunin, 6α, 11–11β-diacetoxygedunin, 12 - Oleic acid, 13 - Palmitic acid, 14 - Stearic acid, 15 - Arachidic acid, 16 - Myristic acid, 17 - Palmitoleic acid, 18 - Linoleic acid, 19 - Linolenic acid, 20 - Behenic acid.

similar problems to antimonials, being a high-cost and highly toxic treatment (Mcgwire and Satoskar, 2014; Falci and Pasqualotto, 2015).

Another issue related to leishmanicidal drugs is the increasing parasite resistance, which makes it necessary to search for pharmacological alternatives (Rodrigues et al., 2006). Andiroba oil (*C. guianensis*) is used by traditional communities for the treatment of wounds (Pinto, 1963). From *Carapa guianensis* oil, limonoids have been identified, with the main ones highlighted as: gedunin, 6α-acetoxygedunin, methyl angolensate, 7-deacetoxy-7-oxogedunin, andirobin, 6-hydroxymethyl angolensate, 17β-hydroxyazadiradione, 1,2-dihydro-3β-hydroxy-7-deacetoxy-7-oxogedunin, and xylolcensin K (Ambrozin et al., 2006; Tappin et al., 2008; Silva et al., 2009). The metabolites in higher concentration are fatty acids (palmitic and oleic acid), followed by stearic, linoleic, linolenic, myristic, palmitoleic, and behenic acids (Salgado et al., 2015).

The seed oil of *C. guianensis* showed no antileishmanial activity, and the cytotoxicity was higher than 1,000 μg/mL against peritoneal macrophages. The limonoid-rich oil fraction demonstrated activity against promastigotes *Leishmania amazonensis* (IC_{50} = 10.53 μg/mL), amastigotes (IC_{50} = 27.31 μg/mL), and exhibited cytotoxicity (IC_{50} = 78.55 μg/mL) (Oliveira et al., 2018). In summary, the leishmanicidal activity may be related to the limonoids; however, there is a lack of data on the physicochemical, pharmacokinetic aspects, and possible mechanism of action. On the other hand, the major compounds of *C. guianensis* are fatty acids, and studies on these compounds are limited.

Using predicton methods, this work reports on the physicochemical properties, pharmacokinetics, toxicological aspects, potential activities, and targets involved of limonoids and fatty acids identified in *C. guianensis* oil, as well as their potential mechanisms of action involved in leishmanicidal activity.

2 Materials and methods

2.1 Criteria for the selection of molecules

The following limonoids were selected: gedunin, 6α-acetoxygedunin, methyl angolensate, 7-deacetoxy-7-oxogedunin, andirobin, 6-hydroxymethyl angolensate, 17β-hydroxyazadiradione, 1,2-dihydro-3β-hydroxy-7-deacetoxy-7-oxogedunin, xylolcensin K (Ambrozin et al., 2006; Tappin et al., 2008; Silva et al., 2009), 11beta-Hydroxygedunin, and 6α,11β-diacetoxygedunin (Oliveira et al., 2018).

TABLE 2 Prediction of pharmacokinetic properties.

		Absorption		Distribution		Metabolism	
Molecules	MDCK	Caco 2	HIA	PP	BBB	CYP Inibition	CYP phase 1
1	L	M	H	S	M	2C9,3A4	3A4
2	L	M	H	F	M	2C9,3A4	3A4
3	L	M	H	S	M	2C9,3A4	3A4
4	M	M	H	S	M	2C9,3A4	3A4
5	L	M	H	F	M	2C9,3A4	3A4
6	L	M	H	F	L	2C9,3A4	3A4
7	L	M	H	S	L	2C9,3A4	CYP3A4
8	M	M	H	S	L	2C9,3A4	CYP3A4
9	L	M	H	F	M	2C9,3A4	CYP3A4
10	L	M	H	F	M	2C9,3A4	CYP3A4
11	M	M	M	F	M	2C9,3A4	CYP3A4
12	H	M	H	S	H	2C19,2C9,3A4	-
13	H	M	H	S	H	2C19,2C9,3A4	-
14	M	M	H	S	H	2C19,2C9,3A4	-
15	M	M	H	S	H	2C19,2C9,3A4	-
16	M	M	H	S	H	2C19,2C9,3A4	-
17	H	M	H	S	H	2C19,2C9,3A4	-
18	H	M	H	S	H	2C19,2C9,3A4	-
19	H	M	H	S	H	2C19,2C9,3A4	-
20	M	M	H	S	H	2C19,2C9,3A4	-

BBB: blood-brain barrier; CYP: cytochrome P450; HIA: human intestinal absorption; S*: strongly; F*: freely; NO: not observed; W: weakly; H: high; L: low; M: medium; 1 - Goiasin, 2 - 6a-acetoxygoiasin, 3 - Methyl angolensate, 4 - 7-deacetoxy-7-oxogoiasin, 5 - Andirobin, 6 - 6-hydroxy-methyl angolensate, 7–17β-hydroxyazadiradione, 8–1,2-dihydro-3β-hydroxy-7-deacetoxy-7-oxogoiasin, 9 - Xylocensin K, 10–11beta-Hydroxygoiasin, 6 a, 11–11β-diacetoxygoiasin, 12 - Oleic acid, 13 - Palmitic acid, 14 - Stearic acid, 15 - Arachidic acid, 16 - Myristic acid, 17 - Palmitoleic acid, 18 - Linoleic acid, 19 - Linolenic acid, 20 - Behenic acid.

The following fatty acids were also selected for prediction studies: oleic acid, palmitic acid, stearic acid, arachidic acid, myristic acid, palmitoleic acid, linoleic acid, linolenic acid, and behenic acid (Salgado et al., 2015; Silva, 2018).

2.2 In silico evaluation

The molecules were drawn using the Marvin (2023) online program (https://marvinjs-demo.chemaxon.com/latest/demo.html), and for the determination of physicochemical properties, the online server Home-ADMElab was used (https://admet.scbdd.com) (Dong, 2024). The Lipinski's Rule of Five or "Rule of Five" was considered (Lipinski, 2004). For pharmacokinetic and toxicity predictions, the PreADMET program (version 2.0, Copyright © 2005–2017) was used, which considers pharmacokinetic properties (A–absorption; D–Distribution; M–Metabolism/Biotransformation; E–Excretion) and evaluation of toxicity parameters (T–Toxicity; Preadmet, 2020).

For the assessment of toxicity in marine organisms, the criteria used were as follows: for toxicity in algae (Costa et al., 2008); for Daphnia sp (Guilhermino et al., 2000); for Medaka (Zucker, 1985); and for Minnow (Costa et al., 2008). The mutagenicity risk was assessed by the Ames test with the following strains of *Samonella Typhimurium*: TA100-10RLI and TA 100-NA mutation in His G46e plasmid pKM101 without S9; TA1535- 10RLI and TA1535-NA mutation in His G46 (Ames et al., 1975). The carcinogenic potential of the compounds was evaluated in rats and mice and referred to as (+) carcinogenic and (−) non-carcinogenic. To predict acute oral toxicity (lethal dose 50%- LD_{50}), the online software PROTOX II was used (Drwal et al., 2014), considering the classification from I to VI, according to ABNT NBR 14725-2 (2019). Adverse events that may occur with the use of the molecule were also evaluated.

The search for potential targets for molecular docking prediction was conducted using the SuperPred Webserver program (Nickel et al., 2014), a server for predicting molecular targets with potential interaction with the investigated ligands. The targets, which showed relevance to the investigated biological activity, were obtained from the Protein Data Bank database (PDB ID 4H6J and 5F19/4OTY). Compounds with the highest scores for therapeutic activity (≥70% probability of binding and ≥70% prediction accuracy) were selected for molecular docking simulations.

TABLE 3 Prediction of toxicity.

Molecules	Alga	Daphnia	Fish		Ames	Carcino
			Medaka	Minnow		Rats/Mice
1	T	T	VT	VT	N	P/P
2	T	T	VT	VT	N	P/P
3	T	T	VT	VT	N	P/N
4	T	T	VT	VT	N	P/P
5	T	T	VT	VT	N	P/P
6	T	T	VT	VT	N	P/N
7	T	T	VT	VT	N	P/P
8	T	T	VT	VT	N	P/N
9	T	T	VT	VT	N	P/N
10	T	T	VT	VT	N	P/P
11	-	-	-	-	-	-
12	T	T	VT	VT	1535-NA	P/P
13	T	T	VT	VT	1535-NA	P/N
14	T	T	VT	VT	1535-NA	P/N
15	T	T	VT	VT	1535-NA	P/N
16	T	T	VT	VT	1535-NA	P/N
17	T	T	VT	VT	1535-NA	P/P
18	T	T	VT	VT	1535-NA	P/P
19	T	T	VT	VT	1535-NA	P/P
20	T	T	VT	VT	1535-NA	P/P

T: toxic; NT: non-toxic; N: negative; P: positive. Parameters: Algae - < 1 mg/L toxic; >1 mg/L non-toxic (Costa, et al., 2008); Daphnia Test: <0.22 μg/mL toxic; >0.22 μg/mL - non-toxic (Guilhermino, et al., 2000); Test on Medaka and Minnow fish: <1 mg/L - very toxic; 1–10 mg/L-toxic; 10–100 mg/L-harmful and >100 mg/L-extremely toxic (Zucker, 1985); Carcino Rat/mice* = carcinogenicity in rat/mice. T-toxic, NT-non-toxic, VT-very toxic, N-negative, P-positive. 1 - Gedunin, 2 - 6α-acetoxygedunin, 3 - Methyl angolensate, 4 - 7-deacetoxy-7-oxogedunin, 5 - Andirobin, 6 - 6-hydroxy-methyl angolensate, 7–17β-hydroxyazadiradione, 8–1,2-dihydro-3β-hydroxy-7-deacetoxy-7-oxogedunin, 9 - Xylocensin K, 10–11beta-Hydroxygedunin, 6 α, 11–11β-diacetoxygedunin, 12 - Oleic acid, 13 - Palmitic acid, 14 - Stearic acid, 15 - Arachidic acid, 16 - Myristic acid, 17 - Palmitoleic acid, 18 - Linoleic acid, 19 - Linolenic acid, 20 - Behenic acid.

2.3 Docking molecular

Molecular targets were determined: Hypoxia-inducible factor 1 alpha (HIF-1-α, PDB 4H6J) and Cyclooxygenase-2 (COX-2, PDB 5F19/4OTY). The crystallographic structure of the enzymes was retrieved from the Protein Data Bank (PDB) under the codes 4H6J (Cardoso et al., 2012) with a resolution of 1.52 Å and 4OTY with a resolution of 2.35 Å.

The structures of the compounds were initially obtained from PubChem (http://pubchem.org) in sdf format. OpenBabel (O'Boyle et al., 2011) was used to generate the 3D coordinates of the compounds and optimized using the Gaussian 09 software. Docking molecular simulations were conducted using the program Molegro Virtual Docker (MVD) version 5.5 (Bitencourt-Ferreira and de Azevedo, 2019).

Redocking was performed using the inhibitor lumiracoxib (LUR) of the COX-2 protein (PDB 4OTY). The enzyme's active site was defined as a spherical region of 12 Å, based on the coordinates of the crystallographic ligand lumiracoxib using the MolDock Score scoring function.

For HIF-1-α, due to the absence of a crystallized inhibitor, data from the literature and the cavity detector of the program (Singh et al., 2023; Kong et al., 2022) and the cavity detector of the MVD with coordinates x: 6.35, y: −26.39, z: −22.37 and a sphere of 12 Å were used. Ligands underwent 10 iterative runs, and the pose with the best scoring result was considered for the analysis of intermolecular interactions using the Discovery Studio Visualizer (Discovery Studio Visualizer Dassault Systèmes BIOVIA, 2021).

2.4 Molecular dynamics (MD)

The stability of the ligand-receptor complexes for the apo form of HIF-1alpha and its form complexed with molecules 3, 6, and the reference inhibitor lificiguat (YC-1) was analyzed. Also, the apo form of COX-2 complexed with molecules 15, 16, and the reference inhibitor lumiracoxib. The AMBER22 simulation package was used to perform 200 ns MD simulations on all complexes prepared using the GPU-accelerated version of the Particle Mesh Ewald Molecular Dynamics (PMEMD) (Lee et al., 2018).

TABLE 4 Prediction of oral toxicity.

Molecules	LD_{50} (mg/kg)	Toxicity class	Side effects
1	980	IV	N
2	1,804	IV	N
3	846	IV	N
4	596	IV	N
5	1,219	IV	N
6	1,162	IV	N
7	496	IV	N
8	696	IV	N
9	676	IV	N
10	559	IV	N
11	-	-	N
12	5,302	VI	N
13	4,010	V	I/T
14	4,499	V	I/T/M
15	4,867	V	N
16	3,033	V	I/M
17	4,906	V	N
18	5,259	VI	N
19	6,838	VI	N
20	5,228	VI	N

LD50 - lethal dose 50%. NO, nothing observed. I - Irritant, T - Tumorigenic, M - Mutagenicity. Category I: I< LD50≤ 5 mg/kg - Extremely Toxic; Category II: 5 < LD50 ≤ 50mg/kg- Highly Toxic; Category III: 50 < LD50 ≤ 300 mg/kg - Moderately Toxic; Category IV: 300 < LD50 ≤ 2,000 mg/kg - Low Toxic; Category V: 2000 < LD50 ≤ 5,000 Unlikely to Cause Acute Damage; Category VI: DL50 > 5,000 No damage. Source: ABNT NBR, 2018; RDC, No. 294, 2019. 1 - Gaduain, 2 - 6α-acetoxygeduain, 3 - Methyl angelonuate, 4 - 7-deacetoxy-7-oxogeduain, 5 - Andirobin, 6 - 6-hydroxy-methyl angelonuate, 7–17β-hydroxyazadiradione, 8–1,2-dihydro-3β-hydroxy-7-deacetoxy-7-oxogeduain, 9 - Xylocensin K, 10–11beta-Hydroxygeduain, 6α, 11–11β-diacetoxygeduain, 12 - Oleic Acid, 13 - Palmitic Acid, 14 - Stearic Acid, 15 - Arachidic Acid, 16 - Myristic Acid, 17 - Palmitoleic Acid, 18 - Linoleic Acid, 19 - Linolenic Acid, 20 - Behenic Acid.

TABLE 5 Molecular target assessment.

Molecules	Probability (%)	Prediction accuracy (%)	Target Name	PDB
3	99.05	85.14	Hypoxia-inducible factor 1 alpha	4H6J
6	95.62	85.14	Hypoxia-inducible factor 1 alpha	4H6J
15	90.73	89.65	Cyclooxygenase-2	5F19/4OTY
16	90.93	89.65	Cyclooxygenase-2	5F19/4OTY

PDB: Protein Data Bank 3- Methyl angelonuate, 6 - 6-hydroxy-methyl angelonuate, 15 - Arachidic Acid, 16 - Myristic Acid.

Proteins and ligands were prepared in ff14SB (Maier et al., 2015) and GAFF (Wang et al., 2004), with atomic charges calculated using the restrained electrostatic potential (RESP) protocol at the HF/6-31G*25 theoretical level using the Gaussian 09 software. The protonation states of the ionizable residues were analyzed by calculating the pKa at neutral pH using the PDB2PQR server (Dolinsky et al., 2007). All systems were solvated in the tLeap module using an octahedral water box with the TIP3P model (Jorgensen et al., 1983). Na + ions were added to maintain the system's electroneutrality. Each step was performed by applying steps of steepest descent minimization followed by 5,000 of conjugated gradient.

The systems were heated from 0 to 300 K, maintained at 300 K (Langevin thermostat), performing 200 ps of MD and 300 ps of density equilibration, and 500 ps without positional restraints at constant pressure. A cutoff point of 10 Å for the systems was used for non-bonded interactions, the Particle Mesh Ewald (PME) method (Petersen, 1995), and the SHAKE algorithm (Elber, 2011) were used to restrict bond lengths involving hydrogen atoms. Finally, MD (production) simulations were performed using 200 ns at a

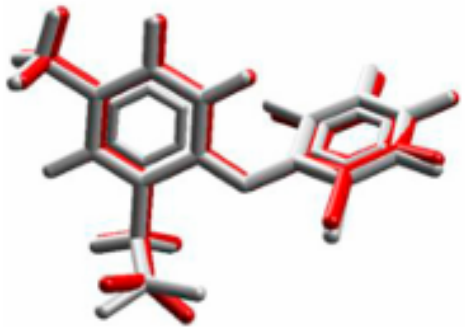

FIGURE 2
Validation of molecular docking protocols using the MVD program. White is the co-crystal ligand and red is the coupling pose.

TABLE 6 Values of the binding energies between the limonoids and HIF1A.

Molecules	ΔE_{ele}	ΔE_{vdW}	ΔG_{GB}	ΔG_{SA}	ΔG_{bind}
YC-1	−10.18	−36.79	21.13	−4.62	−30.47
3	−19.87	−31.24	33.86	−4.09	−20.56
6	−11.69	−20.45	25.51	−2.69	−11.32

Caption: YC-1, lifecigat, 3- Methyl angolensate, 6 - 6-hydroxy-methyl angolensate.

temperature of 300 K without positional restraints. The deviations of the protein and protein-ligand complex systems were analyzed by calculating the root mean square deviation (RMSD), root mean square fluctuation (RMSF), and hydrogen bonds using the CPPTRAJ module (Roe and Cheatham, 2013).

2.5 Binding free energy calculation using MM/GBSA

The MM/GBSA technique accurately calculates the total binding free energy of protein-ligand complexes using the AmberTools23 package (Da Costa et al., 2022; Case et al., 2023). The last 10 ns of the MD simulation trajectories were used to calculate the binding free energy.

3 Results

3.1 In silico evalution

All limonoids already isolated from *C. guianensis* were included in this study. Similarly, identified fatty acids of the species were selected (Figure 1):

Regarding the predictions of the physicochemical characteristics of the fatty acids (12, 13, 14, 15, 17, 18, 19, and 20), they demonstrated a partition coefficient oil-water (LogP) higher than 5.0, while the limonoids have higher molecular masses (MM), with limonoid 11 violating the Lipinski's rule. Molecule 2 showed only one violation in molecular mass (Table 1).

Despite the compounds' permeability ranging from low to high, all molecules appear to be well absorbed in the gastrointestinal tract. Regarding distribution, molecules 2, 5, 6, 9, 10, and 11 exhibit reduced plasma protein binding and moderate distribution to the central nervous system (CNS), except molecule 6, which showed low distribution. Only the fatty acids distribute highly to the CNS, likely due to their high lipid solubility (Chagas et al., 2022). All limonoids inhibit CYP2C9 and CYP3A4, with CYP3A4 being the main enzyme involved in the metabolism of these molecules. Fatty acids are inhibited by CYP2C19, CYP2C9, and CYP3A4 and do not undergo phase 1 metabolism (Table 2).

The toxicity prediction model showed a limitation regarding molecule 11, for which it was not possible to determine the toxicity parameters. All compounds were toxic to algae, Daphnia, and Medaka and Minnow fishes. Regarding mutagenicity, the fatty acids were mutagenic for strain TA1535_NA. The fatty acids were carcinogenic for rats and mice. Except for acids 13, 14, 15, and 16, which were not carcinogenic for mice. The limonoids were not mutagenic, but they were carcinogenic for rats and mice, except for 3, 6, and 8, which were not carcinogenic for mice (Table 3).

Regarding acute oral toxicity, the molecules with the lowest toxic potential are the fatty acids (Class V and VI); however, despite being considered of low toxicity (Class IV), the limonoids appear to have a lower potential for side effects (Table 4).

Based on the predictions related to physicochemical, pharmacokinetic, and toxicity parameters, the molecules considered most promising were 3, 6, 15, 16. Subsequently, the targets with potential for biological activity related to Leishmania were determined (Hypoxia-inducible factor 1 alpha, Cyclooxygenase-2) with a probability of correctness and accuracy greater than 70%, and PDB (Protein Data Bank) code (4H6J and 5F19/4OTY) for docking, obtained through the online server as demonstrated in Table 5.

3.2 Docking molecular simulation

In the redocking with the lumiracoxib (LUR) inhibitor of the COX-2 protein (PDB 4OTY), it was found that the redocked conformation of the ligand perfectly overlapped with the co-crystallized ligand, with an RMSD value of 0.33 Å and satisfactory precision in repositioning the LUR ligand within the active site of COX-2. The RMSD value between the docking pose and the crystallographic ligand pose is less than 2.0 Å (Figure 2).

The validated docking protocol was subsequently used for molecular docking simulation. Comparing the bindings of compounds 3 and 6 to the enzyme Hypoxia-inducible factor 1 (HIF1A), it is observed that compound 3 bound with lower energy and had a lower inhibition constant than 6. Regarding compounds 15 and 16 with Cyclooxygenase-2 (COX2), despite the low binding energy, the inhibition constants were higher than those of 3 and 6, with 16 being very high (Table 6).

Regarding the interactions established between the limonoids and the HIF1A protein, compound 3 did not have any unfavorable bonds, establishing alkyl bonds and hydrogen

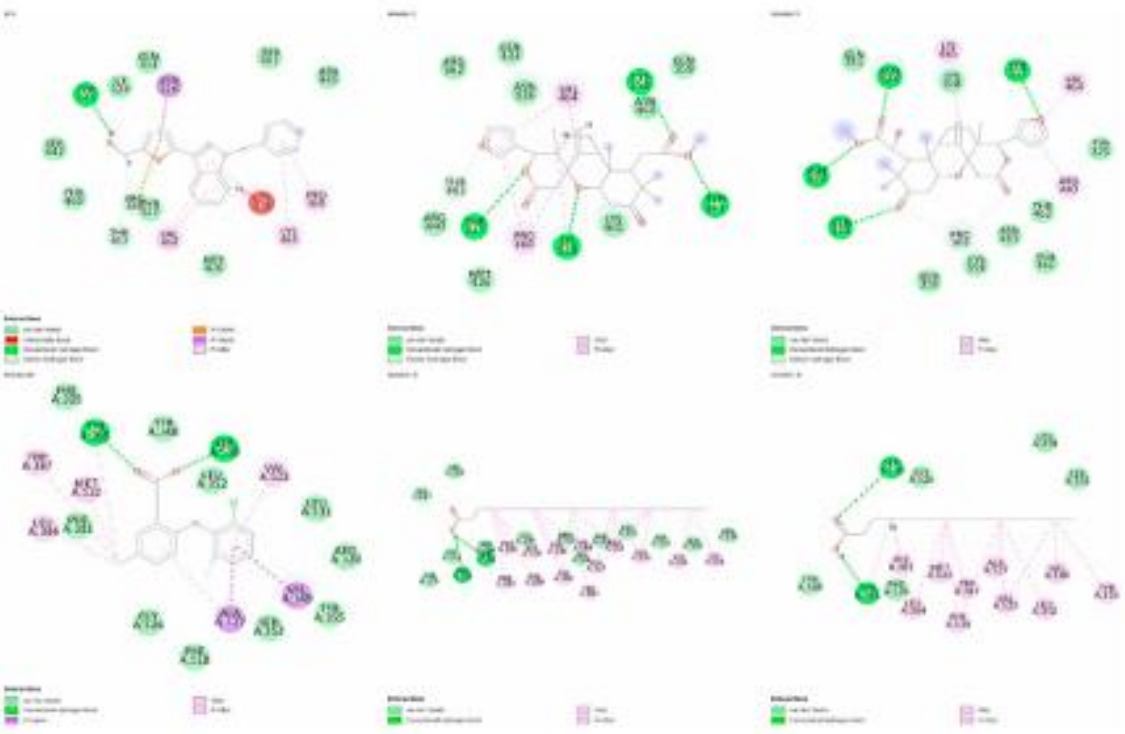

FIGURE 3
Representation of 2D interactions of molecules 3, 6, 15, 16 and inhibitors YC-1, LUR. Image generated with Discovery Studio 3.5 Visualizer.

bonding. Compound 6 presented 1 unfavorable bond, 1 alkyl bond, 1 C-H bond, and 4 hydrogen bonds (Figure 2). Evaluating the interactions established by the fatty acids and the COX-2 protein, unfavorable bonds are observed for both compounds, with hydrogen bonds, alkyl bonds, and C-H bonds also being observed (Figure 3).

3.3 Molecular dynamics simulation

3.3.1 Interactions of the limonoids methyl angolensate and 6-hydroxy-methyl angolensate with HIF1A

Figure 4 shows the RMSDs of HIF1A complexed with ligands 3, 6, and YC-1, displaying stable dynamic behavior and RMSD values of 1.87 Å (molecule 3), 1.55 Å (molecule 6), 1.71 Å (YC-1), and 1.61 Å (HIF1A-6).

Figure 5 shows that all complexes formed by molecules 3, 6, and the YC-1 inhibitor exhibited similar behaviors, with minimal fluctuations below 2 Å, except in the regions between residues 344-346, which showed greater fluctuation and the presence of a significant number of H bonds, suggesting a strong interaction between a ligand-protein complex.

In Table 6, it can be observed that molecule 3 showed the most favorable binding affinity to the HIF1A protein (ΔGbind −20.56 kcal/mol), compared to molecule 6 (ΔGbind −11.32 kcal/mol).

3.3.2 Interactions of fatty acids with COX-2

When comparing the RMSD values over time, it is observed that molecules 15 and 16 exhibit lower values than LUR (Figure 6). Regarding the comparison of RMSD and amino acid residues, in most bonds, proximities were observed between this parameter; however, the lowest RMSD values were observed for molecule 16 (Figure 6).

Regarding the ligand's ability to establish hydrogen bonds with COX-2, a greater number of bonds between the protein and molecule 15 were observed (Figure 7).

In Table 7, it can be observed that molecule 15 showed the most favorable binding affinity to the COX-2 protein (ΔGbind -54.36 kcal/mol), compared to molecule 16 (ΔGbind -35.90 kcal/mol).

4 Discussion

This study evaluated the physicochemical, pharmacokinetic, and toxicity aspects of fatty acids already identified in *C. guianensis* Oil, observing in the physicochemical study that they violate the LogP. The LogP assesses the balance between liposolubility and hydrosolubility, and when it is above 5, it can be a predictive factor for low absorption of the compounds in the gastrointestinal tract. However, pharmacokinetic prediction studies demonstrated that in MDCK cells, the permeability of the compounds was moderate to high, while in Caco2 cells, the permeability was moderate. The high permeability in MDCK cells

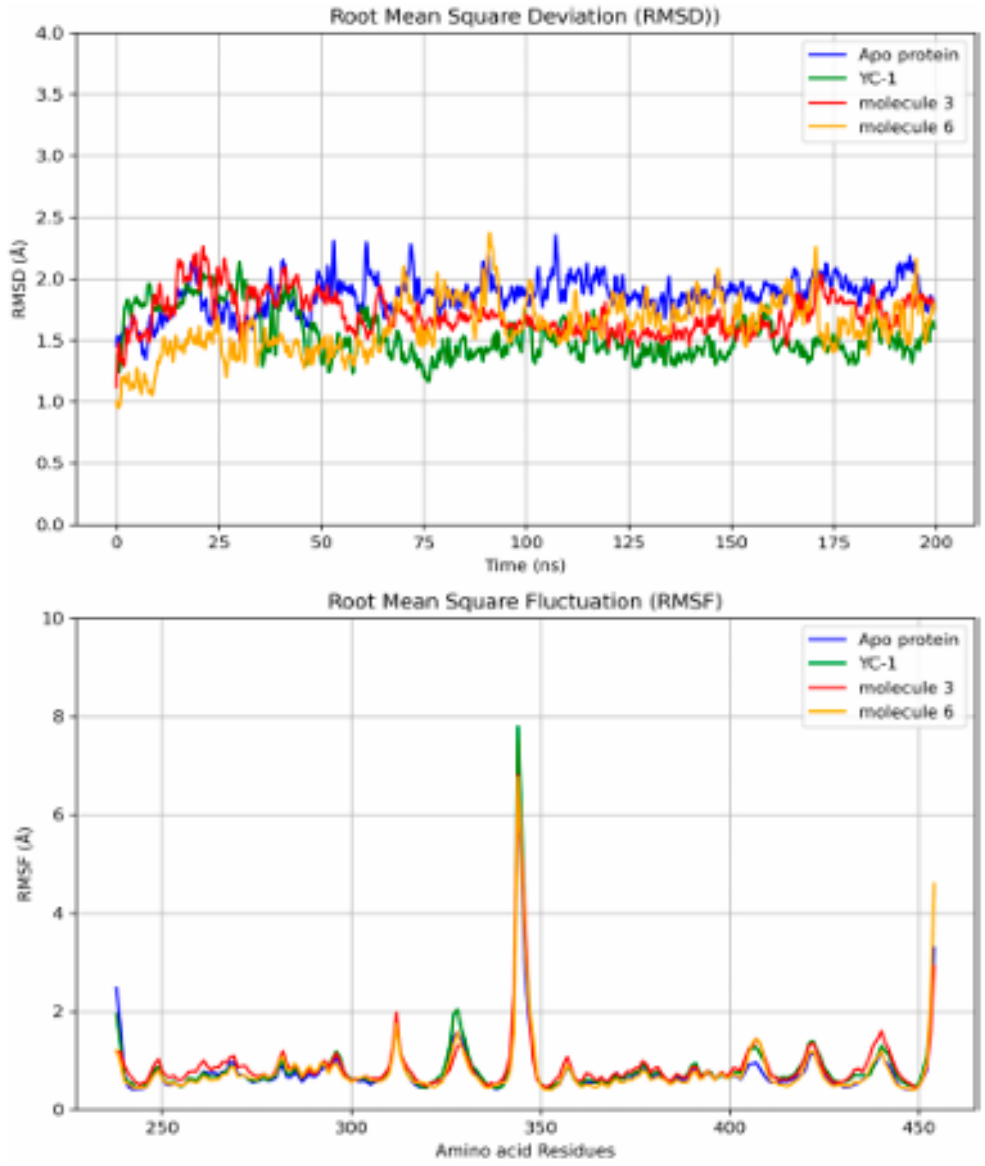

FIGURE 4
Comparisons of RMSD and RMSF of the limonoids and HIF1A as a function of time and amino acid residues. YC-1 - Ilicigual, 3 - Methyl angolensate, 6 - 6-hydroxy-methyl angolensate.

suggests that these compounds may be absorbed by passive diffusion (Chen et al., 2018). That is, they can cross the lipid layer due to their high liposoluble potential. The permeability in Caco2 cells evaluates absorption in the Colon region, which seems to be moderate, and perhaps, the high intestinal absorption of these compounds may occur due to absorption in different locations of the GI tract (Da Silva Miranda et al., 2022).

Due to their MM < 500D and high liposolubility, the evaluated fatty acids appear to freely cross the blood-brain barrier. Therefore, therapeutic concentrations can be achieved centrally and peripherally, expanding their medicinal potential. However, adverse reactions may occur centrally and peripherally. Additionally, these compounds strongly bind to plasma protein and appear not to be metabolized by CYP. It is worth noting that phase 1 metabolism makes the compound more polar and facilitates renal excretion. It is important to emphasize that fatty acids play an essential role in the body, from strengthening immunity to their importance in the inflammatory response (Pereira, 2008).

A concerning point in terms of pharmacokinetics is the inhibitory potential of CYP2C19, CYP2C9, and CYP3A4, which

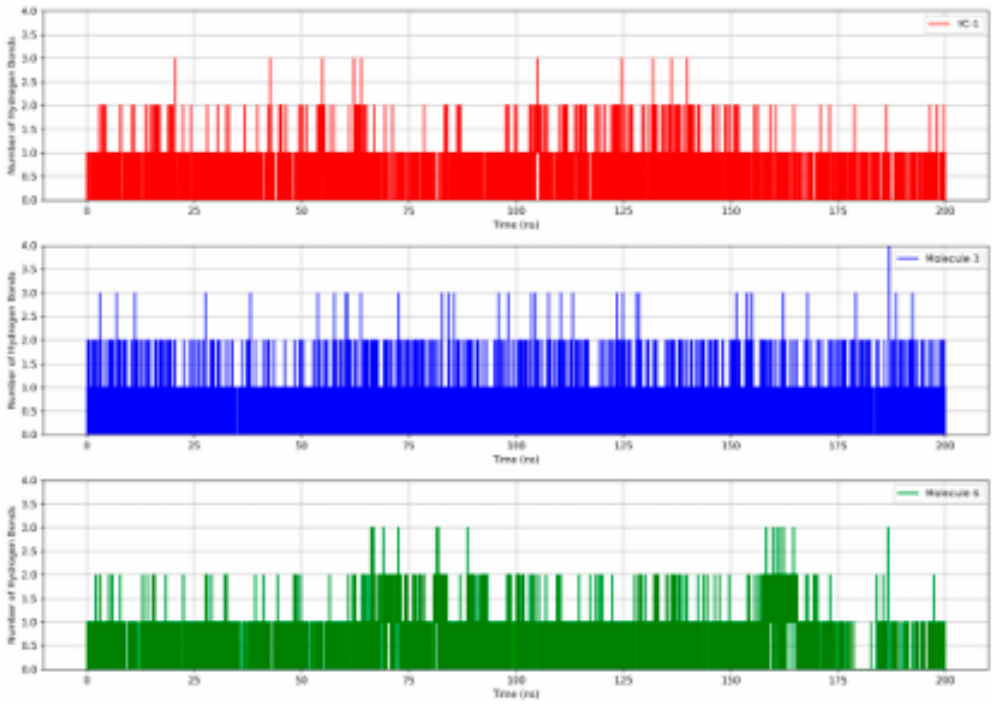

FIGURE 5
RMSD and hydrogen bonds between HIF1A and the YC-1 inhibitor and molecules 3 and 6.

may interfere with the metabolism of other drugs. Since CYP3A4 metabolizes a large number of drugs, its inhibition can lead to an increase in the plasma concentration of these drugs and elevate the risk of toxic effects.

Another important aspect evaluated was the toxicity of fatty acids in algae, crustaceans, and fish. All fatty acids were toxic to algae and crustaceans, while they were not toxic to fish. The model for algae is used to predict acute oral toxicity in terms of mortality (Guilhermino et al., 2000). The Daphnia crustacean model is used to predict acute and subchronic toxicities. The model for Medaka and Minnow fish suggests acute and subchronic toxicity, as well as changes in different organs (Bauer, 2017).

All fatty acids showed mutagenic potential (TA1535-NA), with mutations potentially occurring in both somatic and germline cells, depending on the genes, which may or may not have phenotypic effects, potentially leading to severe clinical consequences. Additionally, compounds 12, 17, 18, 19, and 20 were found to have carcinogenic potential in rats and mice, with carcinogenesis involving the conversion of a normal cell into a malignant cell, requiring prolonged time and repeated exposure to carcinogens (Loureiro et al., 2002). Thus, if used acutely or for short periods, the carcinogenic potential of fatty acids is minimized.

Regarding acute oral toxicity, the molecules with the lowest toxic potential are the fatty acids (Class V and VI). However, molecules 13, 14, and 16 appear to have side effects related to irritation, tumorigenicity, and mutagenicity. Therefore, while fatty acids may not be lethal when ingested, the side effects on organisms are a trade-off of these results, requiring attention to these molecules despite limited toxicity studies.

The limonoids, except for 11, followed the Lipinski rule; however, their permeability in MDCK cells showed that only one molecule had high permeability, suggesting that the mechanism used in cellular diffusion may not be passive diffusion (Chen et al., 2018). Additionally, the results in Caco2 cells showed moderate permeability, suggesting that absorption in the intestine occurs at more than one location, thus explaining the high intestinal absorption. However, limonoids have higher molecular mass (MM) compared to fatty acids, but only molecule 2 has a molecular mass (MM) exceeding 500D. On the other hand, molecule 11 violated the Lipinski rule. Despite limited oral bioavailability in molecules that do not adhere to Lipinski's rule, the therapeutic potential should not be ignored (Lipinski, 2004).

Similarly to fatty acids, limonoids exhibited high intestinal absorption, despite low to moderate permeability in MDCK and moderate permeability in Caco2. These results suggest that perhaps the diffusion mechanism through membranes is not passive and that their absorption may occur in other intestinal regions (Chen et al., 2018). Another similarity with fatty acids was the potential inhibitory effect on CYPs, which could interfere with the metabolism of different classes of drugs (Chen et al., 2018).

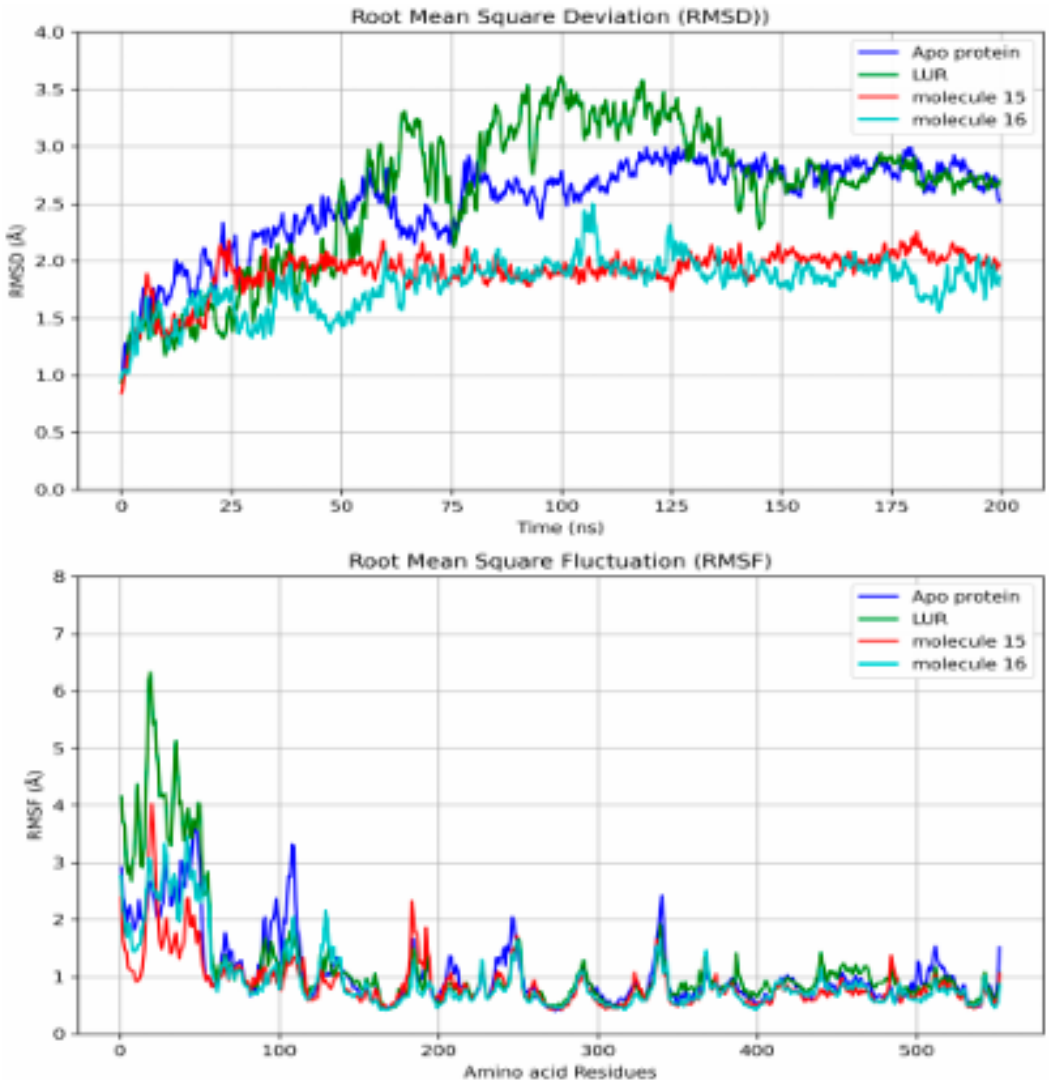

FIGURE 6
Comparisons of RMSD in the binding of fatty acids and COX-2 as a function of time and amino acid residues.

In terms of toxicity, the significant advantage of limonoids over fatty acids is that they did not show mutagenic potential in predictions. A previous study demonstrated that limonoids found in andiroba oil have anti-inflammatory, anticancer, antitumor, and antiallergic properties (Matsui et al., 2014; Higuchi et al., 2017; Tsukamoto, 2019).

One disadvantage of limonoids compared to fatty acids was their higher acute oral toxicity, with their simulated LD50 belonging to class IV. However, it is important to establish the effective dose 50% of limonoids, thus allowing the determination of the therapeutic window of these compounds, ensuring their safety of use. On the other hand, there were no results related to side effects, which is encouraging for the possibility of a promising drug (Miranda-Júnior et al., 2012).

The molecular docking studies of the selected limonoids and fatty acids were conducted against molecular targets of Leishmania, aiming to explore their leishmanicidal potential. These enzymes are necessary for the parasite's survival and represent relevant targets for the development of new drugs (Degrossoli et al., 2007). The limonoids exhibited the best characteristics and molecular affinities, as they formed hydrogen bonds with the Tyr254 residue, which participates in the active site, potentially generating irreversible inhibitors (Cardoso et al., 2012). Comparing the two limonoids and their binding to HIF1A, it can be suggested that limonoid 3 established a better binding.

Regarding fatty acids and their binding to cyclooxygenase 2, inhibition of which is related to anti-inflammatory effects, molecules 15 and 16 bound with favorable binding energy, but 16 had a very unfavorable inhibition constant. Thus, the more promising molecule was 15, which may contribute to the treatment of cutaneous

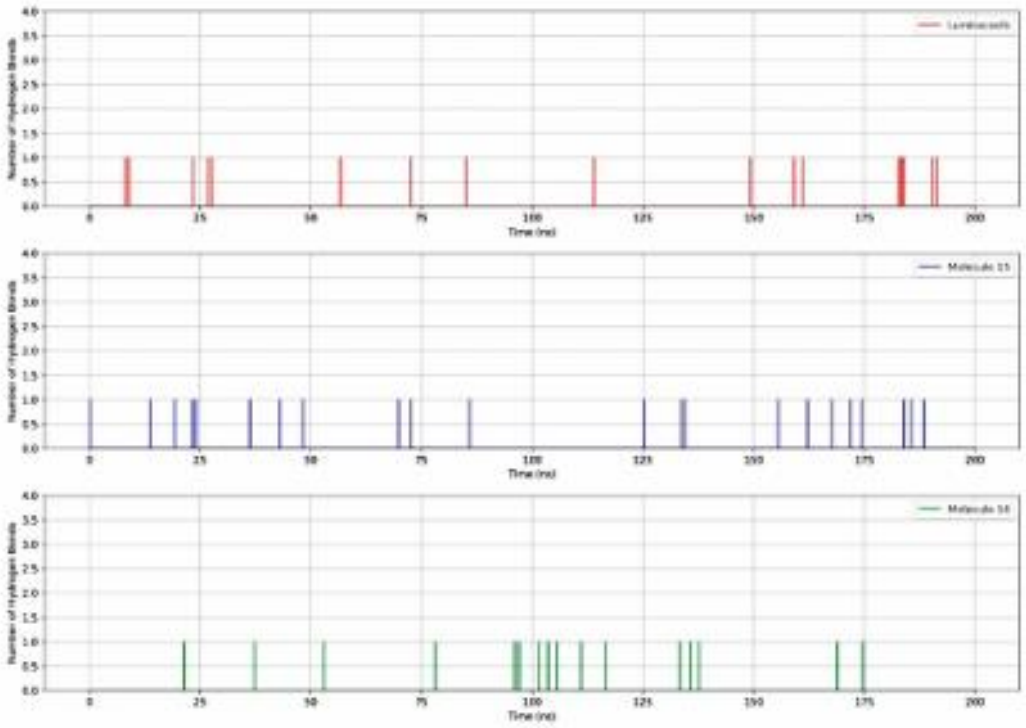

FIGURE 7
RMSD and hydrogen bonds between COX-2, LUR, and molecules 15 and 16.

TABLE 7 Values of the binding energies between fatty acids and COX-2.

Molecules	ΔEele	ΔEvdW	ΔGGB	ΔGSA	ΔGbind
LUR	−37.76	−35.77	44.42	−5.34	−34.46
15	−7.34	−59.96	21.55	−8.61	−54.36
16	−11.89	−40.82	22.82	−6.01	−35.90

Caption: LUR-karanaundi, 15 - Arachidic Acid, 16 - Myristic Acid.

leishmaniasis in the wound healing phase. This process involves interaction between cells and various messenger systems, divided into three phases: inflammatory, proliferative, and remodeling (Velnar et al., 2009).

The results of molecular dynamics provide a detailed and dynamic view of molecular behavior, essential for understanding complex phenomena of molecule-protein binding. Despite the RMSD values of limonoids 3 and 6 being close and many hydrogen bonds being observed for both molecules, the better binding energy was observed for limonoid 3, suggesting that it may be the most promising.

In terms of the dynamics of fatty acids 15 and 16, it was observed that the RMSD of these molecules was lower than that of LUR. However, there was a slight difference between the number of hydrogen bonds and the energy, with compound 15 being the most promising.

5 Conclusion

In summary, the leishmanicidal effect of *C. guianensis* appears to result from the synergistic effect between limonoids and fatty acids. Limonoids have an antiparasitic effect, while fatty acids may contribute to the wound healing process of American cutaneous leishmaniasis. Another relevant point is related to mutagenicity, with only fatty acids presenting this potential, while limonoids act as protectors against mutagenic processes. Therefore, *C. guianensis* oil seems to be very promising for the treatment of cutaneous leishmaniasis.

Data availability statement

The original contributions presented in the study are included in the article/Supplementary Material, further inquiries can be directed to the corresponding author.

Ethics statement

The manuscript presents research on animals that do not require ethical approval for their study.

Author contributions

RCB: Formal Analysis, Investigation, Methodology, Software, Writing–original draft, Writing–review and editing. RAC: Formal Analysis, Methodology, Software, Writing–review and editing, SDPF: Data curation, Investigation, Writing–review and editing, KCOA: Data curation, Investigation, Writing–review and editing, AMRM: Data curation, Investigation, Writing–review and editing, MBC: Supervision, Writing–review and editing. PSBM: Data curation, Investigation, Writing–review and editing. MFD: Supervision, Writing–review and editing.

Funding

The authors declare that financial support was received for the research, authorship, and/or publication of this article. The Dean of Research and Postgraduate Studies at the State University of Pará provided payment for the processing and publication of this article - Notice 02/2023 - PAPQ/PROPESP. Additionally, FAPESPA/CAPES provided support through the program "PDPG Strategic Partnerships in States III (PDPG-FAPIII)," which supports the first author as a FAPESPA/CAPES-BRAZIL Fellow.

Conflict of interest

The authors declare that the research was conducted in the absence of any commercial or financial relationships that could be construed as a potential conflict of interest.

Publisher's note

All claims expressed in this article are solely those of the authors and do not necessarily represent those of their affiliated organizations, or those of the publisher, the editors and the reviewers. Any product that may be evaluated in this article, or claim that may be made by its manufacturer, is not guaranteed or endorsed by the publisher.

References

Aguiar, P. F., and Rodrigues, R. K. (2017). Leishmaniose visceral no Brasil: artigo de revisão. *Revista Universitas Científica* 19 (1), 192–204.

Ambrozin, A. R. P., Leite, A. C., Bueno, F. C., Vieira, P. C., Fernandes, J. B., Bueno, O. C., et al. (2006). Limonoids from andiroba oil and Cedrela fissilis and their insecticidal activity. *J. Braz. Chem. Soc.* 17 (5). doi:10.1590/s0103-50532006000300017

Ames, B. N., McCann, J., and Yamasaki, E. (1975). Methods for detecting carcinogens and mutagens with the salmonella/mammalian-microsome mutagenicity test. *Mutat. Research-Environmental Mutagen. Relat. Subj.* 31 (6), 347–363. doi:10.1016/0165-1161(75)90046-1

Bauer, L. H. (2017). *Sensibilidade do Método de Ensaios de Toxicidade Aguda com Embriões de Peixes na Avaliação de Efluente de Indústria Metalmecânica*. Available at: https://www.lume.ufrgs.br/handle/10183/180460.

Bitencourt-Ferreira, G., and de Azevedo, W. F. (2019). *Molegro Virtual Docker for Docking. em Methods in Molecular Biology*. New York, NY: Springer New York, 149–167.

Cardoso, R., Love, R., Nilsson, C. L., Bergqvist, S., Nowlin, D., Yan, J., et al. (2012). Identification of Cys255 in HIF-1α as a novel site for development of covalent inhibitors of HIF-1α/ARNT PasB domain protein-protein interaction: covalent Allosteric Inhibitors of HIF-1α/ARNT PasB PPI. *Protein Sci. A Publ. Protein Soc.* 21 (12), 1885–1896. doi:10.1002/pro.2172

Case, D. A., Aktulga, H. M., Belfon, K., Cerutti, D. S., Cisneros, G. A., Cruzeiro, V. W. D., et al. (2023). AmberTools. *J. Chem. Inf. Model.* 63 (20), 6183–6191. doi:10.1021/acs.jcim.3c01153

Chagas, C., Kallahan, S., Martins, H. P. d. S., and Delabela, M. F. (2022). Estudo in silico de compostos fenólicos isolados de Inga laurina. *Res. Soc. Dev.* 11 (2), e24511225592. doi:10.33448/rsd-v11i2.25592

Chen, E. C., Broccatelli, F., Pfau, E., Chen, B., Liu, L., Cheong, J., et al. (2018). Evaluating the utility of canine Mdr1 knockout Madin-Darby canine kidney I cells in permeability screening and efflux substrate determination. *Mol. Pharm.* 15 (11), 5103–5115. doi:10.1021/acs.molpharmaceut.8b00688

Costa, C. R., Olivi, P., Botta, C. M. R., and Espindola, E. L. G. (2008). A toxicidade em ambientes aquáticos: discussão e métodos de avaliação. *Química nova* 31 (7), 1820–1830. doi:10.1590/s0100-40422008000700058

Da Costa, R.A., da Rocha, J. A. P., Pinheiro, A. S., da Rocha, E. C. M., Josino, L. P. C., et al. (2022). In silico identification of novel allosteric inhibitors of Dengue virus NS2B/NS3 serine protease. *J. Serbian Chem. Soc.* 87 (6), 693–706. doi:10.2298/jsc210929011d

Da Silva Miranda, C. C., Cardoso Salazar, V. A., and Gomes Coelho, A. (2022). Predição in silico da atividade antiviral e avaliação de características farmacocinéticas e toxicológicas de compostos presentes no óleo essencial de Peltiverta alliacea L. *Rev. Caos Conselh.* 13 (1), e8705.

Degrossoli, A., Bosetto, M. C., Lima, C. B. C., and Giorgio, S. (2007). Expression of hypoxia-inducible factor 1α in mononuclear phagocytes infected with Leishmania amazonensis. *Immunol. Lett.* 114 (2), 119–125. doi:10.1016/j.imlet.2007.09.009

Discovery Studio Visualizer Dassault Systèmes BIOVIA (2021). *Discovery Studio modeling environment, version 2021*. San Diego: Dassault Systèmes.

Dong, J. (2024). *Home-ADMElab: ADMET Prediction, Scbdd.com*. Available at: https://admet.scbdd.com/.

Dolinsky, T. J., Czodrowski, P., Li, H., Nielsen, J. E., Jensen, J. H., Klebe, G., et al. (2007). PDB2PQR: expanding and upgrading automated preparation of biomolecular structures for molecular simulations. *Nucleic acids Res.* 35 (Web Server), W522–W525. doi:10.1093/nar/gkm276

Droval, M. N., Banerjee, P., Dunkel, M., Wettig, M. R., and Preissner, R. (2014). ProTox: a web server for the *in silico* prediction of rodent oral toxicity. *Nucleic acids Res.* 42 (Web Server issue), W53–W58. doi:10.1093/nar/gku401

Elber, R., Ruymgaart, A. P., and e Hess, B. (2011). SHAKE parallelization. *Eur. Phys. J. Special Top.* 200 (1), 211–223. doi:10.1140/epjst/e2011-01525-9

Falci, D. R., and Pasqualotto, A. C. (2015). Anfotericina B: uma revisão sobre suas diferentes formulações, efeitos adversos e toxicidade. *Ciên. Biomed. Rev.* 35 (2), 65–82. doi:10.4322/2357-9730.56021

Guilhermino, L., Diamantino, T., Silva, M. C., and Soares, A. M. V. M. (2000). Acute toxicity test with Daphnia magna: an alternative to mammals in the prescreening of chemical toxicity? *Ecotoxicol. Environ. Saf.* 46 (3), 357–362. doi:10.1006/eesa.2000.1916

Jorgensen, W. L., Chandrasekhar, J., Madura, J. D., Impey, R. W., and Klein, M. L. (1983). Comparison of simple potential functions for simulating liquid water. *J. Chem. Phys.* 79 (2), 926–935. doi:10.1063/1.445869

Kong, X. M., Song, D., Li, J., Jiang, Y., Zhang, X. Y., Wu, X. J., et al. (2022). Preliminary verification of the anti-hypoxia mechanism of Gentiana straminea maxim based on UPLC-triple TOF MS/MS and network pharmacology. *BMC Complementary Med. Ther.* 22 (1), 310. doi:10.1186/s12906-022-03773-0

Lee, T.-S., Cerutti, D. S., Mermelstein, D., LeGrand, S., Giese, T. J., et al. (2018). GPU-accelerated molecular dynamics and free energy methods in Amber18: Performance enhancements and new features. *J. Chem. Inf. Model.* 58 (10), 2043–2050. doi:10.1021/acs.jcim.8b00462

Lipinski, C. A. (2004). Lead- and drug-like compounds: the rule-of-five revolution. *Drug Discov. Today Technol.* 1 (4), 337–341. doi:10.1016/j.ddtec.2004.11.007

Loureiro, A. P. M., Di Mascio, P. E., and Medeiros, M. H. G. (2002). Formação de adutos exocíclicos com bases de DNA: implicações em mutagênese e carcinogênese. *Química nova* 25 (5), 777–793. doi:10.1590/s0100-40422002000500014

Maier, J. A., Martinez, C., Kasavajhala, K., Wickstrom, L., Hauser, K. E., and Simmerling, C. (2015). ff14SB: improving the accuracy of protein side chain and backbone parameters from ff99SB. *J. Chem. theory Comput.* 11 (8), 3696–3713. doi:10.1021/acs.jctc.5b00255

Mann, S., Frasca, K., Scherrer, S., Henao-Martínez, A. F., Newman, S., Ramanan, P., et al. (2021). A review of leishmaniasis: current knowledge and future directions. *Curr. Trop. Med. Rep.* 8 (2), 121–132. doi:10.1007/s40475-021-00232-7

Marvin, J. S. (2023). *Chemaxon.com*. Available at: https://marvinjs-demo.chemaxon.com/latest/demo.html.

Matsui, Y., Kikuchi, T., Inoue, T., Muraoka, O., Yamada, T., and Tanaka, R. (2014). Caraparvilides J–L from the seeds of Carapa guianensis (andiroba) and their effects on LPS-activated NO production. *Mol. (Basel, Switz.)* 19 (11), 17130–17140. doi:10.3390/molecules191117130

McGuire, B. S., and Satoskar, A. R. (2014). Leishmaniasis: clinical syndromes and treatment. *QJM Mon. J. Assoc. Physicians* 107 (1), 7–14. doi:10.1093/qjmed/hct116

Miranda Júnior, R. N. C., Dolabela, M. F., da Silva, M. N., Póvoa, M. M., and Maia, J. G. S. (2012). Antiplasmodial activity of the andiroba (Carapa guianensis Aubl., Meliaceae) oil and its limonoid-rich fraction, *J. ethnopharm.* 142 (3), 679–683. doi:10.1016/j.jep.2012.05.037

Nickel, J., Gohlke, B. O., Erehman, J., Banerjee, P., Rong, W. W., Goede, A., et al. (2014). SuperPred: update on drug classification and target prediction. *Nucleic acids Res.* 42 (W1), W26–W31. doi:10.1093/nar/gku477

O'Boyle, N. M., Banck, M., James, C. A., Morley, C., Vandermeersch, T., and Hutchison, G. R. (2011). Open Babel: an open chemical toolbox. *J. cheminformatics* 3 (1), 33. doi:10.1186/1758-2946-3-33

Oliveira, I. D. S., Moraga Tellis, C. J., Chagas, M. d. S., Behrens, M. D., Calabrese, K. S., Abreu-Silva, A. L., et al. (2018). Carapa guianensis Aublet (andiroba) seed oil: chemical composition and antileishmanial activity of limonoid-rich fractions. *BioMed Res. Int.* 2018, 1–10. doi:10.1155/2018/5032816

Pereira, L. M. (2008). *Effect of oleic and linoleic acids on the inflammatory phase of wound healing in rats. Cell Biochemistry and Function: Cellular biochemistry and its modulation by active agents or disease*, 197–204.

Peterson, H. G. (1995). Accuracy and efficiency of the particle mesh Ewald method. *J. chem. phy.* 103 (9), 3668–3679. doi:10.1063/1.470043

Pinto, G. (1963). *Características físico-químicas e outras informações sobre as principais oleaginosas do Brasil*.

Preadmet (2020). *ADME TOX calculatio Recuperado de*. Available at: http://preadmet.bmdrc.kr.Recuperadode.program.

Rodrigues, A. M., Hueb, M., Santos, T. A. R. R., and Pontes, C. J. F. (2006). Fatores associados ao insucesso do tratamento da leishmaniose cutânea com antimoniato de meglumina. *Rev. Soc. Bras. Med. Trop.* 39 (2), 139–145. doi:10.1590/s0037-86822006000200001

Roe, D. R., and Cheatham, T. E. (2013). PTRAJ and CPPTRAJ: software for processing and analysis of molecular dynamics trajectory data. *J. Chem. theory Comput.* 9 (7), 3084–3095. doi:10.1021/ct400341p

Salgado, H. L. C., Ndush, R. B., Corcet, L. Z. K. M., Carvalho, A. N. S. C., and Santos, A. S. (2015). Enzymatic hydrolysis of crude oil and isolated acylglycerides from Andiroba's seed. *Int. J. Sci.* 7, 132–136.

Silva, D. A., Oliveira, R. R., and Figueiredo, M. R. (2009). Isolation of Limonoids from seeds of Carapa guianensis Aublet (Meliaceae) by high-speed countercurrent chromatography. *Phytochem. Anal.* 20 (1), 77–81. doi:10.1002/pca.1100

Silva, L. R. (2018). Propriedades físico-químicas e perfil dos ácidos graxos do óleo da andiroba. *Nativa* 6 (2), 147. doi:10.31413/nativa.v6i2.4729

Singh, Y., Sanjay, K. S., Kumar, P., Singh, S., and Thareja, S. (2023). Molecular dynamics and 3D-QSAR studies on indazole derivatives as HIF-1α inhibitors. *J. Biomol. Struct. Dyn.* 41 (8), 3524–3541. doi:10.1080/07391102.2022.2051745

Tappin, M. R. R., Nakamura, M. J., Siani, A. C., and Lucchetti, L. (2008). Development of an HPLC method for the determination of tetranortriterpenoids in Carapa guianensis seed oil by experimental design. *J. Pharm. Biomed. Analysis* 48 (4), 1090–1095. doi:10.1016/j.jpba.2008.08.027

Tsukamoto, Y. (2019). Guianoftuits C-1 from fruit oil of andiroba (Carapa guianensis, Meliaceae). *Tetrahedron* 75 (9), 1149–1156.

Yelnar, T., Bailey, T. e., and Strelioff, Y. (2009). The wound healing process: an overview of the cellular and molecular mechanisms. *J. Int. Med. Res.* 37 (5), 1528–1542. doi:10.1177/147323000903700531

Wang, J., Wolf, R. M., Caldwell, J. W., Kollman, P. A., and Case, D. A. (2004) Development and testing of a general amber force field, *J. Comp. Chem.* 25 (9), p. 1157–1174. doi:10.1002/jcc.20035

Zucker, E. H. (1985). Hazard Evaluation Division-Standard evaluation procedure-acute test for freshwater fish. *U.S. EPA Publ.* 540 (9).

CAPÍTULO 3

Estudos quimicos e avaliação da atividade antileishmania de *Carapa guianensis*

Renilson Castro Barros; Renato Araujo da Costa, Heliton Patrick Cordovil Brígido, Juliana Correa-Barbosa Andrey Moacir R. Marinho; Lucas Botelho Jerônimo, Pablo Luis Baia Figuereido, Patrícia Santana Barbosa Marinho, Fernando Tobias Silveira; Marliane Batista Campos; Maria Fâni Dolabela.

Resumo:

O óleo resina de *C. guianensis* é amplamente utilizado pelas comunidades tradicionais amazônicas para o tratamento de feridas de difícil cicatrização. Entretanto, os estudos com extrato (EECGf) e frações obtidos desta espécie são escassos. O presente estudo comparou os aspectos químicos e atividade antiparasitária do óleo de *C. guianensis* ao extrato obtido das folhas. O EECGf e suas frações foram submetidos a análises em cromatografia em camada delgada (CCD) e alta eficiência acoplada a arranjos diiodos (HPLC-DAD) e a ressonância magnética nuclear (H1 RMN). O óleo foi submetido a técnica de hidrodestilação, sendo o óleo essencial posteiormente, submetido a análise em cromatografia gasosa acoplada a massa (CG-MS). Todas as amostras foram submetidas à avaliação da atividade antipromastigota em Leishmania L. *amazonensis*. A as moléculas da amostra mais ativa foram submetidos aos estudos *in silico*. Na prospecção fitoquimica do EECPf foi detectado triterpenos e esteroides, que também estavam presentes na fração hexanica. No HPLC, identificou-se a presença de flavonoides no extrato e frações. No RMN a presença de terpenos. No CG-MS, no óleo essencial de andiroba foram encontrados aldeidos, além disso, os resultados dos estudos computacionais foram promissores, o composto 9 (Undec-2E-enal) é um candidato para inibição da catepsina D

Palavras-chave: *Carapa guianensis*, Leishmania, Aldeidos.

1 Introdução

A leishmaniose é causada por um protozoário *Leishmania*, transmitida pelo flebotomíneos. Existem 3 formas principais da doença, sendo a leishmaniose cutânea (LC) é a forma mais comum e causa lesões cutâneas. Estima-se que 600.000 a 1 milhão de novos casos ocorram anualmente em todo o mundo, porém há subnotificação da doença (WHO, 2023)

O tratamento da leishmaniose é complexo e depende de múltiplos fatores, incluindo a forma clínica da doença, a presença de comorbidades, a espécie do parasita envolvida e a localização geográfica do paciente. Embora seja uma doença tratável e curável, a eficácia da terapia está diretamente relacionada à competência

do sistema imunológico, pois os medicamentos disponíveis não erradicam completamente o parasita. Portanto, pacientes imunocomprometidos têm um risco aumentado de recaídas e complicações (Madusanka; Silva; Karunaweera, 2022) Outro problema relacionado ao tratamento da leishmaniose é elevado à toxicidade dos fármacos, isto é, ao antimoniato de meglumina que possui elevado risco de cardiotoxicidade (Bento et al., 2013), a anfotericina B pode ocasionar nefrotoxicidade (Rahal et al., 2014). Outros medicamentos também são utilizados como a paromomicina que pode causar ototoxicidade, toxicidade renal e hepatotoxicidade (Pokharel; Ghimire; Lamichhane, 2021) e Miltefosina que pode causar problemas gastrointestinais, incluindo anorexia, náusea, vômito e diarreia (Silva et al., 2024).

Torna-se importante a busca de novos fármacos antileishmania e a *Carapa guianensis* pode ser uma fonte promissora de moléculas bioativas. O óleo de *C. guianensis* apresentou atividade antileishmania, sendo sua atividade relacionada aos limonoides, mas os ácidos graxos são os principais constituintes deste óleo. Estudo realizou a predição e o possível mecanismo de ação da atividade antileishmania de Gedunina, 6α-acetoxigedunina, Metil angosenlato, 7-desacetoxi-7-oxogedunina, Andirobina, 6-hidroxi-angolensato metílico, 17β-hidroxiazadiradiona, 1,2-diidro-3β-hidroxi-7-desacetoxi-7oxogedunina, xilocensina k, 11beta-hidroxigedunina, 6α,11-11β-diacetoxigedunina, Ácido oleico, Ácido palmítico, Ácido esteárico, Ácido araquídico, Ácido mirístico, Ácido palmitoleico, Ácido linoleico, Ácido linolênico e Ácido beênico. Apesar de várias moléculas violaram a regra de Lipinski, todas as moléculas foram bem absorvidas no intestino e inibiram o CYP. Todos os compostos mostraram toxicidade em algum modelo, com ácidos graxos sendo mutagênicos e carcinogênicos, e limonoides não sendo mutagênicos e carcinogênicos, pelo menos para ratos. Em modelos *in vivo*, os ácidos graxos foram menos tóxicos. Dockings moleculares foram realizados em esteroides COX-2 (15 e 16) e fator 1 alfa induzível por hipóxia para limonoides (3,6), atuando de forma sinérgica onde os Limonoides 3 e 6 parecem ser promissores como agentes leishmanicidas, e ácidos graxos são promissores como cicatrizantes de feridas (De Barros et al., 2024)

O presente estudo avaliou a atividade antileishmania do óleo de *C. guianensis,* de extrato e frações em isolados de *L. amazonensis* de paciente com a forma difusa e localizada. Estas amostras foram caracterizadas em termos químicos e as moléculas do óleo essencial foram submetidas aos estudos *in silico* para predição de

diferentes parâmetros físico-químicos, farmacocinética, toxidade e toxidade aguda e a docagem molecular.

2 Metodos

2.1 Estudos químicos do extrato de *C. guianensis*

As folhas foram coletadas nas coordenadas: 1.474822, -48.455531 na Universidade Federal do Pará, em Belém do Pará, sua exsicata foi depositada IAN 201.467 e registrado no SISGEN A94E918. O EECGf foi obtido por maceração e submetido ao fracionamento sob refluxo obtendo as frações hexano (FHCGf), diclorometno (FDCGf), acetato de etila (FEACGf) e metanólica (FMCGf). As amostras foram cacaterizadas por cromatografia em camada delgada (CCD) Adaptado de WAGNER, 1984.) cromatografia de alta eficiência (HPLC-DAD) e ressonância magnética nuclear (H1-RMN).

O extrato etanólico (EE) e frações das folhas e foram submetidos à cromatografia líquida de alta eficiência (CLAE) (Alliance e2695 chromatograph (WatersR), sendo solubilizado 1 mg da amostra em 1 mL de metanol e transferiu-se para o cartucho SPE C18. Posteriormente filtrou-se a extração com auxílio de filtro de seringa 0,45 µm (hidrofílico), e transferiu-se para frasco de CLAE (vial) em concentração de 1mg/mL (1:1). O gradiente exploratório linear empregado foi H_2O/ACN 95:5 (tempo= 0 minutos) e 60 minutos (0:100 H20/ACN), com uma vazão de 1,0 mL/min. O intervalo de detecção no ultravioleta-visível variou de 210 a 600 nm.

O EE e frações das folhas foram analisadas em ressonância magnética nuclear (RMN) de hidrogênio ^1H (Bruker Ascend 400 spectrometer (Bruker, Bremen, Germany), sendo o EE (20 mg), e frações metanolicas e acetato (20 mg) solubilizados em metanol deuterado (500 µL). As frações hexano (FH) (20 mg) e diclorometano (FD) (20 mg) solubilizadas em clorofórmio (500 µL). O TMS foi utilizado como padrão interno para a calibração dos espectros. As constantes de acoplamento (J) foram medidas em Hertz, e os deslocamentos químicos foram reportados na escala delta (δ). operado nos modos de ionização por electrospray tanto negativo quanto positivo. Para processar os espectros utilizou-se o programa TopSpin, versão 4.5.

2.2- Obtenção dos óleos e caracterização química

As sementes foram coletadas nas coordenadas: 1.474822, -48.455531 e registrado no SISGEN A94E918. As sementes foram submetidas em processo que consistiu em cozinhar as amêndoas até ficarem macias, o que levou 60 minutos. Em seguida, elas foram secas e passaram por um período de fermentação que durou 30 dias. Após a fermentação, as amêndoas foram cozidas e amassadas manualmente para extração. O material obtido foi deixado em repouso para que o óleo se separe e surgisse naturalmente. Esse óleo foi decantado e acondicionado em frascos de vidro escuro. Todo o processo foi realizado à sombra, protegido da luz direta.

Posteriormente, cerca de 100g do óleo foi submetido a hidrodestilação em aparelho de clevenger modificado durante 3h, (Maia; Andrade, 2009). A composição química do óleo essencial foi analisada em CG-EM (Modelo QP2010 ultra (Shimadzu, Tóquio, Japão) equipado com uma coluna capilar de sílica fundida Rtx-5MS (30m × 0,25mm; espessura de filme de 0,25 μm) (Restek, Bellefonte, EUA). Como gás de arraste, usou-se o Hélio com fluxo de 1 mL/min a 57,5KPa. No CG-EM foi injetado 1 μL de solução de óleo essencial em hexano (na proporção de 5 μL de óleo e 500 μL de hexano), a injeção foi do tipo Split (proporção de divisão 1:20).

A temperatura do injetor e da linha de transferência foi de 250°C; a programação da temperatura do forno foi de 60 – 240°C (3°C/min), seguida por uma isoterma de 10 minutos. As moléculas foram ionizadas por impacto eletrônico com energia de ionização de 70 eV em que a temperatura da fonte de íons foi de 200 ºC. A obtenção dos espectros de massas foi por varredura automática a cada 0,3 s, com fragmentos de massa entre 35 - 400 m/z.

Para a análise quantitativa, um Cromatógrafo gasoso acoplado a um detector de ionização de chama (CG-DIC) também foi utilizado. Os dados quantitativos referentes aos constituintes voláteis foram obtidos utilizando um GC Série 2010, operado em condições similares ao sistema CG-EM. As quantidades relativas de componentes individuais foram calculadas por normalização de área de pico usando o CG-DIC.

Os compostos foram identificados com base na interpretação de seus espectros de massas obtidos e associados aos tempos e índices de retenção presentes nas bibliotecas Adams, FFNSC 2 e NIST (Adams, 2007; Mondello, 2011; Raposo et al., 2018).

2.3 Atividade antipromastigota

Neste estudo, foram utilizados duas cepas de *Leishmania (Leishmania.) amazonensis* (MHOM/BR/2012/M29719/Tomé-Açú/Pará), isolada de caso clínico de leishmaniose cutânea anérgica difusa (LCAD) e *Leishmania (Leishmania.) amazonensis (*MHOM/BR/2012/M29125/Magalhães Barata-Pa.), Isolada de caso clínico de Leishmaniose tegumentar americana, forma clínica: Leishmaniose cutânea localizada (LCL), ambas mantidas no mantida no criobanco (N2) do Laboratório de Leishmanioses Prof. Ralph Lainson, do Instituto Evandro Chagas, Secretaria de Vigilância em Saúde e Ambiente do Ministério da Saúde.

As formas promastigotas de *L.* (L.) *amazonensis* obtidas durante a fase logarítmica de crescimento, foram reunidas por centrifugação em meio RPMI completo 3500 rpm por 10 minutos. O precipitado foi resuspendido em meio RPMI completo, as promastigotas foram quantificadas em câmara de Neubauer e ajustadas para uma concentração correspondente a 4 x 10^6 parasitas/100µL. Esta suspensão foi distribuída em placas com culturas de células com fundo chato previamente dosificadas contendo o extrato vegetal e frações hexanica, dicorometano, acetato e metanol.

Foram preparadas duas placas, o extrato e frações diluídos em metanol, o que permitiu a pré-dosificação da placa. A placa dos óleos resina e essencial diluída em DMSO, o que não permitiu a pré-dosificação da placa. A pré-dosificação da placa do extrato e frações foi realizada da seguinte forma: 1 mg da amostra foi solubilizada em 500µg/mL em metanol, sendo realizada diluições sucessivas para obter-se as seguintes concentrações finais: 200µg/mL, 100 µg/mL, 50 µg/mL, 25 µg/mL, 12,5 µg/mL, 6,25 µg/mL e 3,125 µg/mL. Após as diluições, 10µL de cada solução foram transferidos para cada poço em fluxo laminar e a placa ficou aberta até completa evaporação do solvente.

No caso dos óleos, óleo resina e óleo essêncial, as amostras foram solubilizados em DMSO 1%, sendo realizada diluições sucessivas para obter-se as seguintes concentrações finais: 200µg/mL, 100 µg/mL, 50 µg/mL, 25 µg/mL, 12,5 µg/mL, 6,25 µg/mL e 3,125 µg/mL. Em seguida, as placas foram incubadas a 26°C por 24 horas. O controle negativo consistiu de uma suspensão do parasita e meio de cultura, controle do solvente para as placas pré-dosificadas (metanol evaporado + suspensão do parasito + meio), controle do solvente para o óleo resina e essencial (DMSO + suspensão do parasito + meio) e o controle positivo consistiu de uma

suspensão de promastigotas adicionada de Anfotericina B (25,12,5, 6,25, 3,125, 1,5625, 0,78125 e 0,3906 p/mL). Após o período de incubação de promastigotas com as amostras e fármacos foram adicionados 10 µL de MTT (Brometo de 3- (4,5-dimetiltiazol-2- yl)-2,5-difeniltetrazolium) (5 mg/mL) em cada poço.

A placa for recoberta com papel alumínio, sucedendo-se nova incubação por 4 horas em estufa a 26°C para que o MTT seja metabolizado e consequentemente fossem formados os cristais de formazan (Veiga et al., 2017). Depois de 4 horas, foi adicionado 10 µL de dimetilsufóxido (DMSO), para solubilizar os cristais de formazan gerados, através da agitação manual até completa solubilização dos cristais e novamente foi realizado a incubação por 1h. Posteriormente, realizou-se leitura da densidade óptica (D.O) das amostras em leitor de placas de ELISA sob comprimento de onda de 490 nm. A viabilidade das formas promastigotas foi avaliada com base no metabolismo do MTT, sendo a mesma proporcional ao valor da absorbância gerada. A porcentagem de células (promastigotas) pela fórmula, adaptada de (Ngure et al., 2009)

A Concentração inibitória 50% (CI50) foi determinada por regressão linear (Graph Pad Prism versão 8.0). A análise estatística foi realizada pelo teste t de Student (Biostat 5.0). Os resultados foram classificados de acordo com os seguintes critérios: IC50 $\leq$ 100 µg/mL: amostra ativa, IC50 entre 101 e 200 µg/mL - amostra moderadamente ativa e IC50 $\geq$ 200 µg/mL - amostra inativa (Veiga et al., 2017).

2.4- Estudos *in silico*

Foram realizados estudos *in silico* de moléculas que obtiveram pelo menos atividade moderada ou na literatura para atividade leishmanicida. Além disso, no caso do óleo essencial em que foram obtidas as moléculas presentes, foram selecionados compostos com rendimento igual ou maior a 1% e que não foram publicados em artigo publicado pelo autor, sendo selecionadas: 2-Pentilfurano, Valerato de propila, Pentanoato de butila, n-nonanal, 2E-nonen-1-al, n-decanal, 2E-decenal, 2E,4E-decadienal, Undec-2E-enal, y-Dodecalactona e cis-6-Octadecenoato de metila

As moléculas do óleo essencial foram desenhadas utilizando o programa online Marvin (2023) (https://marvinjs-demo.chemaxon.com/latest/demo.html), e para a determinação das propriedades físico-químicas, foi utilizado o servidor online HomeADMElab (https://admet.scbdd.com) (Dong, 2024). A Regra dos Cinco de Lipinski e Veber foi considerada (Lipinski, 2004; Veber et al., 2002). Para as previsões

farmacocinéticas e de toxicidade, foi utilizado o programa PreADMET (versão 2.0, Copyright © 2005–2017), que considera as propriedades farmacocinéticas (A–Absorção; D–Distribuição; M–Metabolismo/Biotransformação; E–Excreção) e a avaliação de parâmetros de toxicidade (T–Toxicidade; Preadmet, 2020).

Para a avaliação da toxicidade em organismos marinhos, foram utilizados os seguintes critérios: para toxicidade em algas (Costa et al., 2008); para Daphnia sp (Guilhermino et al., 2000); para Medaka (Zucker, 1985; e para Minnow (Costa et al., 2008). O risco de mutagenicidade foi avaliado pelo teste de ames com as seguintes cepas de *Salmonella Typhimurium*: TA100-10RLI e TA100-NA com mutação em *His* G46e plasmídeo pKM101 sem S9; TA1535-10RLI e TA1535-NA com mutação em *His* G46 (Ames; 1975). O potencial carcinogênico dos compostos foi avaliado em ratos e camundongos e classificado como (+) carcinogênico e (−) não carcinogênico. Para prever a toxicidade oral aguda (dose letal 50% - LD50), foi utilizado o software online PROTOX III (Drwal et al., 2014) considerando a classificação de I a VI, também foram avaliados eventos adversos que podem ocorrer com o uso da molécula.

2.5. Docagem molecular e Refinamento da energia

O docking molecular seguido do refinamento da energia pelo método MM/GBSA foi realizado usando a plataforma ChemFlow (Barreto, et al., 2023), que integra três módulos principais: DockFlow, LigFlow e ScoreFlow.

A estrutura dos compostos 4, 6, 7 e 9 foram baixados do banco de dados PubChem no formato 3D e submetidos a uma optimização estrutural. A estrutura cristalográfica da cathepsin D (PDB ID: 6QBH) foi obtida do Protein Data Bank (PDB), contendo o inibidor co-cristalizado S43. A preparação da proteína incluiu a remoção de moléculas de água, adição de hidrogênios e ajuste dos estados de protonação dos resíduos no pH fisiológico no servidor PDB2PQR (Dolinsky et al., 2007)

No módulo DockFlow, o docking molecular foi realizado com o software PLANTS, a pontuação inicial de encaixe foi realizada com o ChemPLP que combina o PLP (Piecewise Linear Potential) com o Chemscore do GOLD (Korb; Stutzle; Exner, 2009). Para validação do protocolo, um redocking do inibidor S43 foi conduzido, avaliando a sobreposição entre a pose predita e a co-cristalizada. O inibidor re-encaixado foi então sobreposto ao co-cristalizado de referência usando PyMOL 2.3 e

o desvio quadrático médio (RMSD) foi calculado. O centro do sítio ativo foi definido com base nas coordenadas do inibidor (x = 8.778, y = 16.692, z = 6.870), e uma esfera de 15 Å delimitou a cavidade de ligação, garantindo acessibilidade para os ligantes.

No módulo LigFlow, os ligantes foram parametrizados utilizando o ANTECHAMBER, as cargas atômicas foram geradas pelo método AM1-BCC e os arquivos de parâmetros baseados no campo de força GAFF2.

No módulo ScoreFlow, as energias foram refinadas pelo método MM/GBSA (Molecular Mechanics/Generalized Born Surface Area), implementado no MMPBSA.py do AmberTools23. Essa abordagem permite uma estimativa mais precisa das energias livres de ligação, considerando interações moleculares detalhadas, reduzindo falsos positivos frequentemente associados às funções de pontuação padrão dos programas de docking.

3 Resultados

3.1 Análise química do extrato, frações e óleo de *C. guianensis*

O EECGf (rendimento de 13%) foi submetido a reextração sob refluxo obtendo-se as frações hexano (FHCGf, rendimento= 3,6%), diclorometano (FDCGf, rendimento= 2,6%), acetato de etila (FEACGf; rendimento= 2,8%) e metanolica (FMCGf, rendimento= 7,4%). Todas as amostras foram sumetidas a análises em CCD, sendo dectados triterpenos e esteroides (EECGf, FHCGf) e flavonoides (EECGf, FDCGf, FEACGf e FMCGf).

Análises e HPLC- DAD sugerem a presença de flavonoides no EECGf (TR entre 25 a 30min.; Fig.1.1). As frações FDCGf, FEACGf e FMCGf apresentaram prefis cromatograficos semelhantes (Fig. 1.3.; 1.4.; 1.5.).

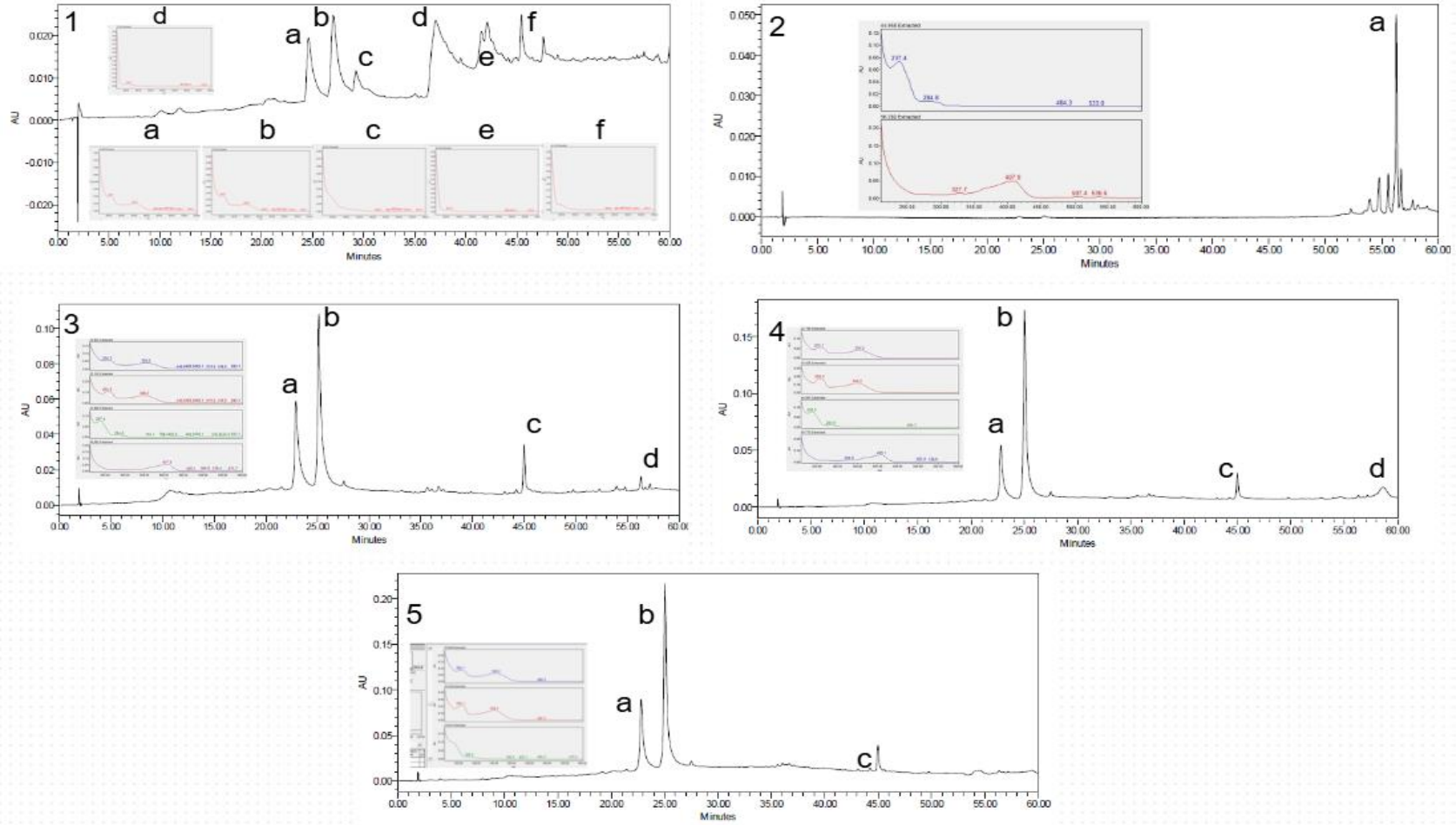

Figura 1. Análises cromatográficas e espectros em ultravioleta de *C. guianensis*.

Legenda: 1- Extrato etanólico obtido das folhas de *C. guianensis*; 2- Fração hexano de *C. guianensis*; 3- Fração diclorometano de *C. guianensis* 4- fração acetato de etila de *C. guianensis;* 5- Fração metanólica de *C. guianensis.* Condições Cromatográficas: t=0 min. H_2O/ACN 95:5; t= 60 min. 0:100 H_20/ACN, fluxo= 1,0 mL/min., temperatura=40°C, λ=210 a 600 nm

A última análise realizada nestas amostras foram H1-RMN, que sugerem a presença de terpenos no extrato etanólico (EECGf), fração hexânica (FHCGf), fração diclorometano (FDCGf), fração acetato de etila (FAECGf) e fração metanólica (FMCGf) (Material Suplementar) (Tabela 1).

Tabela 1- Análise pelo grupo funcional (CH2) em H1 RMN de extrato e frações.

Grupo funcional	EECGf - Deslocamento (ppm)	FHCGf Deslocamento (ppm)	FDCGf- Deslocamento (ppm)	FACGf- Deslocamento (ppm)	FMCGf Deslocamento (ppm)
metileno (CH_2)	-	0.68 e 0.81, 0.98 e 1.68, 1.00 e 1.98, 1.60 e 2.04, 2.35 e 2.76.	0.86 e 0.90, 1.25 e 1.64.	1.10 e 1.92, 1.11 e 1.23, 2.17 e 2.63.	1.10 e 1.92, 1.20 e 1.27, 2.17 e 2.61.

Fonte: Adaptado de Popova et al., 2009; Sarria et al., 2014; Amorim et al., 2020; Álvarez et al., 2024.

Na análise do óleo essencial por CG-MS detectou-se a presença de diferentes classes químicas, tais como ácidos graxos, ésteres, aldeídos, cetonas, entre outras. Ainda foram detectados 54 metabolitos diferentes, sendo que a maioria das moléculas estava em concentrações inferiores a 1%. Os constituintes em concentrações superiores a 1% foram: 2 ácidos graxos (Ácido hexadecanoico e ácido oleico); 5 aldeídos (n-Nonanal; 2E-Nonen-1-al; n-Decanal; 2E-decenal;2E-4E- Decadienal; Undec-2E-enal); 6 esteres (Valerato de propila; Pentanoato de butila; Hexadecanoato de metila; Hexadecanoato de etila; Palmitato de propila; cis-6-Octadecenoato de metila); 1 lactona (γ-Dodecalactona); 1 furano (2- Pentilfurano) (Tabela 2).

Tabela 2 - Resultado da cromatografia gasosa do óleo essencial de andiroba.

IRC	IRL	CONSTITUINTE	TEOR	CLASSIFICAÇÃO
799	801ª	n-Hexanal	0,68	Aldeído
861	863ª	n-Hexanol	0,03	Álcool
887	889ª	2-Heptanona	0,05	Cetona
895	898ª	Butanoato de Propila	0,04	Ester
899	899b	Valerato de etila	0,43	Ester
900	901ª	Heptanal	0,29	Aldeído
951	947ª	2E-Heptenal	0,4	Aldeído
959	958ª	6-metil-Heptan-2-ol	0,01	Outros
964	959ª	n-Heptanol	0,23	Álcool
972	967ª	Ácido hexanoico	0,16	Ácido graxo
975	978b	Álcool vinil-amílico	0,22	Álcool
990	991b	2-Pentilfurano	2,12	Furano
995	996b	Valerato de propila	2,05	Ester
998	997ª	Hexanoato de etila	0,24	Ester
1001	998ª	n-Octanal	2,1	Aldeído
1005	1005ª	Propanoato de pentila	0,09	Ester
1025	1030b	2-etil-Hexanol	0,04	Álcool
1035	1036b	Oct-3-en-2-ona	0,18	Cetona

IRC	IRL	CONSTITUINTE	TEOR	CLASSIFICAÇÃO
1049	1042ª	γ-Hexalactona	0,04	**Lactona**
1054	1053b	2E-Octen-1-al	0,59	Aldeído
1067	1063ª	n-Octanol	0,34	Álcool
1089	1090b	Metil heptil cetona	0,26	Cetona
1091	1092ª	Pentanoato de butila	1,3	Ester
1099	1197ª	2-Nonanol	0,61	Álcool
1102	1100ª	n-Nonanal	6,67	Aldeído
1156	1157aa	2E-Nonen-1-al	1,36	Aldeido
1175	1174ª	Terpinen-4-ol	0,06	Monoterpeno
1196	1196ª	Octanoato de etila	0,28	Ester
1203	1201ª	n-Decanal	3,09	Aldeído
1211	1210ª	Nona-2E,4E-dienal	0,28	Aldeido
1259	1260ª	2E-Decenal	2,73	Aldeído
1298	1300ª	n-Tridecano	0,29	Alcano
1313	1315ª	2E,4E-Decadienal	2,81	Aldeído
1361	1357b	Undec-2E-enal	1,77	Aldeido
1375	1375b	α-Copaeno	0,4	Sesquiterpeno
1378	1380ª	4E-Decenoato de etila	0,21	Ester
1398	1406b	α-Gurjuneno	0,63	Sesquiterpeno
1430	1430ª	β-Copaeno	0,59	Sesquiterpeno
1483	1487ª	Aristoloqueno	0,51	Sesquiterpeno
1493	1495ª	2-Tridecanona	0,19	Cetona
1498	1500ª	n-Pentadecano	0,71	Alcano
1562	1561ª	E-Nerolidol	0,16	Sesquiterpeno
1668	1670ª	epi-β-Bisabolol	0,52	Sesquiterpeno
1675	1676ª	γ-Dodecalactona	1,11	Lactona
1924	1925b	Hexadecanoato de metila	3,86	Ester
1971	1977b	Ácido hexadecanoico	23,61	Ácido graxo
1993	1992ª	Hexadecanoato de etila	6,25	Ester
2089	2091C	Palmitato de propila	2,44	Ester
2091	2093b	Linoleato de metila	0,55	Ester
2098	2104C	cis-6-Octadecenoato de metila	3,13	Ester
2125	2124ª	Octadecanoato de metila	0,36	Ester
2166	2168C	Ácido oleico	4,34	Ácido graxo
2192	2198b	Estearato de etila	0,47	Ester

Classificação dos constituintes:
(continuação)

CLASSIFICAÇÃO	TEOR (%)
Aldeidos	22,87
Alcano	1
Alcool	1,47
Acidos graxos	28,11
Lactona	1,15
Ester	22,35
Monoterpenos	0,06
Hidrocarbonetos	2,13
Sesquiterpenos	0,68
Outros	2,76
Total	81,88%

3.2. Atividade antileishmania

O fracionamento do EECGf não contribui para a atividade antipromastigota M29125, pois as CI_{50} das frações FHCGf ($p>0,05$), FDCGf ($p>0,05$) e FMCGf ($p>0,05$) foram superiores a do EECGf. Somente a FEACGF teve uma CI_{50} inferior ao EECGF, mas sem diferença significativa ($p>0,05$; Tabela 3). De forma similiar ao observado para as promastigota M29125, o fracionamento EECGf não contribuiu para a atividade contra promastigota de M29719, tendo sido observado uma elevação significativa da CI_{50} FHCGf ($p<0,05$), FDCGf ($p<0,05$) e menores diferenças foram observadas para as frações FEACGf ($p<0,05$) e FMCGf ($p<0,05$) (Tabela 3).

Quando se compara as atividades antipromastigota entre os isolados M29125 e M29719, maiores CI_{50} foram observadas para o isolado M29719 em todas as amostras testadas, exceto FDCGf (Tabela 3). Em termos estatísticos, estas diferenças não são significativas entre as cepas ($p> 0,05$).

O ORCG parece ser mais promissor que o OECG ($p<0,05$), pois as CI50 foram menores nos dois isolados de Leishmania. Apesar de ser menos ativo, o OECG pode conter moléculas com potencial antiparasitário (Tabela 3).

Tabela 3- Atividade Antipromastigota de partes da *Carapa guianensis*.

	CI_{50} µg/mL + DP		
Amostras	**M29125**	**M29719**	**P**
EECGf	175±0,13	180±0,10	P>0,05
FHCGf	230±0,18	250±0,12	P<0,05
FDCGf	232±0,06	220±0,05	P<0,05
FEACGf	170±0,10	190±0,09	P>0,05
FMCGf	180±0,08	185±0,11	P>0,05
ORCG	89±0,15	95±0,22	P<0,05
OECG	140±0,06	137±0,18	P>0,05
Anfotericina B	0,1788±0,0005	0,1655±0,00045	P>0,05

Legenda: CI_{50} – Concentração inibitória 50%; M29719- isolada de leishmaniose anergica difusa; M29125- isolada de leishmaniose tegumentar localizada; Extrato Etanólico (ET); Fração de hexano (FH); Fração diclorometano (FD); Fração acetato de Etila (FEA); Fração metanol (FMe); Óleo Resina (OR); Óleo essencial (OE). Inativo = Inativo; A = Ativo; MA = Moderadamente Ativo.

3.3 Avaliação *in silico*

Como o ORCG mostrou-se mais promissor contra promastigotas de *L. amazonensis* foi realizado um estudo *in silico* e publicado (De Barros et al., 2024b). Algumas moléculas majoritárias presentes OECG estão presentes no ORCG, tendo sido excluídas do presente estudo (Ácido hexadecanoico, ácido oleico, Hexadecanoato de etila e Palmitato de propila). Desta forma, foram incluídas as seguintes moléculas: 1- 2-Pentilfurano, 2 – Valerato de propila, 3 – Pentanoato de butila, 4 – n-nonanal, 5 – 2E-nonen-1-al, 6 – n-decanal, 7 – 2E-Decenal, 8—2E,4E-

decadienal, 9 – Undec-2E-enal, 10- y-Dodecalactona, 11- cis-6-Octadecenoato de metila (Figura 2):

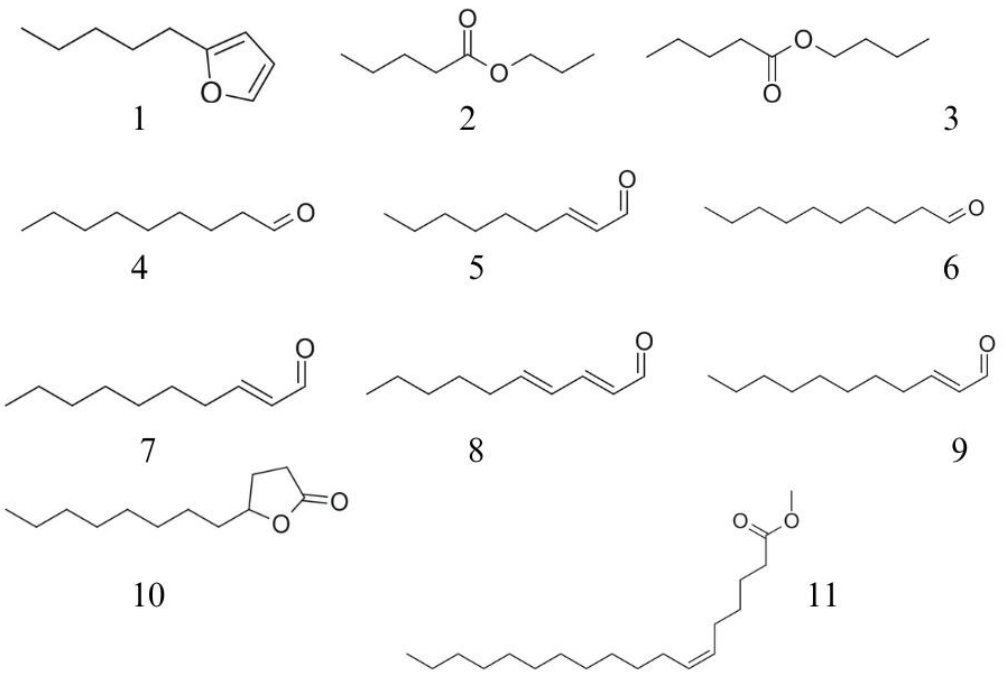

Figura 2- Moléculas selecionadas para estudo *in silico*. 1- 2-Pentilfurano, 2 – Valerato de propila, 3 – Pentanoato de butila, 4 – n-nonanal, 5 – 2E-nonen-1-al, 6 – n-decanal, 7 – 2E-Decenal, 8—2E,4E-decadienal, 9 – Undec-2E-enal, 10- y-Dodecalactona, 11- cis-6-Octadecenoato de metila.

Predições das propriedades físico-químicas sugerem que todas as moléculas seguem os critérios estabelecidos por Lipinski e Veber. Também, a superfície polar foi inferior a 140 Å (Tabela 4).

Tabela 4- Predição das propriedades físico-químicas,

Moleculas	MM	LogP	nHBA	Nhbd	TPSA
1	138,100	4,092	1	0	13,14
2	144,120	2,656	2	0	26,30
3	158,130	3,058	2	0	26,30
4	142,140	3,178	1	0	17,07
5	140,120	3,312	1	0	17,07
6	156,150	3,609	1	0	17,07
7	154,140	3,744	1	0	17,07
8	152,120	3,091	1	0	17,07
9	168,150	4,209	1	0	17,07
10	198,160	3,483	2	0	26,30
11	296,270	7,687	2	0	26,30

Regra de Lipinski e Veber: LogP - oeficiente de partição óleo-água menor ou igual a 5≤ 5; TPSA: área de superfície polar topológica (TPSA) menor ou igual a 140 Å≤140 Å; nHBA: aceitadores de ligação de hidrogênio≤ 10; nHBD doadores de ligação de hidrogênio≤ 5; MM – massa molecular ≤ 500D (Lipinski, 2004; Veber, 2002). 1- 2-Pentilfurano, 2 – Valerato de propila, 3 – Pentanoato de butila, 4 – n-nonanal,

5 – 2E-nonen-1-al, 6 – n-decanal, 7 – 2E-Decenal, 8—2E,4E-decadienal, 9 – Undec-2E-enal, 10- y-Dodecalactona, 11- cis-6-Octadecenoato de metila.

Todas as moléculas apresentam algumas características farmacocinéticas similares, isto é, possuem elevada absorção trato gastrointestinal, elevada ligação a PP e potencial inibitória de 3 CYP (Tabela 5).

Tabela 5- Predição das propriedades farmacocinéticas

	Absorção		Distribuição			Metabolismo	
Moleculas	**MDCK**	**Caco 2**	**HIA**	**PP**	**BBB**	**CYP Inibition**	**CYP**
1	H	M	H	H	M	2C9, 2C19, 3A4	W 2D6
2	M	M	H	H	M	2C9, 2C19, 3A4	W 2D6
3	M	M	H	H	M	2C9, 2C19, 3A4	3A4
4	H	M	H	H	H	2C9, 2C19, 3A4	W 3A4
5	H	M	H	H	H	2C9, 2C19, 3A4	-
6	H	M	H	H	H	2C9, 2C19, 3A4	-
7	H	M	H	H	H	2C9, 2C19, 3A4	-
8	H	M	H	H	H	2C9, 2C19, 3A4	-
9	H	M	H	H	H	2C9, 2C19, 3A4	-
10	M	M	H	H	H	2C9, 2C19, 3A4	W 2D6, W3A4
11	M	M	H	H	H	2C9, 2C19, 3A4	-

BBB: barreira hematoencefálica; CYP: citocromo P450; HIA: absorção intestinal humana; W: fraco; H: alto; L: baixo; M: médio; 1- 2-Pentilfurano, 2 – Valerato de propila, 3 – Pentanoato de butila, 4 – n-nonanal, 5 – 2E-nonen-1-al, 6 – n-decanal, 7 – 2E-Decenal, 8—2E,4E-decadienal, 9 – Undec-2E-enal, 10- γ-Dodecalactona, 11- cis-6-Octadecenoato de metila.

Uma variação significatica significativo no potencial mutagênico e carcinogênico, isto é, as moléculas 8, 9, 10 e 11 parecem não ser mutagênicas. Enquanto as moléculas 4, 5, 6. 7 não foram carcinogênicas (Tabela 6).

Tabela 6- Predição de toxicidade.

Moleculas	**Alga**	**Daphnia**	**Fish**		**Ames (TA)**	**Carcino Rato/Cam ***
			Medaka	**Minnow**		
1	T	T	VT	VT	1535_10RL; 1535_NA; 100_NA	P/P
2	T	T	VT	VT	1535_NA; 100_NA	N/P
3	T	T	VT	VT	1535_NA; 100_NA	N/P
4	T	T	VT	VT	1535_NA	N/N
5	T	T	VT	VT	1535_NA; TA100_NA	N/N
6	T	T	VT	VT	N	N/N
7	T	T	VT	VT	100_NA	N/N
8	T	T	VT	VT	N	P/P
9	T	T	VT	VT	N	N/P
10	T	T	VT	VT	N	P/P
11	T	T	VT	VT	N	P/P

T: tóxico; NT: não tóxico; N: negativo; P: positivo. Parâmetros: algas — <1 mg/L tóxico; >1 mg/L não tóxico; teste com dáfnia: < 0,22 µg/mL tóxico; > 0,22 µg/mL — não tóxico; teste em peixes medaka e minnow: < 1 mg/L — muito tóxico; 1–10 mg/L — tóxico; 10–100 mg/L — prejudicial e > 100 mg/L — extremamente tóxico; carcinogenicidade em rato/camundongo * = carcinogenicidade em rato/camundongo. T — Tóxico, NT — Não tóxico, VT — muito tóxico, N — negativo, P — positivo. 1- 2-Pentilfurano, 2 – Valerato de propila, 3 – Pentanoato de butila, 4 – n-nonanal, 5 – 2E-nonen-1-al, 6 – n-

decanal, 7 – 2E-Decenal, 8—2E,4E-decadienal, 9 – Undec-2E-enal, 10- γ-Dodecalactona, 11- cis-6-Octadecenoato de metila.

As moléculas com menor toxicidade oral (2, 3) apresentaram elevado potencial mutagênico e a molécula 1 foi a com maior potencial toxico. As demais moléculas apresentaram mesma classe de toxicidade (Tabela 7).

Tabela 7- Prediction de toxicidade oral

Moleculas	LD50 (mg/kg)	Classe
1	1200	IV
2	35420	VI
3	35420	VI
4	5000	V
5	5000	V
6	5000	V
7	5000	V
8	5000	V
9	5000	V
10	4400	V
11	3000	V

LD50 — dose letal 50%. I — Irritante, T — tumorigênico, M — mutagenicidade. Categoria I: 1 < LD50 ≤ 5 mg/kg — extremamente tóxico; categoria II: 5 < LD50 ≤ 50 mg/kg — altamente tóxico; categoria III: 50 < LD50 ≤ 300 mg/kg — moderadamente tóxico; categoria IV: 300 < LD50 ≤ 2000 mg/kg — baixa toxicidade; categoria V: 2000 < LD50 ≤ 5000 — improvável de causar dano agudo; categoria VI: DL50 > 5000 — nenhum dano. 1- 2-Pentilfurano, 2 – Valerato de propila, 3 – Pentanoato de butila, 4 – n-nonanal, 5 – 2E-nonen-1-al, 6 – n-decanal, 7 – 2E-Decenal, 8—2E,4E-decadienal, 9 – Undec-2E-enal, 10- γ-Dodecalactona, 11- cis-6-Octadecenoato de metila.

Baseados nos resultados da toxicidade foram selecionados as moléculas 4, 6, 7 e 9 para a predição dos possíveis alvos moleculares, sendo todas as moléculas pertencentes a classe dos aldeídos. Todas as moléculas ligaram com elevada acurácia na Catepsina D (Tabela 8). Sendo este alvo selecionado para a docagem molecular.

Tabela 8 - Avaliação de alvos moleculares

Moleculas	Probabilidade	Acurácia	Nome do alvo	PDB
4	93,42%	98,95%	Catepsina D	4OD9/6QBH
6	93,42%	98,95%	Catepsina D	4OD9/6QBH
7	92,24%	98,95%	Catepsina D	4OD9/6QBH
9	92,24%	98,95%	Catepsina D	4OD9/6QBH

PDB: Protein Data Bank; 4 – n-nonanal, 6 – n-decanal, 7 – 2E-Decenal, 9 – Undec-2E-enal,

4.3 Docagem molecular e Cálculo de Energia Livre de Ligação

A validação do protocolo de docking molecular foi realizada por meio do redocking do inibidor co-cristalizado S43 na estrutura cristalográfica da catepsina D (PDB ID: 4OD9/6QBH). O desvio quadrático médio (RMSD) entre a estrutura reanalisada e a co-cristalizada foi de 0,033 Å (Figura 3).

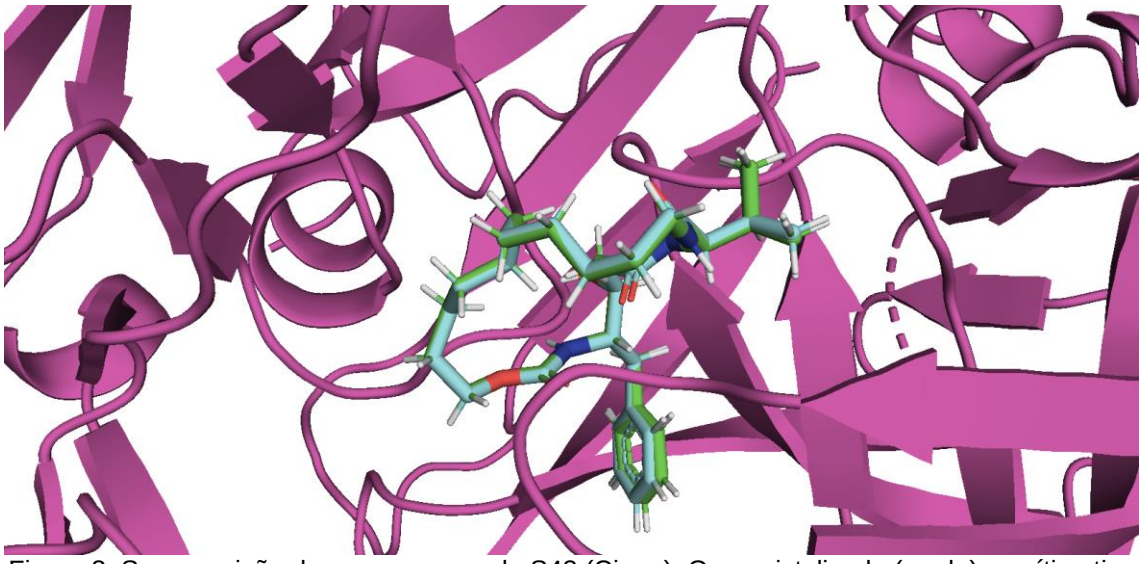

Figura 3: Superposição da reancoragem do S43 (Ciano). O co-cristalizado (verde) no sítio ativo usando PyMOL (RMSD = 0,033 Å).

As moléculas 4, 6, 7 e 9 foram submetidas a simulações de docking molecular contra a Catepsina D. As funções de pontuação e as energias livres destas moléculas sugerem que a ligações entre as moléculas e a catepsina D são favoráveis. Entretanto, a molécula 9 exibiu um melhor desempenho, sugerindo maior afinidade pelo sítio ativo da proteína em comparação aos demais compostos testados. O inibidor S43, utilizado como controle, apresentou a menor energia de docking e a menor energia livre de ligação (Tabela 9).

Tabela 9- Energias de ligação das moléculas presentes no óleo essencial de *C. guianensis*

Moleculas	**ChemPLP**	**ΔG**
4	-62.5549	-22.6975
6	-59.4354	-22.9030
7	-64.7954	-25.6680
9	-70.7703	-29.5836
S43	-127.043	-59.3822

Legenda: **ΔG**: Kcal/mol. 4 – n-nonanal, 6 – n-decanal, 7 – 2E-Decenal, 9 – Undec-2E-enal.

Todas as moleculas, a se ligar a Catepsina D não apresentaram ligações desfavoráveis, porém observam-se algumas diferenças entre as ligações destes aldeídos a proteína. Quando se compara a molecula 4 (figura 4B) e a molécula 6 (Figura 4C) As moléculas 7 e 9, que possuem 10 carbonos e 11 carbonos em sua estrutura, a molécula 9 (figura 4E) parece ser mais favoraravel que a molécula 7 (figura 4D), observa-se que o aumento do número de carbonos favorece a ligação. Em termos de ligação, a molécula 9 apresentou um perfil similar das demais moléculas, todos as moléculas estabeleceram ligações de hidrogênio com Ser80 e Gly79, interações hidrofóbicas com Tyr78, Phe126 e Ile134 (Figura 4).

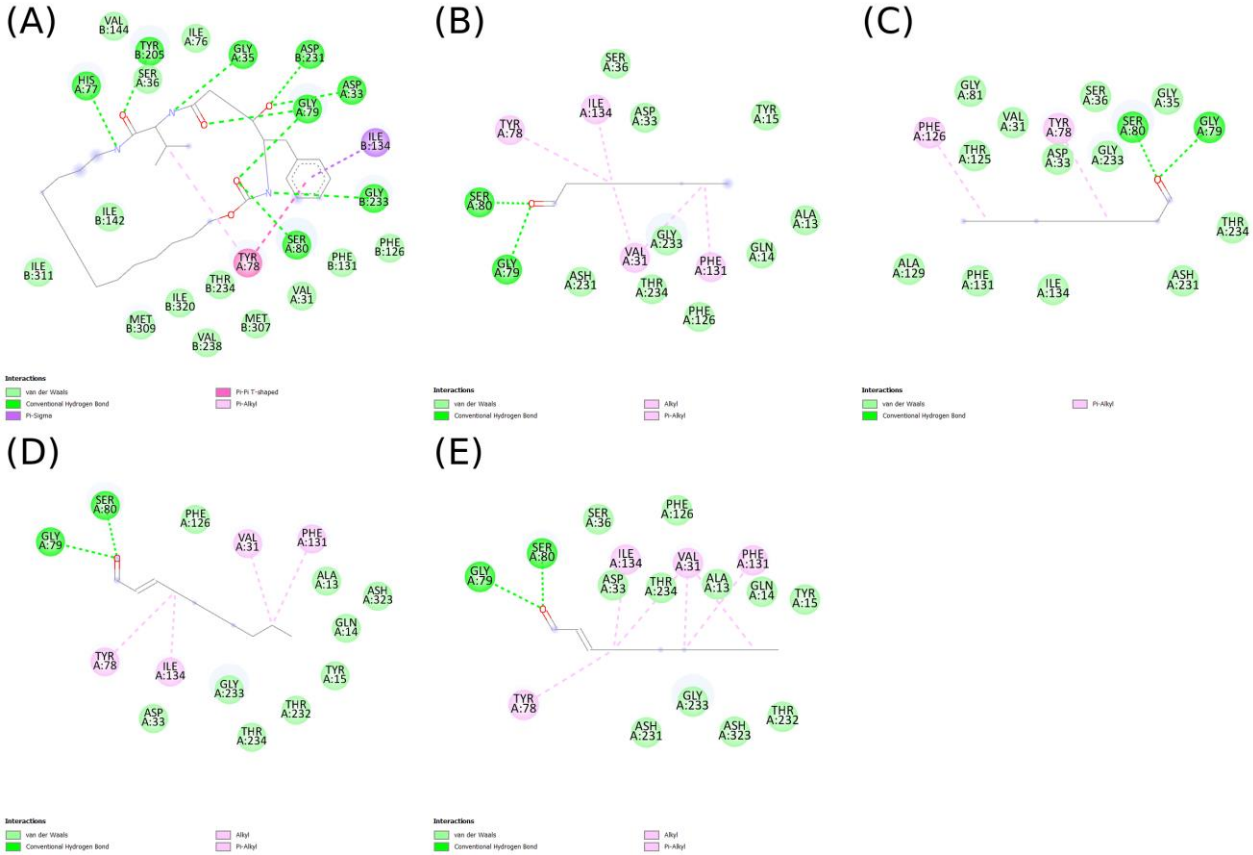

Figura 4- Representação das interações 2D do inibidor S43 (A), 4 (B), 6 (C), 7 (D) e 9 (E). Figura gerada com o Discovery Studio 3.5 Visualizer. 4 – n-nonanal, 6 – n-decanal, 7 – 2E-Decenal,, 9 – Undec-2E-enal.

4 Discussão

Na medicina tradicional amazônica, o óleo de sementes de *C. guianensis* é utilizado para o tratamento de feridas de difícil cicatrização (De Souza et al., 2017) porém atualmente é comum adicionar outros óleos no produto, o que pode influenciar na atividade, visando buscar outro tratamento para leishmaniose tegumentar, cujo a característica é uma ferida, utilizando técnicas fitoquímicas nas folhas e óleo verificou a diferença dos componentes químicos entre extrato e frações, óleo resina e óleo essencial.

Essas diferenças impactam nos resultados da atividade antipromastigota, sendo elucidado que a atividade antipromastigota presente no óleo resina é devido a presença de limonóides (Oliveira et al., 2018) No entanto, verificou-se que o extrato etánolico das folhas de andiroba e frações, que possuem flavonoides e terpenos, não possuem atividade antipromastigota. Outrossim, o óleo essencial que é composto por

esteres, aldeídos e ácidos graxos (Tabela 2) possuem atividade moderada, sendo atividade cicatrizante devido aos ácidos graxos (Chia et al., 2018)

A atividade biológica de aldeídos ainda é pouco explorada, sendo realizado a investigação do potencial *in silico* dessas moléculas. A análise das interações moleculares revelou que todos os compostos testados estabeleceram ligações de hidrogênio com Ser80 e Gly79, resíduos críticos para a estabilização do complexo proteína-ligante na catepsina D. Essas interações são fundamentais para a afinidade dos compostos pelo sítio ativo, uma vez que promovem um encaixe estável e favorecem a interação com a cavidade enzimática. Estudos anteriores demonstraram que inibidores potentes da catepsina D frequentemente interagem com esses resíduos, reforçando sua importância no mecanismo de inibição da enzima (Abideen et al., 2022;Houstecka et al., 2020).

As moléculas selecionas pertencem a classe dos aldeídos e tiveram o mesmo alvo de ação molecular, a catepsina-D que tem a função no parasito de digestão das proteínas da célula hospedeira, sendo essencial para a sobrevivência do parasita nesta célula (Sojka et al., 2016). Desta forma, o bloqueio dessa via pode ser um alvo interessante para atividade anti-leishmanicida. Nas células tumorais ocorre a superexpressão de catepsina-D o que pode favorecer a degradação da matriz célula promovendo a metástase (Mijanovic et al., 2021). Também esta enzima parece envolvida no processo de apoptose e respostas celulares ao estresse oxidativo (Mijanovic et al., 2021). A princípio, a inibição de catepsina-d parece ser interessante um alvo de tratamento leishmaniose, merecendo uma atenção especial.

Esses achados indicam que o composto 9 (Undec-2E-enal) é um candidato promissor para inibição da catepsina D, embora sua afinidade ainda seja inferior à do inibidor de referência. Modificações estruturais estratégicas podem ser exploradas para otimizar sua interação com o sítio ativo e melhorar sua estabilidade termodinâmica.

5 Conclusão

Neste estudo, verificou-se que a presença dos limonóides é um fator para atividade antipromastigota do óleo resina de *Carapa guianensis*. No entanto, apesar da atividade moderada antipromastigota do óleo essencial de *Carapa guianensis*, existem moléculas promissoras para essa atividade biológica, os aldeídos, que estudos em relação a atividades biológicas são escassos. Portanto os resultados dos

estudos *in silico* indicam que existe um potêncial de ação antileishmania dessas moléculas, sendo necessário estudos adicionais.

6 REFERÊNCIAS

ABIDEEN, S. A. et al. Deciphering the dynamics of cathepsin D as a potential drug target to enhance anticancer drug-induced apoptosis. **Journal of Molecular Liquids**, v. 361, p. 119677, 2022.

Adams, R.P., 2007. Identification of essential oil components by gás chromatography/massspectrometry. Allured Publishing Corporation, Carol Stream, Ilinois, EUA. [s.d.].

AMES, B. N.; MCCANN, J.; YAMASAKI, E. Methods for detecting carcinogens and mutagens with the salmonella/mammalian-microsome mutagenicity test. **Mutation Research/Environmental Mutagenesis and Related Subjects**, v. 31, n. 6, p. 347–363, dez. 1975.

BARRETO GOMES, D. E. et al. ChemFlow─ From 2D Chemical Libraries to Protein–Ligand Binding Free Energies. **Journal of Chemical Information and Modeling**, v. 63, n. 2, p. 407–411, 2023.

BENTO, D. B. et al. Oxidative stress in mice treated with antileishmanial meglumine antimoniate. **Research in veterinary science**, v. 95, n. 3, p. 1134–1141, 2013.

COSTA, C. R. et al. A toxicidade em ambientes aquáticos: discussão e métodos de avaliação. **Química Nova**, v. 31, n. 7, p. 1820–1830, 2008.

DE BARROS, R. C. et al. In silico studies on leishmanicide activity of limonoids and fatty acids from Carapa guianensis Aubl. **Frontiers in Chemistry**, v. 12, 30 jul. 2024a.

DE BARROS, R. C. et al. In silico studies on leishmanicide activity of limonoids and fatty acids from Carapa guianensis Aubl. **Frontiers in Chemistry**, v. 12, 30 jul. 2024b.

DE SOUZA, B. A. A. et al. Effects of andiroba oil (Carapa guianensis) on wound healing in alloxandiabetic rats. **Int Arch Med**, v. 10, p. 1–6, 2017.

DOLINSKY, T. J. et al. PDB2PQR: Expanding and upgrading automated preparation of biomolecular structures for molecular simulations. **Nucleic Acids Research**, v. 35, n. SUPPL.2, jul. 2007.

Dong, J. (2024). Home-ADMElab: ADMET Prediction, Scbdd.com. Available at: https://admet.scbdd.com/. [s.d.].

DRWAL, M. N. et al. ProTox: a web server for the in silico prediction of rodent oral toxicity. **Nucleic Acids Research**, v. 42, n. W1, p. W53–W58, 1 jul. 2014.

GUILHERMINO, L. et al. Acute Toxicity Test with Daphnia magna: An Alternative to Mammals in the Prescreening of Chemical Toxicity? **Ecotoxicology and Environmental Safety**, v. 46, n. 3, p. 357–362, jul. 2000.

HOUŠTECKÁ, R. et al. Biomimetic Macrocyclic Inhibitors of Human Cathepsin D: Structure–Activity Relationship and Binding Mode Analysis. **Journal of medicinal chemistry**, v. 63, n. 4, p. 1576–1596, 2020.

KORB, O.; STUTZLE, T.; EXNER, T. E. Empirical scoring functions for advanced protein− ligand docking with PLANTS. **Journal of chemical information and modeling**, v. 49, n. 1, p. 84–96, 2009.

LIPINSKI, C. A. Lead- and drug-like compounds: the rule-of-five revolution. **Drug Discovery Today: Technologies**, v. 1, n. 4, p. 337–341, dez. 2004.

MADUSANKA, R. K.; SILVA, H.; KARUNAWEERA, N. D. Treatment of cutaneous leishmaniasis and insights into species-specific responses: a narrative review. **Infectious diseases and therapy**, v. 11, n. 2, p. 695–711, 2022.

MAIA, J. G. S.; ANDRADE, E. H. A. Database of the Amazon aromatic plants and their essential oils. **Química Nova**, v. 32, n. 3, p. 595–622, 2009.

MIJANOVIC, O. et al. Cathepsin D—managing the delicate balance. **Pharmaceutics**, v. 13, n. 6, p. 837, 2021.

Mondello, L., 2011. FFNSC 2: Flavors and Fragrances of Natural and Synthetic Compounds, Mass Spectral Database. John Wiley & Sons Inc, New York. [s.d.].

NGURE, P. K. et al. In vitro antileishmanial activity of extracts of Warburgia ugandensis (Canellaceae), a Kenyan medicinal plant. v. 3, n. 2, p. 61–66, 2009.

OLIVEIRA, I. DOS S. DA S. et al. Carapa guianensis Aublet (Andiroba) Seed Oil: Chemical Composition and Antileishmanial Activity of Limonoid-Rich Fractions. **BioMed Research International**, v. 2018, n. 1, p. 5032816, 2018.

POKHAREL, P.; GHIMIRE, R.; LAMICHHANE, P. Efficacy and safety of paromomycin for visceral leishmaniasis: a systematic review. **Journal of Tropical Medicine**, v. 2021, n. 1, p. 8629039, 2021.

RAHAL, A. et al. Oxidative stress, prooxidants, and antioxidants: the interplay. **BioMed research international**, v. 2014, n. 1, p. 761264, 2014.

RAPOSO, J. D. A. et al. Seasonal and circadian study of the essential oil of Myrcia sylvatica (G. Mey) DC., a valuable aromatic species occurring in the Lower Amazon River region. **Biochemical Systematics and Ecology**, v. 79, p. 21–29, ago. 2018.

SILVA, L. R. S. DA et al. Análise dos benefícios do desenvolvimento de vacinas contra Leishmaniose em relação ao tratamento clássico. **CONTRIBUCIONES A LAS CIENCIAS SOCIALES**, v. 17, n. 6, p. e7407, 11 jun. 2024.

SOJKA, D. et al. Parasite cathepsin D-like peptidases and their relevance as therapeutic targets. **Trends in parasitology**, v. 32, n. 9, p. 708–723, 2016.

VEBER, D. F. et al. Molecular properties that influence the oral bioavailability of drug candidates. **Journal of medicinal chemistry**, v. 45, n. 12, p. 2615–2623, 2002.

VEIGA, A. et al. Leishmania amazonensis and Leishmania chagasi: In vitro leishmanicide activity of Virola surinamensis (rol.) warb. **Experimental Parasitology**, v. 175, p. 68–73, abr. 2017.

WAGNER, H.; BLADT, S.; ZGAINSKI, E. M. Plant drug analysis. Springer- Verlag, Berlin, 1984. [s.d.].

WHO. World Health Organization (2023). Leishmaniasis. Available at: https://www.who.int/news-room/fact-sheets/detail/leishmaniasis. [s.d.].

Zucker, E. H. (1985). Hazard Evaluation Division-Standard evaluation procedure-acute test for freshwater fish. U.S. EPA Publ. 540 (9). [s.d.].

5. DISCUSSÃO INTEGRADORA

Na busca de alternativas terapêuticas para o tratamento da leishmaniose é importante compreender a interação parasito hospedeiro. Ao infectar o homem, o parasita desenvolve várias estratégias que visam assegurar sua sobrevivência e evasão do sistema imune (Cunningham, 2002; Dos-Santos et al., 2016).

A resposta imune mediada por células Th1 $CD4^+$ é essencial para ativação de macrófagos e eliminação do parasita, sendo o óxido nítrico um componente fundamental nesse processo (Machado et al., 2004; Silveira et al., 2008). Outras espécies reativas de oxigênio também são essenciais nesse processo (Bogdan et al., 2000; Silveira et al., 2008). Entretanto, o parasita desenvolve estratégias para resistir ao estresse oxidativo (Olivier et al., 2005). Os fármacos disponíveis, como o antimoniato de meglumina (MA), causam alterações oxidativas que estão envolvidas tanto na atividade antiparasitária quanto na toxicidade do fármaco (Solomon et al., 2024). A forma nanoestruturada do MA favorece o aumento de expressão de NOS TNF-α e lFN-y, diminuição de IL3 e ativa caspase-3 induzindo a apoptose de células parasitárias (Yadegari et al., 2023).

Desta forma, o MA atua nos pontos críticos que favorecem a sobrevivência do parasita no hospedeiro, isto é, para sobreviver o parasito diminui o estresse oxidativo, o MA eleva o estresse; o parasita altera a resposta imune para favorecer seu crescimento e o MA reverte este processo. Porém, as mudanças oxidativas ocasionadas por MA estão envolvidas em sua toxicidade. A nefrotoxicidade da Anfotericina B também tem sido associada ao estresse oxidativo (Baginski et al., 2006), a toxicidade da paromomicina tem sido associada a ROS, outros fármacos, utilizam para o tratamento da leishmaniose que tem sido atribuída ao estresse oxidativo a atividade e toxicidade a isotionato de pentamida (Bento et al., 2013) e miltefosina (Olivier et al., 2005; Pinto-Martinez et al., 2018).

Na busca de alternativas terapêuticas, alguns estudos com plantas medicinais demonstraram uma relação direta entre o estresse oxidativo e a atividade antiparasitária (Veiga et al., 2022; Brígido et al., 2024). A princípio, parece interessante buscar um novo fármaco que gera espécies reativas de O e N para o tratamento da leishmaniose. Entretanto, estas mesmas espécies podem ocasionar diferentes eventos adversos com potencial grave.

Diante destas reflexões, o presente estudo tenta buscar uma possível alternativa terapêutica para o tratamento de leishmaniose que tivesse potencial

antiparasitário sem o envolvimento do estresse oxidativo e alterasse o processo inflamatório envolvido na doença. Desta forma, o óleo de *C. guianensis* pareceu promissor, visto que a atividade antiparasitária dos limonoides já é relatada (Oliveira, 2018) e atividade cicatrizante dos ácidos graxos também está relatada na literatura (Chia, 2018). No entanto, os mecanismos envolvidos nestas atividades biológicas não é conhecido. Visando compreender melhor o potêncial farmacológico destas moléculas foi realizado estudo *in silico* (de Barros et al., 2024).

A primeira preocupação foi em relação se um possível medicamento com estas moléculas pudessem ser usados por via oral. Os estudos de predições das propriedades físico-químicas e farmacocinéticas sugerem que a via pode ser a oral (de Barros et al., 2024).

Os medicamentos disponíveis, exceto a miltefosina, são de uso intravenoso e intramuscular. Ressalta-se que a maioria dos pacientes com leishmaniose moram em locais afastados e tem reações adversas e dificuldades de acesso a serviços de saúde, logo a via oral é mais adequada que a via parenteral, favorecendo a adesão ao tratamento e melhorando a resposta ao tratamento (Laniado-Laborín; Cabrales-Vargas, 2009; Solomon et al., 2024).

Como os fármacos disponíveis para o tratamento da leishmaniose apresentam elevada toxicidade, torna-se importante buscar novas alternativas menos tóxicas. O presente estudo realizou as predições de toxicidade para limonoides e ácidos graxos por meio de diferentes abordagens *in sílico*. No entanto, todas moléculas demonstraram toxicidade nos modelos de algas, *Daphnia* e peixes.

A toxicidade para *Daphinia* sugere que o uso de uma molécula em curto prazo, em concentrações subletais, podem ocasionar efeitos tóxicos (da Silva et al., 2024) e são recomendados estudos *in vivo* para avaliar a toxicidade renal, hepática, cardíaca e em outros órgãos.

A toxicidade pode resultar em efeitos adversos da molécula sobre o crescimento, metabolismo ou sobrevivência do organismo, sendo uma escolha ecotoxicológica e pode ser para avaliação de moléculas candidatas a fármacos (Giaginis et al., 2012). O uso deste modelo *in silico* sugere efeito toxicológico agudo, sendo considerado na avaliação preliminar (de Barros et al., 2024). Todas as moléculas aumentadas de toxicidade neste modelo. A predição de toxicidade oral aguda indicou que os limonóides apresentavam baixa toxicidade, enquanto os ácidos graxos exibiam um potencial ainda menor, de forma geral."

Estudos *in silico* demonstraram que os limonoides podem afetar a membrana celular dos parasitas através do estresse oxidativo, porém apresentam baixa toxicidade para humanos em doses terapêuticas (de Barros et al., 2024). A toxicidade foi relacionada para o uso de doses elevadas, podendo causar problemas gastrointestinais, além de afetar a função cognitiva e a funcionalidade motora (Porfírio-Dias et al.,2020). Entretanto, a exposição de ratos de forma prolongada levou ao surgimento de hepatotoxicidade (Costa-Silva, 2008), porém estas alterações não foram observadas no presente estudo.

Em relação aos ácidos graxos incluídos nesses estudos, são compostos que podem interagir com as membranas de algas reduzindo a permeabilidade, levando o ao estresse oxidativo e inibição do crescimento (Sun et al., 2018). Diante disso, todas foram tóxicas para algas.

Os efeitos tóxicos dos ácidos graxos para *Daphinia* podem resultar na formação de agregados lipídicos afetando a função respiratória (Tkaczyk et al., 2021). Para verificar se os ácidos graxos possuem toxicidade aguda foi realizada a predição de toxicidade oral, sendo menor toxicidade observadas efeitos indesejáveis (13,14 e 16), mutagênico (14 e 16) e tumorigênico (13 e 14). Verificou-se se os ácidos graxos e limonoides possuem potencial mutagênico e carcinogênico, novos estudos *in silico* foram realizados, os limonóides não foram mutagênicos e os ácidos graxos possuem potencial mutagênico em ST1535NA. Em síntese, estes resultados sugerem o potencial genotóxico intrínseco de ácidos graxos, sendo necessário estudos adicionais.

Esperava-se que os ácidos graxos pudessem ser carcinogênicos e os limonóides não apresentassem efeito tóxico. Tal premissa se fundamentou no fato que mutações no DNA podem ocasionar alterações em genes que regulam o ciclo celular como proto-oncogenes e genes supressores de tumor (Zacharias et al., 2020). Vale ressaltar que nem toda substância é carcinogênica (Kolbye e Carr, 1984). No presente estudo, observa-se que os ácidos graxos foram mutagênicos e apresentavam potencial carcinogênico para ratos e camundongos (12,17,18,19,20) ou apenas ratos (13,14,15).

Os limonoides não apresentaram potencial mutagênico, porém, foram carcinogênicos, o que faz pensar em outros mecanismos envolvidos neste processo, como aumento a taxa de ativação celular sem causar mutações (Chia, 2018) podem

causar estresse oxidativo nas diversas expressões gênicas sem alterar no presente estudo.

Desta forma, é importante investigar os mecanismos envolvidos no processo de apoptose dos limonoides. Todas as moléculas foram tóxicas para *Medaka* e *Minnow* nos estudos *in silico*. Os estudos em peixes demonstraram bons indicadores de toxicidade aguda (de Barros et al., 2024), porém a predição em ratos demonstrou a segurança das moléculas. Além disso, pode sinalizar o quanto moléculas lipofílicas podem se acumular, ocasionando alterações endócrinas e outras alterações (Geyer et al., 1993).

Desta forma, ao que parece, as possíveis ações ocasionadas pelos limonoides e ácidos graxos não são letais, mas são alterações em órgãos ou sistemas que podem desencadear reações tóxicas ou reações adversas. Nesse contexto, é importante a realização de estudos de toxicidade oral em doses repetidas associadas a "*screening*" hipocrático, função renal e hepática, hemograma, análise imunohistoquímica e dosagens de citocinas e NO. Estas análises permitem prever as possíveis reações adversas e toxicidade.

Depois destas análises selecionou-se 2 limonoides (3 e 6) e 2 ácidos graxos (15 e 16) apresentaram melhor perfil de toxicidade para a docagem molecular e dinâmica molecular. Estudos preliminares demonstraram que os limonoides am HIF-1a na célula humana esta proteína está envolvida na adaptação celular à hipóxia (de Barros et al., 2024) e interage com o sistema imune contribuindo para modulação da inflamação e apoptose (Ferraris, 2011; Ferraris, 2012).

A leishmaniose não atua por meio do gene HIF-1a, mas pode induzir sua expressão nos macrófagos (Aghaei et al., 2020) o resultado desta ativação pode modular a inflamação e apoptose, alterando o ciclo de vida do parasito (Mendonça et al., 2020).

Os ácidos graxos avaliados inibiram a COX-2, que é uma enzima essencial no processo inflamatório e induzida por estímulos inflamatórios, lesões e infecções (de Barros et al., 2024). A COX pode atuar regulando a resposta inflamatória, contribuindo com sua resolução ou cronificação (Rajakariar; Yaqoob; Gilroy, 2006). O uso de inibidores de COX-2 para o tratamento da leishmaniose pode ter efeitos positivos como o aumento de produção de óxido nítrico e de espécies reativas de oxigênio que são letais para o parasito e supressão da resposta inflamatória (Bhattacharjee, et al., 2012). Por outro lado, esta inibição pode interferir no equilíbrio da resposta imune TH1

e TH2, o que pode não ser bom para o tratamento da infecção (Bhattacharjee, et al., 2012). De qualquer forma, o controle da inflamação pode ser útil para o tratamento da leishmaniose, porém deve estar associado a um fármaco com propriedades antiparasitárias.

Sempre que se avalia a antileishmania de ORCG atribui-se esta atividade aos componentes fixos (Limonoides). Entretanto, no OECG pode conter outras moléculas ativas no parasito. Então, foi obtido OECG, feito a caracterização química e identificados diferentes ésteres e aldeídos. Aldeídos isolados de plantas medicinais mostraram-se ativos em doenças de chagas e leishmaniose (Machado et al.,.2012). Logo, avaliar a atividade in silico de moléculas pertencentes a esta classe parece interessante, também parece interessante avaliar a atividade do OECG.

O OECG mostrou-se menos ativo quanto às formas promastigotas M29125 e M29719 que o ORCG, sugerindo a importância dos limonóides para esta atividade. Nos estudos in silico, avaliou-se 5 aldeídos presentes OECG, 4 ésteres, 1 lactona e 1 furano. A inclusão de ésteres se fundamenta na premissa que estes metabólitos possam alterar a integridade da membrana do parasito (Rabinovitch; Zilberfarb; Ramazeilles, 1986. Enquanto, lactonas podem ter atividade inibitória na enzima tripanomatioma redutase- (Possart et al., 2021) e furanos inibem a síntese do ergosterol (Sathiyamoorthy et al., 2024).

Todos os componentes são a regra de Lipinski e parecem ser bem absorvidos por via oral. Sendo o principal critério utilizado para seleção das moléculas que foram para docagem a toxicidade. Neste contexto, as moléculas 6 (n-decanal), 8 (2E,)9, e 10 as mais promissoras. No entanto, somente as moléculas 4,5,6,7 não foram carcinogênicas, a molécula 6 também não foi mutagênica, enquanto a molécula 9 não foi mutagênica e carcinogênica para rato. A molécula 7 foi mutagênica, porém, não foi carcinogênica e a molécula 4 foi mutagênica e não carcinogênica para ratos. Essas moléculas não foram tóxicas quando avaliadas por via oral e diante desses resultados foram selecionadas para os estudos in silico.

As moléculas selecionadas pertencem a classe dos aldeídos e tiveram o mesmo alvo de ação molecular, catepsina-D que tem a função no parasito de digestão das proteínas da célula hospedeira, sendo essencial para a sobrevivência do parasita nesta célula (Sojka et al., 2016). Desta forma, o bloqueio desta via pode ser um alvo interessante para atividade anti-leishmanicida. Nas células tumorais ocorre a superexpressão de catepsina-D, o que pode favorecer a degradação da matriz célula

promovendo a metástase (Mijanovic et al., 2021). Também esta enzima parece envolvida no processo de apoptose e respostas celulares ao estresse oxidativo (Mijanovic et al., 2021). A princípio, a inibição da catepsina-D parece ser interessante um alvo de tratamento leishmaniose, merecendo uma atenção especial.

Além de avaliar atividade antileishmania, do ORCG e OECG, foi avaliado a atividade antipromastigota de EECGf, FHCGf, FDCGf, FEACGf e FMCGf, certamente as composições químicas do extrato e frações é muito diferente dos óleos, sendo detectado a presença de flavonoides no EECGf e FDCGf, FEACGf e FMCGf. Além disso, em análise de RMN, verificou-se a presença de terpenos a partir dos deslocamentos encontrados nas frações foram sugestivos da presença de hidrogênios referentes a grupos metilenos contidos em diferentes diterpenos e triterpenos cicloartano (Popova et al., 2009). Na espécie em questão já foram identificados variados terpenos, como triterpenoides (Sarria et al., 2014; Amorim et al., 2020) e sesquiterpenos (Álvarez et al., 2024),

Após todos os estudos químicos e avaliação da atividade antipromastigota, percebe-se que o ORCG ainda é a melhor alternativa para o tratamento da leishmaniose e os compostos fixos são importantes para esta atividade. Entretanto, os ensaios in vivo são importantes para compreender a atividade antiparasitária e antiinflamatória de ORCG.

6. CONCLUSÃO

Ao final deste estudo conclui-se que o ORCG foi o mais promissor como anti-leishmania, sendo contido neste óleo constituintes fixos, limonóides e constituintes voláteis, a resposta antileishmania pode resultar de um efeito sinérgico resultante da inibição de vias envolvidas na resposta inflamatória (COX-2) pelos ácidos graxos, associada anti-parasitario, promovido catepsina-d pelos aldeídos e pela inibição do HIF1-a pelos limonóides. Torna-se urgente investigar se associação da inbição destas diferentes vias pode levar ao sinergismo para os efeitos tóxicos subletais em modelo de roedores. Desta forma, pode se sugerir a segurança do ORCG no tratamento da leishmaniose tegumentar.

REFERÊNCIAS

AGHAEI, M. et al. The role of Bax in the apoptosis of Leishmania-infected macrophages. **Microbial Pathogenesis**, v. 139, p. 103892, fev. 2020.

ALVAR, J. et al. Leishmaniasis Worldwide and Global Estimates of Its Incidence. **PLoS ONE**, v. 7, n. 5, p. e35671, 31 maio 2012.

BAGINSKI, M.; CZUB, J. Amphotericin B and its new derivatives-mode of action. **Current drug metabolism**, v. 10, n. 5, p. 459–469, 2009.

BARBOSA, I. R. et al. Aspectos da Coinfecção Leishmaniose visceral e HIV no Nordeste do Brasil. **Revista Baiana de Saúde Pública**, v. 37, n. 3, p. 672–687, 2013.

BARREIRO, E. J. et al. Modelagem molecular: uma ferramenta para o planejamento racional de fármacos em química medicinal. **Química nova**, v. 20, p. 300–310, 1997.

BENTO, D. B. et al. Oxidative stress in mice treated with antileishmanial meglumine antimoniate. **Research in Veterinary Science**, v. 95, n. 3, p. 1134–1141, dez. 2013.

BOGDAN, C.; RÖLLINGHOFF, M.; DIEFENBACH, A. The role of nitric oxide in innate immunity. **Immunological reviews**, v. 173, p. 17–26, 2000.

BRASIL. Manual de vigilância da leishmaniose tegumentar. 1. ed. Brasília, 2017. 191Pp.

BRASIL. Ministério da Saúde. Secretaria de Vigilância em Saúde. Departamento de Vigilância das Doenças Transmissíveis. Manual de recomendações para diagnóstico, tratamento e acompanhamento de pacientes com a coinfecção leishmania-HIV. Brasília: Ministério da Saúde, 2015. [s.d.].

BRÍGIDO, H. P. C. et al. Aspidosperma nitidum reduces parasite load and modulates cytokines in BALB/c mice infected with Leishmania (Leishmania) amazonensis. **Frontiers in Chemistry**, v. 12, 2024.

BROGI, S. et al. **In silico methods for drug design and discovery**. **Frontiers in chemistry**Frontiers Media SA, , 2020.

COSTA, R. K. E.; HOLANDA, E. C.; ANDRADE, S. M. Visceral Leishmaniasis and Human Immunodeficiency Virus Coinfection: epidemiological profile of cases reported in São Luís-Maranhão, Brazil. Res Soc Dev 10: e2310413317. **Res Soc Dev**, 2021.

CUNNINGHAM, A. C. Parasitic adaptive mechanisms in infection by Leishmania. **Experimental and molecular pathology**, v. 72, n. 2, p. 132–141, 2002.
DE BARROS, R. C. et al. In silico studies on leishmanicide activity of limonoids and fatty acids from Carapa guianensis Aubl. **Frontiers in Chemistry**, v. 12, 2024.

DE SOUZA FILHO, L. A. et al. TENDÊNCIAS REGIONAIS DA LEISHMANIOSE VISCERAL EM PESSOAS VIVENDO COM HIV NO BRASIL. **The Brazilian Journal of Infectious Diseases**, v. 27, p. 103059, out. 2023.

DO SOCORRO SILVA DA VEIGA, A. et al. Activity of alkaloids from Aspidosperma nitidum against Leishmania (Leishmania) amazonensis. **Scientific Reports**, v. 12, n. 1, 1 dez. 2022.

DOS-SANTOS, A. L. A. et al. Innate immunomodulation to trypanosomatid parasite infections. **Experimental parasitology**, v. 167, p. 67–75, 2016.

FASOULAKIS, Z. et al. MicroRNAs Determining Carcinogenesis by Regulating Oncogenes and Tumor Suppressor Genes During Cell Cycle. **MicroRNA**, v. 9, n. 2, p. 82–92, 4 mar. 2020.

GHASEMIAN YADEGARI, J. et al. Antileishmanial, cellular mechanisms, and cytotoxic effects of green synthesized zinc nanoparticles alone and in combined with glucantime against Leishmania major infection. **Biomedicine & Pharmacotherapy**, v. 164, p. 114984, ago. 2023.

KOLBYE, A. C.; JELLEFF CARR, C. The evaluation of the carcinogenicity of environmental substances. **Regulatory Toxicology and Pharmacology**, v. 4, n. 4, p. 350–354, dez. 1984.

LANIADO-LABORÍN, R.; CABRALES-VARGAS, M. N. Amphotericin B: side effects and toxicity. **Revista iberoamericana de micología**, v. 26, n. 4, p. 223–227, 2009.

LOGGETTO, P. et al. Regional collaboration for the development of national childhood cancer plans in Latin America and the Caribbean. **Revista Panamericana de Salud Pública**, v. 47, p. 1, 25 set. 2023.

MACHADO, M. et al. Monoterpenic aldehydes as potential anti-Leishmania agents: activity of Cymbopogon citratus and citral on L. infantum, L. tropica and L. major. **Experimental parasitology**, v. 130, n. 3, p. 223–231, 2012.

MACHADO, P. R. L. et al. Mecanismos de resposta imune às infecções. **Anais Brasileiros de Dermatologia**, v. 79, p. 647–662, 2004.

MENDONÇA, L. S. O. et al. Characterization of serum cytokines and circulating microRNAs that are predicted to regulate inflammasome genes in cutaneous leishmaniasis patients. **Experimental Parasitology**, v. 210, p. 107846, mar. 2020.

MIJANOVIC, O. et al. Cathepsin D—managing the delicate balance. **Pharmaceutics**, v. 13, n. 6, p. 837, 2021.

NAMBA, Adriana Mieco; DA SILVA, Vinícius Barreto; DA SILVA, C. H. T. P. Dinâmica molecular: teoria e aplicações em planejamento de fármacos. **Eclética Química**, v. 33, p. 13-24, 2008.

ORGANIZAÇÃO PAN-AMERICANA DA SAÚDE; ORGANIZAÇÃO DA SAÚDE. Leishmaniose visceral. 2023. Disponível em: https://www.paho.org/pt/topicos/leishmaniose/leishmaniose-visceral. Acesso em: 12 dez. 2024.

ORGANIZAÇÃO PAN-AMERICANA DA SAÚDE/ORGANIZAÇÃO DA SAÚDE. Diretrizes para o tratamento das leishmanioses na Região das Américas. 2022. Disponível em: https://iris.paho.org/bitstream/handle/10665.2/56487/9789275725030_por.pdf?sequence=4&isAllowed=y. Acesso em: 12 dez. 2024.

PIETRALONGA, T. C. et al. ESTUDO COMPUTACIONAL DE REATIVADORES DA ACETILCOLINESTERASE INIBIDA PELO PESTICIDA AGRÍCOLA FENAMIFÓS. **Revista Ifes Ciência**, v. 1, n. 2, p. 51–64, 2015.

POSSART, K. et al. Sesquiterpene lactones with dual inhibitory activity against the trypanosoma brucei pteridine reductase 1 and dihydrofolate reductase. **Molecules**, v. 27, n. 1, p. 149, 2021.

RABINOVITCH, M.; ZILBERFARB, V.; POUCHELET, M. Leishmania mexicana: destruction of isolated amastigotes by amino acid esters. **The American journal of tropical medicine and hygiene**, v. 36, n. 2, p. 288–293, 1987.

RAJAKARIAR, R.; YAQOOB, M. M.; GILROY, D. W. COX-2 in inflammation and resolution. **Molecular interventions**, v. 6, n. 4, p. 199, 2006

ROCHA, E. C. M. DA et al. High-Throughput Molecular Modeling and Evaluation of the Anti-Inflammatory Potential of Açaí Constituents against NLRP3 Inflammasome. **International Journal of Molecular Sciences**, v. 25, n. 15, p. 8112, 2024.
.
RODRIGUES, V. S. et al. EP-286 - NOVAS POSSIBILIDADES TERAPÊUTICAS PARA TRATAMENTO DE LEISHMANIOSE VISCERAL (LV) EM PESSOAS VIVENDO COM HIV (PVHIV): A ASSOCIAÇÃO ENTRE ANFOTERICINA B LIPOSSOMAL COM MILTEFOSINA COMO ALTERNATIVA DE TRATAMENTO PARA LV RECIDIVANTE EM PVHIV. **The Brazilian Journal of Infectious Diseases**, v. 28, p. 104194, out. 2024.

SATHIYAMOORTHY, J. et al. Elucidation of furanone as ergosterol pathway inhibitor in Cryptococcus neoformans. **Journal of Biomolecular Structure and Dynamics**, v. 42, n. 12, p. 6013–6026, 2024.

SGANZERLA, A.; DO ROSARIO XAVIER, B. H. Da Filosofia Da Natureza À Filosofia Moral: Análise De Uma Ética Animal Em Hans Jonas. **Revista Dissertatio de Filosofia**, v. 52, p. 185–212, 2020.

SILVEIRA, F. T. et al. Revisão sobre a patogenia da Leishmaniose Tegumentar Americana na Amazônia, com ênfase à doença causada por Leishmania (V.) braziliensis e Leishmania (L.) amazonensis. **Revista Paraense de Medicina**, v. 22, n. 1, p. 9–20, 2008.

SOJKA, D. et al. Parasite cathepsin D-like peptidases and their relevance as therapeutic targets. **Trends in parasitology**, v. 32, n. 9, p. 708–723, 2016.
SOLOMON, M. et al. Comparison of Intralesional Sodium Stibogluconate versus Intralesional Meglumine Antimoniate for the Treatment of Leishmania major Cutaneous Leishmaniasis. **Acta Dermato-Venereologica**, v. 104, 2024.

SOTOMAYOR, M.; SCHULTEN, K. Single-molecule experiments in vitro and in silico. **Science**, v. 316, n. 5828, p. 1144–1148, 2007.

SOUSA, Marcia Leite de et al.** Coinfecção Leishmania-HIV no Brasil: aspectos epidemiológicos, clínicos e laboratoriais. *Epidemiologia e Serviços de Saúde*, v. 20, n. 4, p. 519-526, 2011. DOI: 10.5123/S1679-49742011000400003. [s.d.].

SOUZA, E. C. et al. Apresentação clínica da leishmaniose visceral em pacientes portadores do HIV: análise dos fatores relacionados ao aparecimento da doença. **Brazilian Journal of Health Review**, v. 3, n. 2, p. 1766–1777, 2020.

SUN, X.-M. et al. Influence of oxygen on the biosynthesis of polyunsaturated fatty acids in microalgae. **Bioresource Technology**, v. 250, p. 868–876, fev. 2018.

TKACZYK, A. et al. Daphnia magna model in the toxicity assessment of pharmaceuticals: A review. **Science of The Total Environment**, v. 763, p. 143038, abr. 2021.

VASCONCELOS, R. S.; KOVALESKI, D. F.; JUNIOR, Z. C. T. Doenças Negligenciadas: revisão da literatura sobre as intervenções propostas. **Saúde & Transformação Social/Health & Social Change**, v. 6, n. 2, p. 114–131, 2015.

APÊNDICE A

Figura 1S. RMN 1H Extrato etanolico (EECGf)

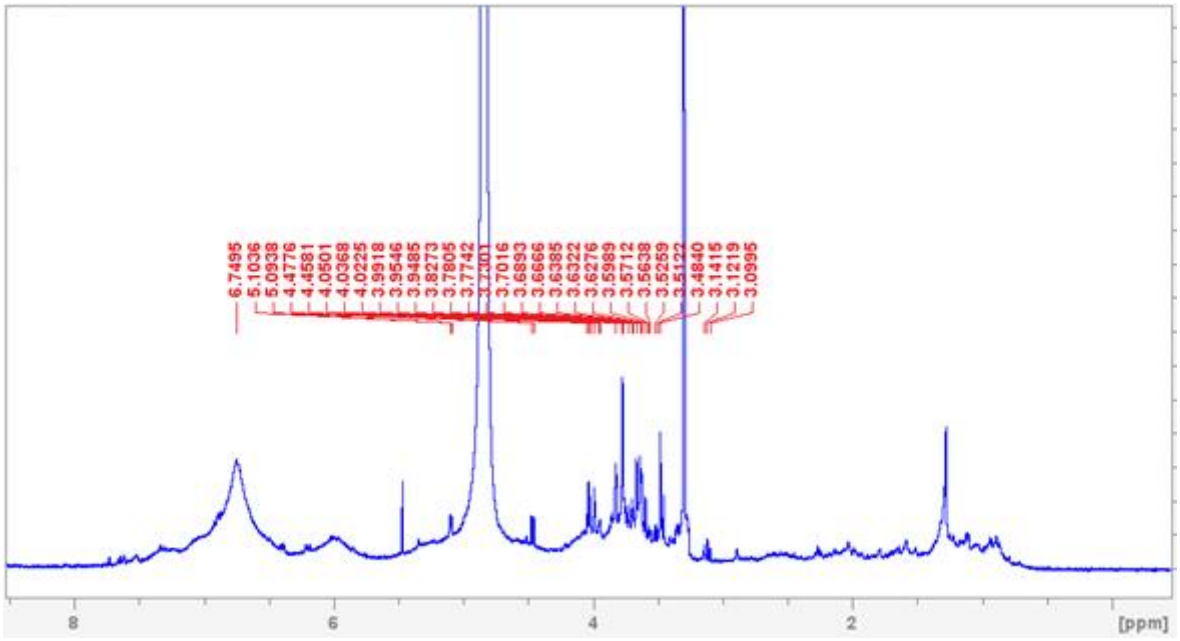

Figura 2S. Fração Hexano (FHCGf)

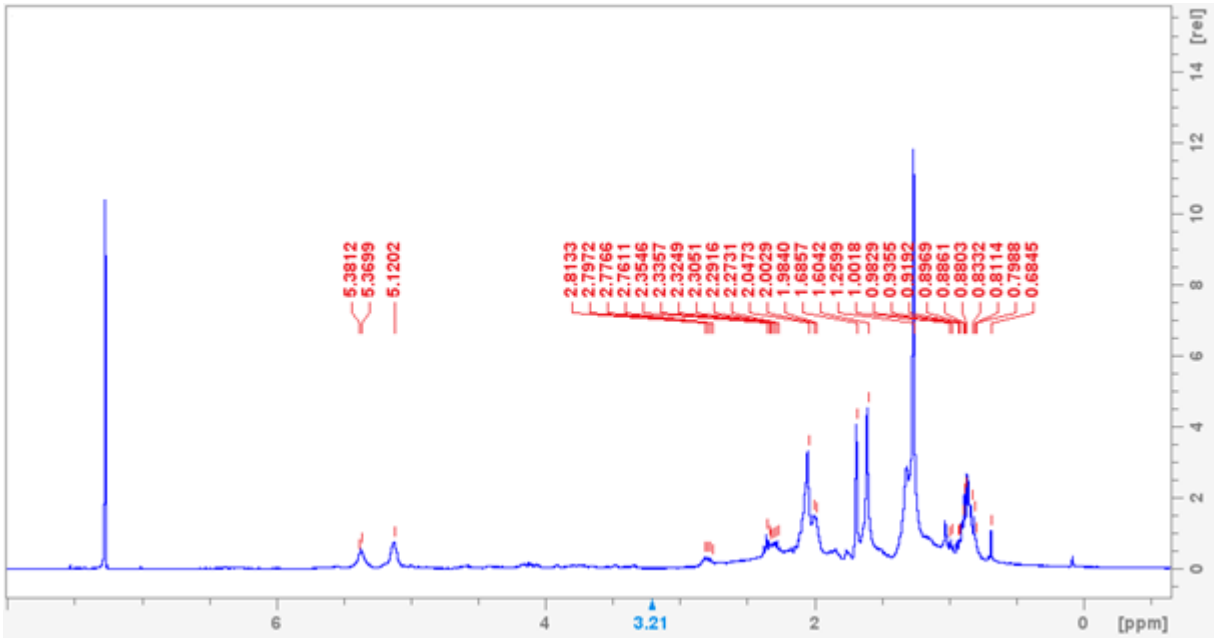

Figura S3. Fração Diclorometano (FDCGf)

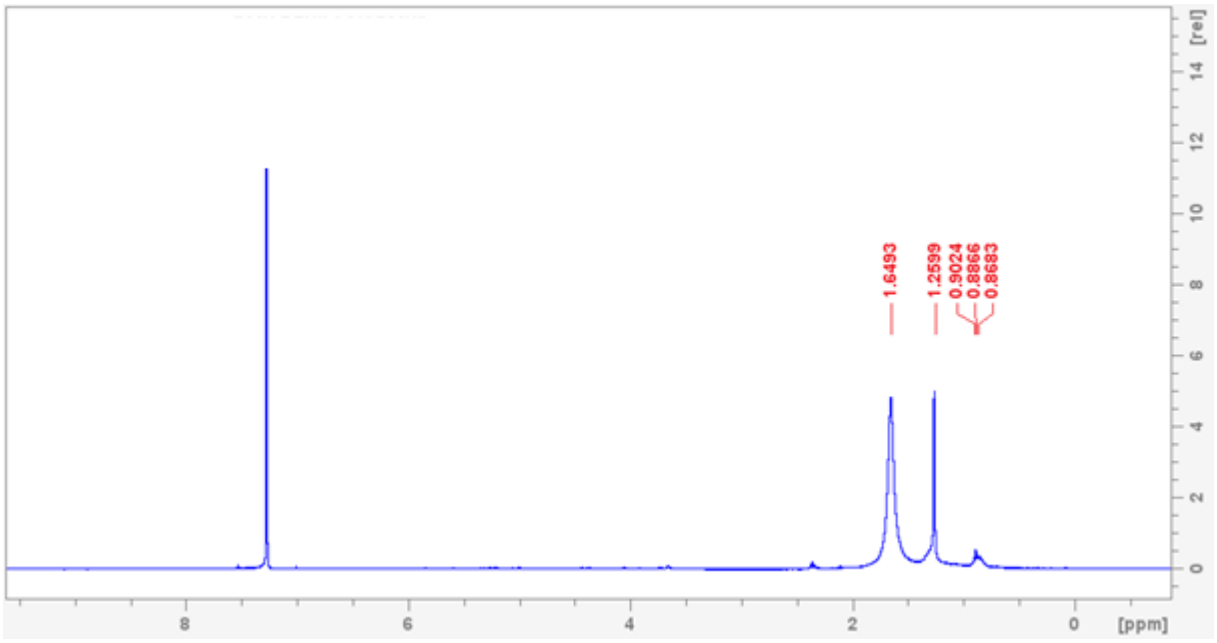

Figura S4. Fração Acetato de etila (FEACGf)

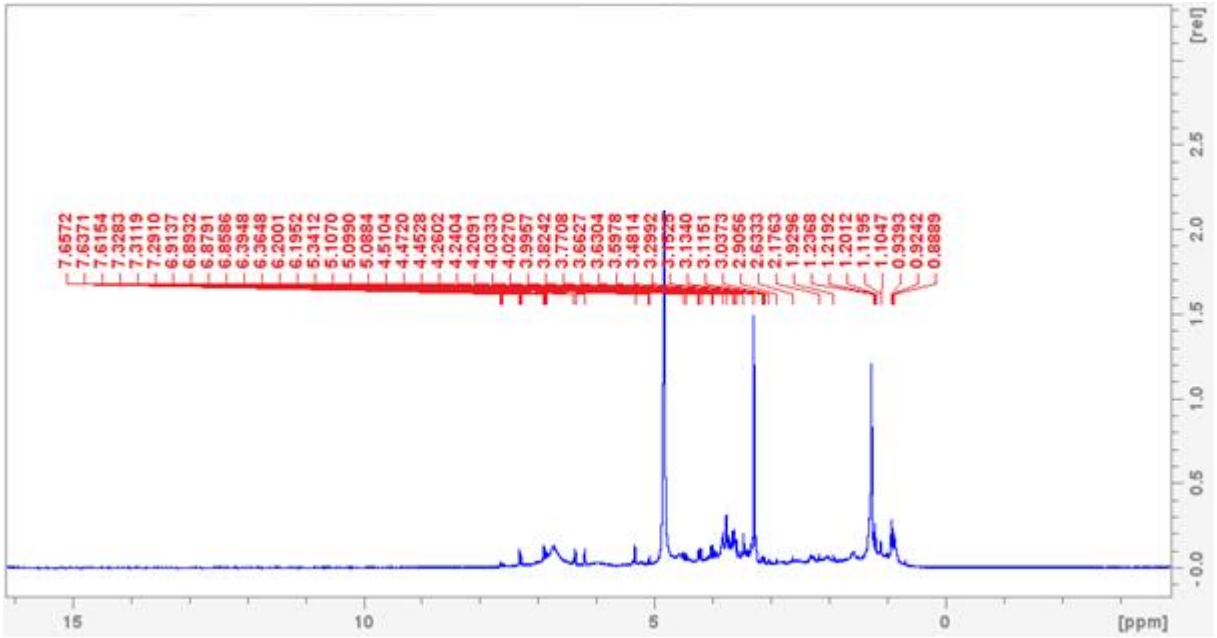

Figura S5. Fração Metanol (FMCGf)

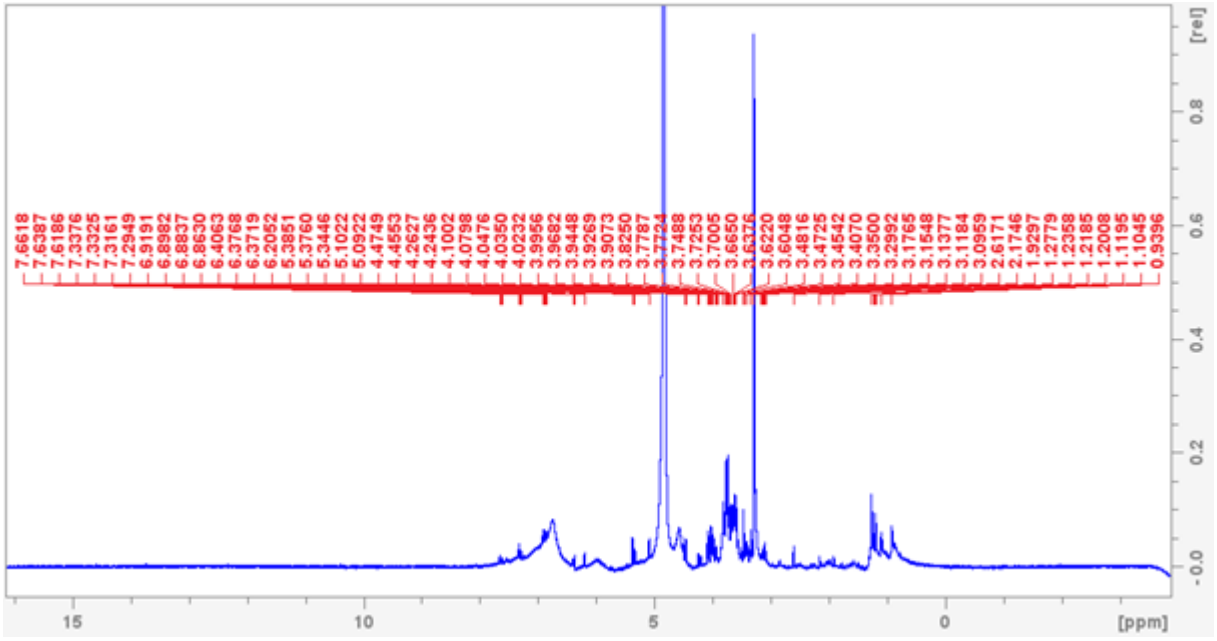
7.6618
7.6387
7.6186
7.3376
7.3325
7.3161
7.2949
6.9191
6.8982
6.8837
6.8630
6.4063
6.3768
6.3719
6.2052
5.3851
5.3760
5.3446
5.1022
5.0922
4.4749
4.4553
4.2627
4.2436
4.1002
4.0798
4.0476
4.0350
4.0232
3.9956
3.9682
3.9448
3.9269
3.9073
3.8250
3.7787
3.7724
3.7488
3.7253
3.7005
3.6650
3.6376
3.6220
3.6048
3.4816
3.4725
3.4542
3.4070
3.3500
3.2992
3.1765
3.1548
3.1377
3.1184
3.0959
2.6171
2.1746
1.9297
1.2779
1.2358
1.2185
1.2008
1.1195
1.1045
0.9396
[rel]
0.8
0.6
0.4
0.2
-0.0
15
10
5
0
[ppm]

ANEXO A

Article

Prediction of the Binding to the Nuclear Factor NF-Kappa-B by Constituents from *Teucrium polium* L. Essential Oil

Renilson Castro de Barros [1], Renato Araújo da Costa [2], Nesrine Guenane [3,4], Boulanouar Bakchiche [3,4,*], Farouk Benaceur [3,4], Omer Elkiran [5], Suelem Daniella Pinho Farias [6], Vanessa Regina Silva Mota [6] and Maria Fani Dolabela [1,*]

check for updates

Academic Editors: Wirginia Kukula-Koch and Magdalena Bartnik

Received: 15 November 2024
Revised: 28 December 2024
Accepted: 5 January 2025
Published: 14 January 2025

Citation: de Barros, R.C.; da Costa, R.A.; Guenane, N.; Bakchiche, B.; Benaceur, F.; Elkiran, O.; Farias, S.D.P.; Mota, V.R.S.; Dolabela, M.F. Prediction of the Binding to the Nuclear Factor NF-Kappa-B by Constituents from *Teucrium polium* L. Essential Oil. *Curr. Issues Mol. Biol.* **2025**, *47*, 48. https://doi.org/10.3390/cimb47010048

[1] Pharmaceutical Sciences Postgraduate Program, Federal University of Pará, Belém 66075-110, PA, Brazil; renilsonbarros098@gmail.com
[2] Federal Institute of Education Sciences of the State of Pará, Campus Abaetetuba, Abaetetuba 68440-000, PA, Brazil; renato.costa@ifpa.edu.br
[3] Laboratory of Biological and Agricultural Sciences (LBAS), Amar Telidji University, Laghouat 03000, Algeria; n.guenane.gpr@lagh-univ.dz (N.G.); f.benaceur@lagh-univ.dz (F.B.)
[4] Research Unit of Medicinal Plant (RUMP), Biotechnology Research Center (CRBt), Laghouat 03000, Algeria
[5] Department of Environmental Health, Vocational School of Health Services, Sinop University, 57000 Sinop, Turkey; omer_elkiran@hotmail.com
[6] Federal of Pharmacy, Federal University of Pará, Belém 66075-110, PA, Brazil; suelem.farias@ics.ufpa.br (S.D.P.F.); regina1435vanessa@gmail.com (V.R.S.M.)
* Correspondence: b.bakchiche@lagh-univ.dz (B.B.); fani@ufpa.br (M.F.D.)

Abstract: *Teucrium polium* L. is a plant with various claims of ethnobotanical use, primarily for inflammatory diseases. Chemical studies have already isolated different types of terpenes from the species, and studies have established its pharmacological potential. The present study evaluates the components of *T. polium* essential oil cultivated in the Algerian Saharan Atlas. GC-MS identified the major components as fenchone (31.25%), 3-carene (15.77%), cis-limonene oxide (9.77%), and myrcene (9.15%). In the in silico prediction, molecules with more than 1% abundance were selected. Regarding Lipinski's rule, all molecules followed the rule. All molecules were found to be toxic in at least one model, with some molecules being non-genotoxic (6, 8, 10, 11, 12, 13) and others being non-mutagenic (5, 7, 9, 14). Three molecules were selected that showed the best results in pharmacokinetic and toxicity studies: the molecules that did not present carcinogenic potential (7—myrtenal; 9—myrtenol; 14—verbenol). The molecular target was established, and it seems that all three bound to the nuclear factor NF-

1. Introduction

Teucrium polium L. (Lamiaceae) is found in Europe, North Africa, and Asia. The following medicinal claims are attributed to it: treatment of inflammatory diseases, gastrointestinal disorders, diabetes, rheumatisms, indigestion, abdominal pain, colds, and urogenital diseases [1,2].

Chemical studies conducted on *T. polium* oil have identified compounds belonging to the following classes: sesquiterpenes (α- and τ-cadinols), (E)-β-caryophyllene and its oxide forms, neoclerodane diterpenoids, and monoterpenes. The proportions of these chemical

kappa-B. Based on the docking and molecular dynamics results, these molecules have potential as anti-inflammatory and antitumor therapies, with further in vitro and in vivo studies needed to evaluate their activity and toxicity.

Keywords: fuclear factor NF-kappa-B; *Teucrium polium* L.; monoterpenes; sesquiterpenes; verbenol; myrtenal; myrtenol

constituents vary according to the collection site [2,3] and, possibly, factors such as the time of plant collection and the part used for oil extraction, among others. The following compounds have already been identified in *T. polium* oil and listed as major components in at least one study: β-caryophyllene [4–8], germacrene D [5], limonene [5,9], p-cymene, 2,4-di-tert-butylphenol [9], α-pinene [6,10], α-thujene, terpinen4-ol [10], ledol oxide (II), linalyl acetate, β-eudesmol [11], α-cardinol, caryophyllene oxide, epi-α-muurolol, cadalene, longiverbenone, carvacrol [6], 11-acetoxyeudesman-4-α-ol, αbisabolol [7], β-pinene, α-muurolol, α-cadinol, α-muurolol, α-cardinol, α-cardinol [8], caryophyllene, γ-muurolene, cadinol, α-gurjunene, rosifoliol, 3-carene, γ-muurolene, α-phellandrene [12], carvacrol, torreyol [13], lycopersen, dodecane, 1,5-dimethyl decahydro naphthalene, tridecane [14], myrcene, menthofuran, ocimene, pulegone [15], β-eudesmol [16], β-pinene, limonene, α-phellandrene, linalool, terpinen-4-ol, γ- and δcadinenes, cedrol, cedrenol, and guaiol. In summary, more than 80 molecules have been identified in *T. polium* oils [17].

The essential oil of *T. polium*, with α-pinene, linalool, and caryophyllene oxide as its major components, demonstrates activity against Gram-positive bacteria (*Staphylococcus aureus* and *Staphylococcus epidermidis*) and Gram-negative bacteria [18]. Essential oils obtained from subspecies also show activity against *Acinetobacter baumannii* and *Staphylococcus aureus* [18].

T. polium is known for its antidiabetic effects through various mechanisms, such as increasing insulin secretion and levels, inducing the regeneration of pancreatic β-cells, reducing oxidative damage, promoting glucose uptake in muscle tissues, inhibiting αamylase activity, and enhancing GLUT-4 translocation [2]. The antidiabetic effect has also been observed in male Wistar rats induced with diabetes by STZ injection (60 mg/kg, i.p.) and treated with *Teucrium polium* extract (100,

200, and 400 mg/kg) via daily gavage for 6 weeks. The results showed that the group treated with the extract exhibited reductions in glucose, triglycerides, and serum cholesterol, in addition to an attenuation of oxidative stress in aortic and cardiac tissues [19].

Due to its antimicrobial and antidiabetic potential, as well as its variation in chemical composition, it is crucial to identify the possible pharmacological markers of the species and their potential mechanisms of action, toxicity, and other aspects. In this context, in silico studies prove to be an important tool for predicting molecular structures and potential mechanisms of action of such compounds, as this type of study allows for the computational simulation of compounds from databases to predict various parameters such as physicochemical, pharmacokinetic, and toxicological properties [20].

This work is based on the analysis of the essential oil (EO) extracted from *T. polium*, with the major molecules selected for investigation related to physicochemical, pharmacokinetic, and toxicological predictions, biological activities, and potential targets of action. Subsequently, molecular modeling of the selected compounds is performed.

Materials and Methods

Chemical Studies

2.1.1. Plant Material, and Extraction of the Essential Oil

The aerial parts of *T. polium* L. (Lamiaceae) were collected in April 2023 from Laghouat city (located in the south part of the Algerian Saharan Atlas); the GPS coordinates were 33°47′59″ N 2°51′54″ E. The plant material was taxonomically identified by the botanical survey, and its voucher specimen (LBAS Tp/04/23) was deposited in the Herbarium of the Laboratory of Biological and Agricultural Sciences, University of Amar Telidji, Laghouat, Algeria. After drying and grinding the plant, 100 g of powder was mixed with 1.5 L of distilled water in a round-bottomed flask and placed in a Clevenger-type apparatus for hydrodistillation. After 3 h, the essential oil was recuperated and stored in a sealed vial at 4 °C until analysis.

2.1.2. Chromatographic Analysis

For the analysis of the essential oil, a Shimadzu GCMS QP 2010 ULTRA (Kyoto, Japan) with an RXI-5MS capillary column (30 m × 0.25 mm inner diameter, film thickness 0.25 μm) was used. The percentage composition of the

essential oil was written by calculating gas chromatography flame ionization detection (GC-FID) peaks.

The RXI-5MS capillary column (30 m˙ × 0.25 mm i.d., film thickness 0.25 µm) was used with helium as the carrier gas. The injector temperature was 250 °C, and the split flow was 1 mL/min. The GC oven temperature was kept at 40 °C for 3 min, programmed to 240 °C at a rate of 4 °C/min, and then kept constant at 240 °C for 53 min. For chemical component identification, Wiley and NIST electronic libraries were used [21,22]. For this study, service was purchased from Kastamonu University Central Research Laboratory "MERLAB" in Turkey.

In Silico Evaluation

The molecules were drawn using the Marvin JS online program (https://marvinjsdemo.chemaxon.com/latest/demo.html (accessed on 1 October 2024) and saved in the

"Smiles" format for use on online servers (Table S1), while, for the determination of physicochemical properties, the online server Home-ADMElab was used (https://admet.scbdd. com) [23]. The Lipinski's rule of five or "Rule of Five" was considered [24]. For pharmacokinetic and toxicity predictions, the PreADMET program (version 2.0, Copyright © 2005–2017) was used, which considers pharmacokinetic properties (A—absorption; D—distribution; M—metabolism/biotransformation; E—excretion) and the evaluation of toxicity parameters (T—toxicity; PREADMET, 2020).

For the assessment of toxicity in marine organisms, the criteria used were as follows. For toxicity in algae [25], *Daphnia* sp. [26], medaka [27], and for [25], the mutagenicity risk was assessed by the Ames test with the following strains of *Salmonella typhimurium*: TA100-10RLI and TA 100-NA mutation in His G46e plasmid pKM101 without S9 and TA1535-10RLI and TA1535-NA mutation in His G46 [28].

The carcinogenic potential of the compounds was evaluated in rats and mice and referred to as (+) carcinogenic and (–) non-carcinogenic. To predict acute oral toxicity (lethal dose 50%-LD_{50}), the online software PROTOX II was used [29], considering the classification from I to VI [30]. Adverse events that may occur with the use of the molecules were also evaluated.

Molecular Target and Docking

Based on the results obtained from in silico studies, particularly regarding carcinogenicity and mutagenicity, the molecules myrtenal, myrtenol, and verbenol

were selected for docking. Initially, these molecules were submitted to the SuperPred Webserver [31], a validated server based on machine learning and similarity that utilizes the Smiles codes of promising molecules [32,33] (Table S1). The server predicts molecular targets with potential interactions with the investigated ligands that may be related to anti-inflammatory activity and cancer.

The only target that showed relevance for the investigated biological activity was the nuclear factor NF-kappa-B p105, obtained from the protein data bank (PDB ID 1SVC), as the compounds with this target achieved scores for therapeutic activity interaction (≥ 90% binding probability and ≥90% prediction accuracy). Other targets, such as DNA-(apurinic or apyrimidinic site) lyase and the LSD1/CoREST complex, were not used because, despite their potential therapeutic activity, they showed a binding probability and a prediction accuracy below 90%.

Initially, the molecular structures of parthenolide, myrtenal, myrtenol, and verbenol were retrieved from the PubChem database and optimized using the DFT/B3LYP/cc-pVDZ quantum method with the Gaussian 09 program. The crystallographic structure of the nuclear factor NF-kappa-B p105 enzyme was obtained from the protein data bank (PDB ID: 1SVC) [34]. This PDB structure consisted of 364 amino acids, corresponding to residues 2 to 365 of the full 968-amino-acid sequence [35]. Among the 968 residues, the domain spanning amino acids 42 to 367, known as the Rel homology domain (RHD), binds to DNA at the major groove and is responsible for the transcriptional activity of the protein. Therefore, this region represents a potential binding site for small molecules aimed at inhibiting DNA transcription and was selected as the protein's binding site, as proposed in the study [36].

Molecular docking was performed using the Molegro Virtual Docker (MVD) version 5.5 program [37]. The center of the sphere was defined with coordinates x: 40.37, y: 27.49, and z: 44.60, with a radius of 12 Å. The scoring function used was the MolDock Score. In addition, the inhibitor parthenolide [38] was included as a positive control in the study to enable a direct comparison of binding energy values and interactions with amino acid residues between the phytocompounds and this reference compound.

An analysis of intermolecular interactions was carried out using the Discovery Studio Visualizer (Dassault Systèmes BIOVIA, Discovery Studio Modeling Environment, version 2021, San Diego: Dassault Systèmes, 2021).

Molecular Dynamics

To gain further insights into the dynamic behavior and intermolecular interactions, the protein in its unbound form (apo) and in a complex with parthenolide (reference inhibitor), myrtenal, myrtenol, and verbenol was subjected to molecular dynamics (MD) simulations using the GPU-accelerated Amber22 software [39]. The restrained electrostatic potential (RESP) procedure was used to calculate the atomic charges of the ligands using the Gaussian 09 program at the HF/6-31G theory level [40]. The structures of the protein and the ligands were treated using the amber force field ff14SB and the general amber force field (GAFF), respectively [41,42]. The protonation states of the amino acid residues were calculated at pH 7.4 using the PDB2PQR server [43]. A TIP3P water box with a 12 Å radius was used to solvate the systems, and counterions were added to neutralize the system's charges. To neutralize the systems and maintain a physiological concentration (0.15 M), Na^+ and Cl^- ions were added [44].

Each solvated system was minimized in four stages: (i) ions and water molecules, (ii) hydrogen atoms, (iii) water molecules and hydrogen atoms, and (iv) the entire system. All steps were performed using 5000 steps with the steepest descent method and 5000 additional steps with the conjugate gradient algorithm. Subsequently, each system was heated for 200 ps to 300 K under a constant volume with positional restraints on the solute. An unrestrained equilibration step of 1 ns under a constant pressure was performed. Langevin dynamics was employed to control the temperature (300 K) with a collision frequency of 2 ps^{-1}. The SHAKE algorithm [44] was used to restrain the bond lengths involving hydrogen atoms, while the particle mesh Ewald (PME) method [45] was employed to handle long-range electrostatic interactions. A 10 Å cutoff was applied for non-bonded interactions.

Finally, 200 ns of production was conducted without positional restraints at a constant temperature of 300 K. The pressure was controlled by a Berendsen barostat. The structural analysis of each system was performed by calculating the root mean square deviations (RMSD) and the root mean square fluctuations (RMSF) of the backbone atoms of the protein.

MM-GBSA Binding Free Energy Calculation

To estimate the binding free energy (ΔGbind) of the compounds parthenolide, myrtenal, myrtenol, and verbenol with the nuclear factor NF-kappa-B p105 protein, we used the MM-GBSA method implemented in the AmberTools23 [46].

The calculations utilized the final 10 ns (1000 frames) of the MD simulation trajectories. Established literature provides detailed descriptions of the MM-GBSA equations [47,48].

Results

Characterization of T. polium Essential Oil

Thirty-three chemical compounds were identified, representing 92.62% of the *T. polium* essential oil from the aerial parts (Table 1, Figure 1). Generally, the total amounts of monoterpene hydrocarbons in the essential oil were higher than in other groups. In the characterization of *T. polium* oil, 14 molecules were identified with concentrations of 1% or greater (Figure 1), with the major compounds being fenchone (31.25%), 3-carene (15.77%), limonene oxide, cis- (9.77%), and myrcene (9.15%). An additional 10 compounds were present with concentrations of 1% or greater.

Table 1. Essential oil composition of the aerial parts of *Teucrium polium*.

	RRI	References	Compounds	RA (%)
1	946	939–957	Camphene	0.40
2	953	937–953	Verbenene	0.26
3	1008	997–1027	3-Carene	15.77
4	1009	990–1009	α-Phellandrene	0.75
5	1055	1059–1087	Fenchone	31.25
6	1064	1027–1050	β-Ocimene, (E)-	1.02
7	1089	1089	p-Cymene	0.65
8	1122	1106–1134	α-Campholenal	0.59
9	1132	1122–1144	Limonene oxide, cis-	9.77
10	1140	1140–1175	Myrcene	9.15
11	1146	1146	Verbenol	1.02
12	1150	1110–1150	δ-2-Carene	0.72
13	1160	1121–1158	Pinocarvone	0.91
14	1162	1147–1176	Linalool oxide	0.64
15	1165	1134–1165	cis-Verbenol	0.36
16	1169	1122–1169	3-Carene	0.80
17	1182	1182	cis-Pinocarveol	2.92
18	1186	1159–1191	α-Terpineol	0.46
19	1194	1169–1200	Myrtenol	1.47
20	1195	1171–1206	Myrtenal	2.31
21	1204	1190–1224	Verbenone	0.38
22	1235	1206–1235	Carvone	0.28
23	1254	1259–1284	Bornyl acetate	0.31
24	1270	1270–1302	Terpinen-4-ol acetate	0.54
25	1290	1290–1316	Myrtenyl acetate	0.70

26	1484	1458–1491	Germacrene D	2.56
27	1500	1474–1501	Bicyclogermacrene	1.56
28	1521	1508–1539	δ-Cadinene	1.18
29	1577	1562–1590	Spathulenol	1.47
30	1640	1610–1650	α-Muurolol, epi-	0.43
31	1649	1649–1686	α-Bisabolol	0.34

Table 1. *Cont.*

	RRI	References	Compounds	RA (%)
32	1654	1619–1662	α-Cadinol	0.35
33	1677	1676	(Z)-Nerolidyl acetate	1.30
		Grouped compounds (%)	Monoterpene hydrocarbons	43.15
			Oxygenated monoterpenes	43.74
			Sesquiterpenes hydrocarbons	5.73
			Total identified compounds (%)	92.62

RRI: Relative retention indices, RA (≥0.25): relative area (peak area relative to the total peak area) [49,50].

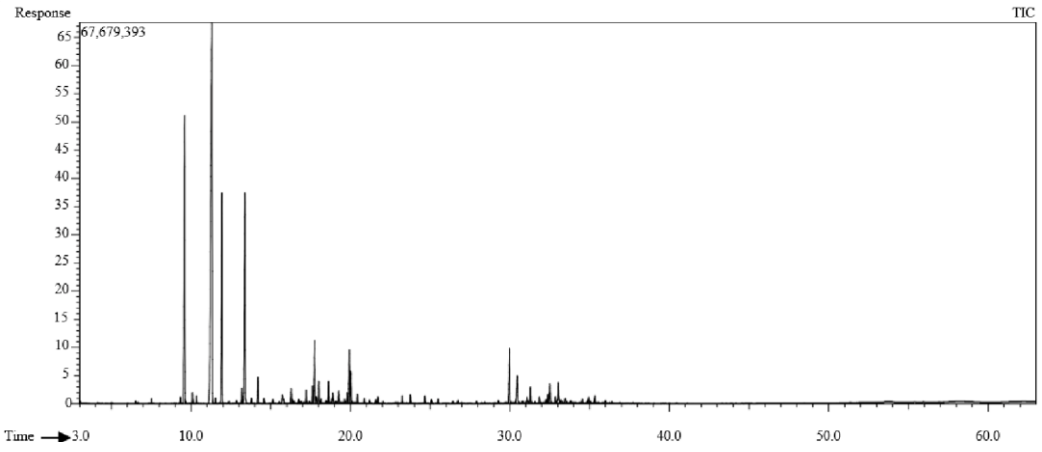

Figure 1. Gas chromatography flame ionization detector (GC-FID) profile of the essential oil of *Teucrium polium*.

In this study, terpenes were selected, including four monoterpenes (3-carene, Figure 2a; myrcene, Figure 2d; β-ocimene, Figure 2m, (E)-; verbenol, Figure 2n), five monoterpenoids (fenchone, Figure 2a; limonene oxide, cis-, Figure 2c; cis-pinocarveol, Figure 2e; myrtenal, Figure 2g; myrtenol, Figure 2i), three sesquiterpenes (germacrene D, Figure 2f; bicyclogermacrene, Figure 2h; δ-cadinene, Figure 2l), and two sesquiterpenoids (spathulenol, Figure 2j; (Z)-nerolidyl acetate, Figure 2k).

Predictions of Physicochemical, Pharmacokinetic, and Toxicity Aspects

No molecule violated Lipinski's rule with adaptation; however, it is worth noting that all exhibited very low polar surface areas (0 to 26.3 Å) and reduced numbers of hydrogen bond acceptors and donors (Table 2).

An analysis of the pharmacokinetic parameters suggests that all molecules had moderate permeability in Caco-2 cells, moderate-to-high permeability in MDCK cells, and high intestinal absorption. Some molecules appeared to have a low potential for binding to plasma proteins and a moderate distribution to the central nervous system (CNS) (3 and 7), while others, despite their high plasma protein binding, seemed to have a high potential for distribution to the CNS (4, 6, 8, 11, 12, 13, and 14). All molecules underwent phase 1 metabolism by CYP3A4 and inhibited at least one CYP enzyme (Table 3).

All molecules were shown to be toxic to some marine organisms; however, the molecules that appeared to have no mutagenic potential (6, 8, 10, 11, 12, and 13) were carcinogenic to mice and rats (6, 8, 11, 12, and 13) or only to rats (10). On the other hand, the molecules that were not carcinogenic to any animal species (5, 7, 9, and 14) showed mutagenic potential (Table 4). Considering all the evaluated toxicities, it can be suggested that, despite their mutagenic potential, molecules 5, 7, 9, and 14 were the most promising.

Table 2. Prediction of physicochemical properties.

Molecules	MM	LogP	TPSA	nHBA	nHBD
1	152.237	2.402	17.07	1	0
2	136.238	2.999	0.00	0	0
3	152.237	2.520	12.53	1	0
4	136.238	3.475	0.00	0	0
5	152.237	1.970	20.23	1	1
6	204.357	4.891	0.00	0	0
7	150.221	2.178	17.07	1	0
8	204.357	4.725	0.00	0	0
9	152.237	1.971	20.23	1	1
10	220.356	3.386	20.23	1	1
11	264.409	4.967	26.30	2	0
12	204.357	4.725	0.00	0	0
13	136.238	3.475	0.00	0	0
14	152.237	1.970	20.23	1	1

Lipinski's rule: LogP—oil–water partition coefficient ≤ 5; TPSA: topological polar surface area ≤ 140 Å; nHBA: number of hydrogen bond acceptors ≤ 10; nHBD: number of hydrogen bond donor groups ≤ 5; MM— molecular mass ≤ 500D [24]. 1—fenchone; 2—3-carene; 3—limonene oxide, cis-; 4—myrcene; 5—cis-pinocarveol; 6—germacrene D; 7—myrtenal; 8—bicyclogermacrene; 9—myrtenol; 10—spathulenol; 11—(Z)-nerolidyl acetate; 12—δ-cadinene; 13—β-ocimene, (E)-; 14—verbenol.

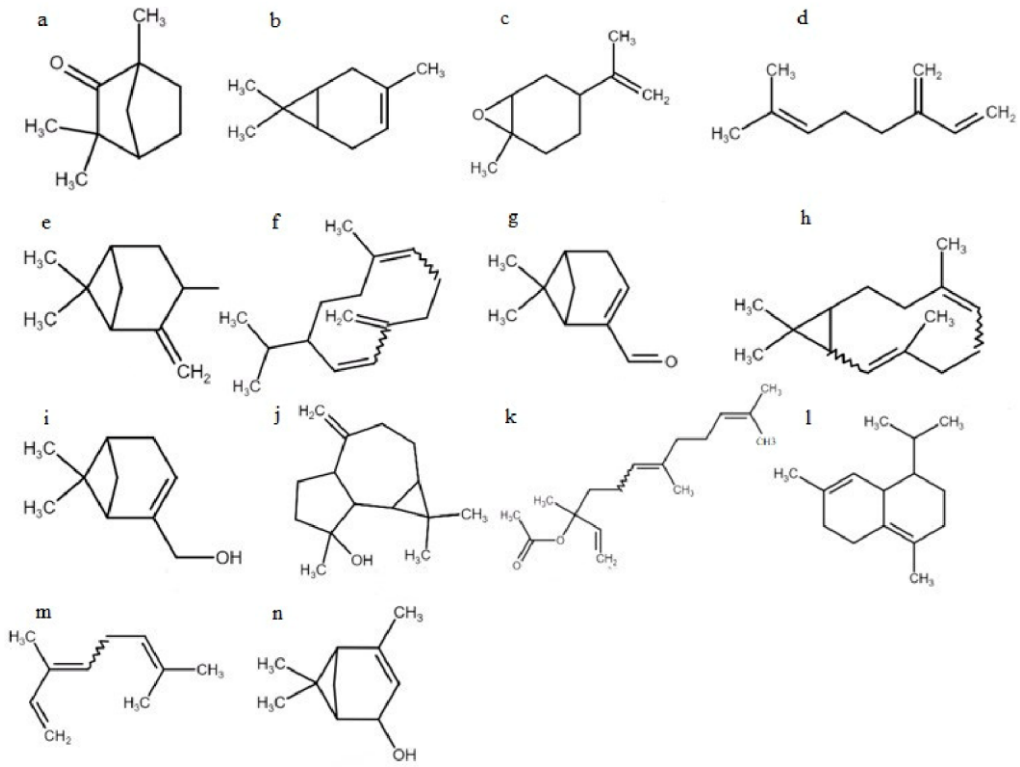

Figure 2. Molecules found in *T. polium* essential oil: (**a**)—fenchone; (**b**)—3-carene; (**c**)—limonene oxide, cis-; (**d**)—myrcene; (**e**)—cis-pinocarveol; (**f**)—germacrene D; (**g**)—myrtenal; (**h**)—bicyclogermacrene; (**i**)—myrtenol; (**j**)—spathulenol; (**k**)—(Z)-nerolidyl acetate; (**l**)—δ-cadinene; (**m**)—β-ocimene, (E)-; (**n**)—verbenol.

Another aspect evaluated was the potential acute oral toxicity of the molecule, with the highest LD50 found for compound 11 (Class VI). Other molecules exhibited an LD50 greater than 2000 mg/kg (1, 2, 7, 8, 10, 12, 13, and 14). The possible side effects of these molecules were also assessed, with no events reported for 3, 5, 6, 12, and 13 (Table 5).

Table 3. Prediction of pharmacokinetic properties.

	Absorption			Distribution		Metabolism	
Molecules	**MDCK**	**Caco 2**	**HIA**	**PP**	**BBB**	**CYP Inibition**	**CYP Phase 1**
1	M	M	H	H	M	2C9, 3A4	3A4
2	H	M	H	H	H	2C9	3A4
3	H	M	H	L	M	2C9, 3A4	W 3A4
4	H	M	H	H	H	2C9, 3A4	3A4
5	M	M	H	L	H	2C9, 3A4	W 3A4
6	M	M	H	H	H	2C9, 2C19	3A4
7	H	M	H	L	M	2C9	W 3A4
8	M	M	H	H	H	2C9	3A4
9	H	M	H	L	H	2C9	W 3A4
10	H	M	H	L	H	2C9, 3A4	3A4
11	M	M	H	H	H	2C19, 2C9, 3A4	3A4
12	M	M	H	H	H	2C19, 2C9	3A4
13	M	M	H	H	H	2C19, 2C9	3A4

14	H	M	H	H	H	2C9	W 3A4

M: medium; 1—fenchone; 2—3-carene; 3—limonen … nan intestinal absorption; W: wea … rveol; 6—germacrene δ-D; 7—myrtenal; 8—bicyclogermacrene; 9—myrtenol; 10— … -; 4—myrcene; 5—cis-pinoca … cadinene;

Table 4. Prediction of toxicity.

Molecules	Alga	Daphnia	Medaka Fish	Minnow Fish	Ames	Carcino Rato/Cam *
1	T	NT	VT	VT	TA1535_10RLI	N/P
2	T	NT	VT	VT	TA100_10RLI	N/P
3	T	NT	VT	VT	TA1535_10RL; 100_10RLI; 1535_NA	P/P
4	T	T	VT	VT	TA1535_NA	P/N
5	T	NT	VT	VT	TA100_10RLI; 1535_NA	N/N
6	T	T	VT	VT	N	P/P
7	T	NT	VT	VT	TA1535_10RLI; 100_10RLI	N/N
8	T	T	VT	VT	N	P/P
9	T	NT	VT	VT	TA1535_10RLI; 100_10RLI	N/N
10	T	T	VT	VT	N	P/N
11	T	T	VT	VT	N	P/P
12	T	T	VT	VT	N	P/P
13	T	T	VT	VT	N	P/P
14	T	NT	VT	VT	TA1535_10RLI; TA100_10RLI	N/N

T: toxic; NT: non-toxic; N: negative; P: positive. Parameters: algae—<1 mg/L toxic; >1 mg/L non-toxic [25]; daphnia test: < 0.22 µg/mL toxic; > 0.22 µg/mL—non-toxic [26]; test on medaka and minnow fish: < 1 mg/L—very toxic; 1–10 mg/L—toxic; 10–100 mg/L—harmful and > 100 mg/L—extremely toxic [27], carcino rat/mice * = carcinogenicity in rat/mice. T—toxic, NT—non-toxic, VT—very toxic, N—negative, P—positive. 1—fenchone; 2—3-carene; 3—limonene oxide, cis-; 4—myrcene; 5—cis-pinocarveol; 6—germacrene D; 7—myrtenal; 8—bicyclogermacrene; 9—myrtenol; 10—spathulenol; 11—(Z)-nerolidyl acetate; 12—δ-cadinene; 13—β-ocimene, (E)-; 14—verbenol.

Table 5. Prediction of oral toxicity.

Molecules	LD50 (mg/kg)	Toxicity Class	Side Effects
1	3087	V	I
2	2799	V	I/T
3	1447	IV	-
4	2561	V	I/T
5	1971	IV	-
6	1471	IV	-
7	2448	V	I
8	2766	V	I/T/M
9	1736	IV	I
10	3278	V	I/T
11	5923	VI	T

12	2090	V	-
13	2652	V	-
14	2280	V	I

LD50—lethal dose 50%. I—irritant, T—tumorigenic, M—mutagenicity. Category I: 1 < LD50 ≤ 5 mg/kg— extremely toxic; category II: 5 < LD50 ≤ 50 mg/kg—highly toxic; category III: 50 < LD50 ≤ 300 mg/kg— moderately toxic; category IV: 300 < LD50 ≤ 2000 mg/kg—low toxicity; category V: 2000 < LD50 ≤ 5000 unlikely to cause acute damage; category VI: DL50 > 5000 no damage. Source: [30] 1—fenchone; 2—3-carene; 3—limonene oxide, cis-; 4—myrcene; 5—cis-pinocarveol; 6—germacrene D; 7—myrtenal; 8—bicyclogermacrene; 9—myrtenol; 10—spathulenol; 11—(Z)-nerolidyl acetate; 12—δ-cadinene; 13—β-ocimene, (E)-; 14—verbenol.

Predictions of Potential Molecular Targets of Compounds in T. polium Essential Oil

Based on the studies of the physicochemical predictions, pharmacokinetics, and toxicity, it can be suggested that the most promising molecules were 7, 9, and 14. Subsequently, targets with potential for biological activity related to cancer (nuclear factor NF-kappa-B p105 subunit) were identified with a correction and precision probability greater than 90%, and the PDB (protein data bank) code (1SVC) for docking was obtained through the online server, as shown in Table 6.

Table 6. Molecular target assessment.

Molecules	Probability	Prediction Accuracy	Target Name	PDB
7	91.76%	96.09%	NF-kappa-B	1SVC
9	96.52%	96.09%	NF-kappa-B	1SVC
14	92.39%	96.09%	NF-kappa-B	1SVC

PDB: protein data bank; NF-kappa-B: nuclear factor NF-kappa-B p105 subunit; 7—myrtenal; 9—myrtenol; 14—verbenol.

Docking Molecular Simulation

The compounds myrtenal, myrtenol, and verbenol, as well as the reference inhibitor parthenolide, were evaluated for their interactions with the residues of the NF-κB protein. These interactions are crucial for understanding the ligands' affinity and specificity for the protein's active site. Parthenolide exhibited hydrogen bonds with the residues Gly68, Ser66, and Pro65, along with extensive van der Waals interactions with several residues such as Gly116, Gly141, and Val115, reinforcing its role as an established NF-κB protein inhibitor (Figure 3). In comparison, the compound myrtenal formed hydrogen bonds with the residues Arg57, Arg59, and Gly141, and alkyl-type interactions with Pro65 and Val115. This distribution of interactions suggests that myrtenal has a robust binding pattern similar to that of parthenolide, including critical interactions with Arg59 and Gly141 which may explain its higher stability observed in molecular dynamics analyses. Myrtenol interacted through hydrogen bonds with Tyr60 and Val61, while establishing pi–alkyl interactions with Arg59 and Val115 and alkyl

interactions with Phe56 and His67. Although myrtenol exhibited multiple interactions at the active site, the combination of these interactions appeared to induce greater structural instability, as observed in the molecular dynamics results (Figure 4).

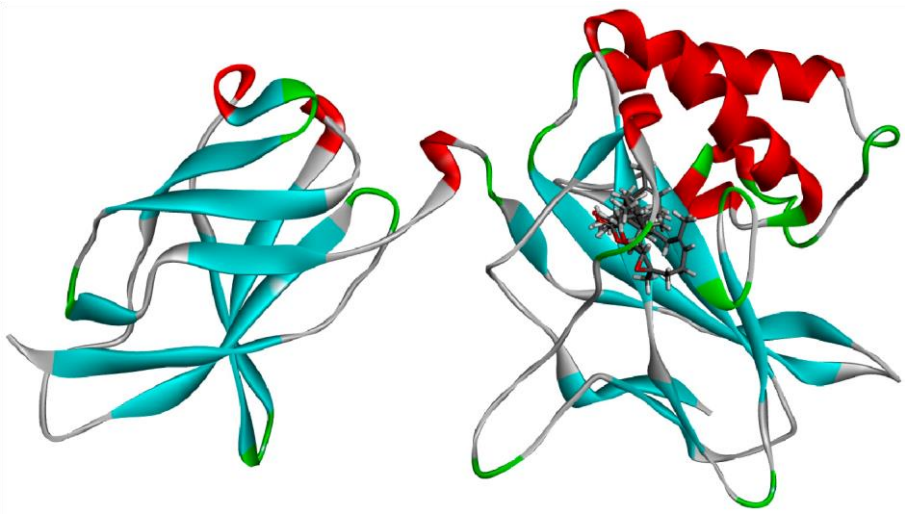

Figure 3. Illustration of the compounds docked on the active site of the NF-κB protein.

Verbenol, on the other hand, displayed hydrogen bonds with Pro65 and Gly68, as well as pi-alkyl interactions with Arg59 and alkyl interactions with Phe56, Val115, and Ile142. The interaction pattern of verbenol lies between that of myrtenal and myrtenol, highlighting its potential as a promising ligand, with a greater affinity for the active site than myrtenol but a lower dynamic stability compared to myrtenal (Figure 4).

Molecular Dynamics Result

The RMSD graph (Figure 5A) demonstrates the structural stability of the NF-κB protein in its unbound form (apo) and in complexes with the reference inhibitor parthenolide, as well as with the compounds myrtenal, myrtenol, and verbenol over 200 ns of simulations. It was observed that the complex with myrtenal presented the lowest average RMSD value

(4.11 Å), indicating a superior dynamic stability compared to the other ligands, including parthenolide (6.76 Å). This result suggests that myrtenal may interact very efficiently with the protein's active site, potentially on par with or better than the reference inhibitor. Myrtenol and verbenol exhibited average RMSD values of 5.44 Å and 7.29 Å, respectively, with myrtenol showing a greater structural instability, while verbenol displayed a behavior intermediate between that of myrtenol and that of parthenolide.

The RMSF graph (Figure 5B) corroborates these findings by revealing the protein's residual fluctuations in different regions. In the binding site region (residues 16–26), myrtenal demonstrated lower fluctuations compared to the other ligands, indicating a greater local stabilization capability. Parthenolide, although effective, exhibited slightly higher residual fluctuations in this region, highlighting the potential of the proposed molecules to achieve competitive or even superior performance. Myrtenol, on the other hand, induced more pronounced fluctuations in various regions, which may indicate fewer specific interactions or the need for more significant conformational adjustments to fit into the active site. Verbenol, with fluctuations similar to those of parthenolide, displayed a promising dynamic profile.

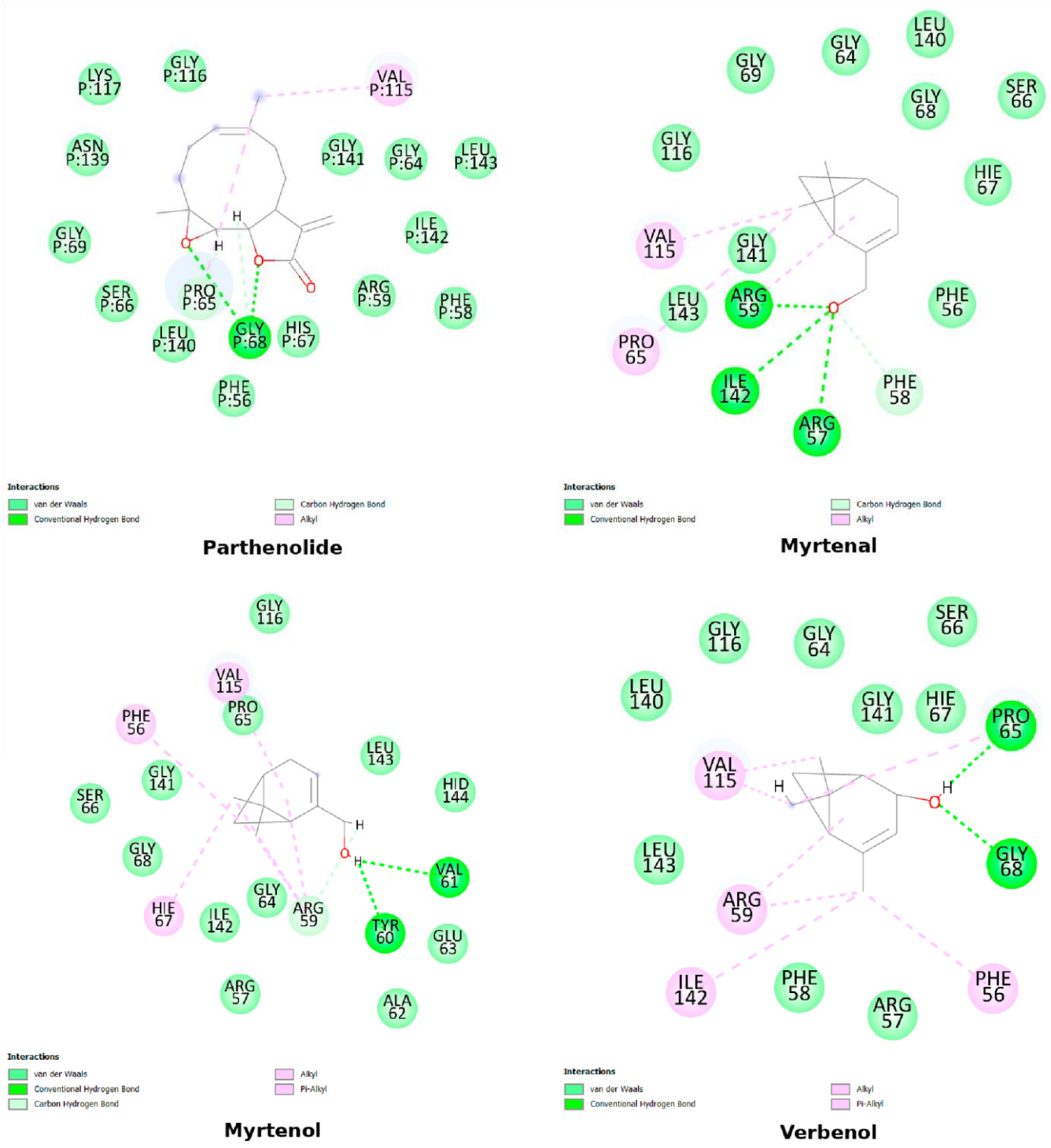

Figure 4. Representation of the 2D interactions of the molecules parthenolide, myrtenal, myrtenol, verbenol, and the protein nuclear factor NF-kappa-B. Image generated with Discovery Studio 3.5 Visualizer.

These data are particularly significant, as they highlight the potential of myrtenal, myrtenol, and verbenol as viable alternatives to the reference inhibitor parthenolide. While parthenolide is widely recognized as an effective NF-κB protein modulator, the proposed compounds, especially myrtenal, demonstrate dynamic properties that make them promising for therapeutic applications. Myrtenal's superior stability suggests that it could be explored as a highly

competitive candidate, offering a foundation for chemical optimizations and further studies.

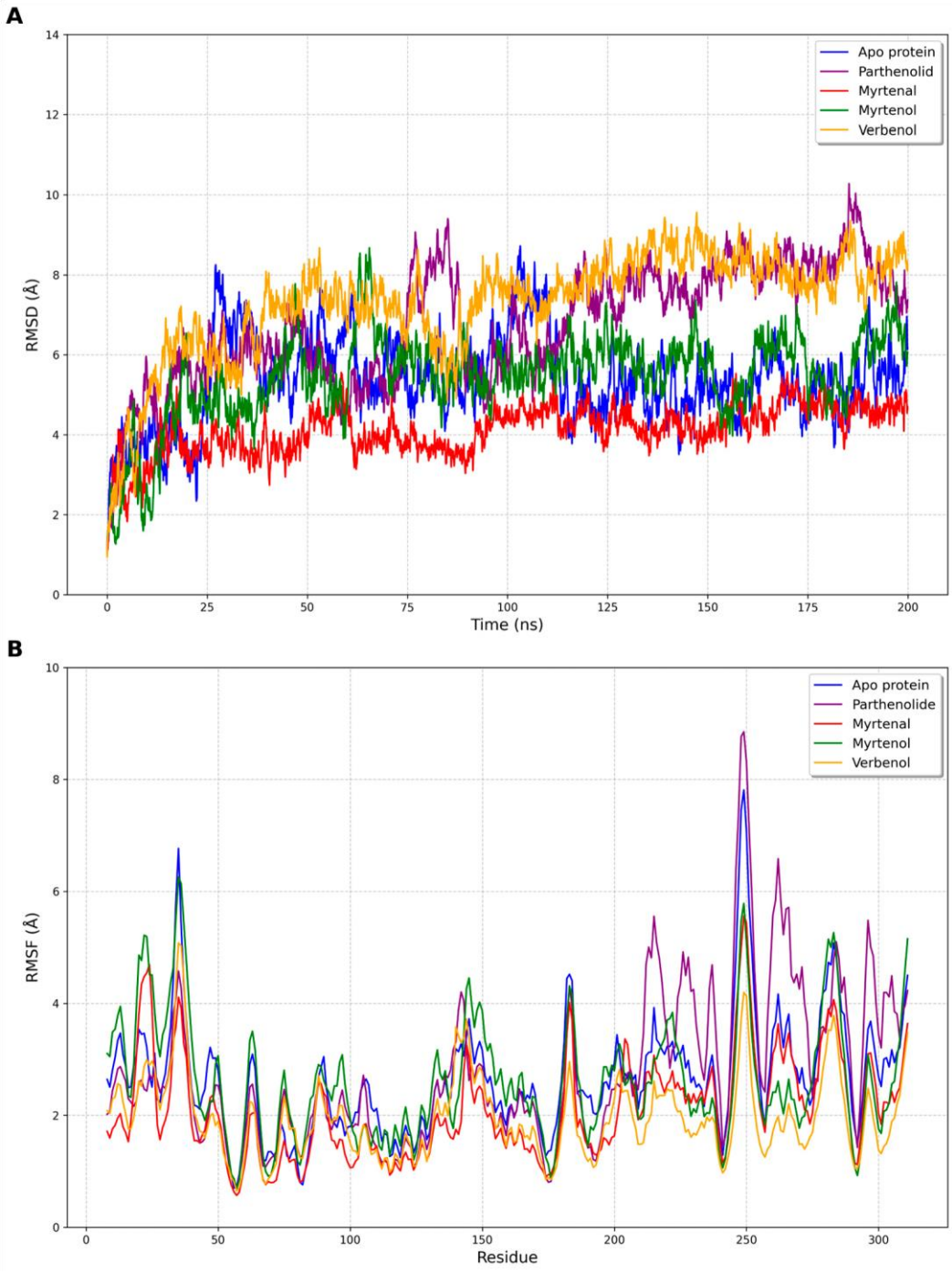

Figure 5. Chart of RMSD (**A**) and RSMF (**B**) of the apo form of the protein nuclear factor NF-kappa-B and complexed with parthenolide, myrtenal, myrtenol, and verbenol.

The RMSD graph (Figure 5A) illustrates the structural stability of the NF-κB protein in its unbound form (apo) and when complexed with parthenolide, myrtenal, myrtenol, and verbenol over 200 ns of simulations. The average RMSD values for the protein in the apo, parthenolide, myrtenal, myrtenol, and verbenol forms were 5.39 Å, 6.76 Å 4.11 Å, 5.44 Å, and 7.29 Å, respectively (Figure 5A). The myrtenal compound exhibited a greater stability and less fluctuations

compared to myrtenol and verbenol, with a value close to that of the apo protein, indicating that this compound is dynamically more efficient in stabilizing the protein.

The RMSF graph (Figure 5B) illustrates the average residual fluctuations over time for each residue of the protein in its different forms. It was observed that the largest

fluctuations were particularly pronounced in specific residues, especially between residues 32–37 and residues 246–253, corresponding to loop regions, which are more flexible. In the region where the ligand was accommodated, between residues 16–26, there was a lower fluctuation level in the complex with myrtenal, a phenomenon which is consistent with the RMSD data. Notably, the complex with myrtenol showed the highest fluctuations in several regions of the protein, corroborating the RMSD observation that this ligand induces a greater structural instability. The fluctuations observed in the complexes with myrtenal and verbenol were comparable to and smaller than those with myrtenol, suggesting that these ligands have a lesser impact on the protein's dynamics.

The greater instability observed with myrtenol may be associated with a weaker or less specific binding to the active site or to the induction of larger conformational adjustments in the protein to accommodate the ligand. In contrast, the relatively stable behavior of the protein in complexes with myrtenal and verbenol suggests that these ligands are more compatible with the active site, resulting in smaller conformational fluctuations. These data are crucial for understanding the structure–function relationship and can guide future studies in the chemical modification of these ligands to enhance their efficacy and specificity.

MM-GBSA Binding Energies

The binding energies (ΔGbind) were calculated for the parthenolide-1SVC, myrtenal1SVC, myrtenol-1SVC, and verbenol-1SVC complexes using the MM-GBSA method. The interaction energy components, including the van der Waals energies (ΔEvdw), electrostatic energies (ΔEele), polar solvation free energy (ΔGGB), and apolar solvation free energy (ΔGSA), were analyzed for each complex (Table 7).

Table 7. Binding energies and their components calculated by MM-GBSA (in kcal/mol).

Complex	ΔEvdw	ΔEele	ΔG_{GB}	ΔG_{SA}	ΔG_{bind}
Parthenolide	-24.24 ± 2.72	0.10 ± 3.25	-24.14 ± 5.15	8.67 ± 3.65	-15.47 ± 2.25
Myrtenal-1SVC	-8.92 ± 2.99	-98.53 ± 8.44	81.12 ± 5.85	-107.46 ± 7.33	-26.33 ± 3.57
Myrtenol-1SVC	-5.59 ± 2.89	-58.77 ± 8.62	40.73 ± 5.94	-58.37 ± 7.47	-17.64 ± 3.65
Verbenol-1SVC	-17.01 ± 2.59	-81.45 ± 8.51	76.32 ± 7.24	-98.46 ± 8.28	-22.14 ± 3.36

The results show that the myrtenal-1SVC complex presented the most favorable binding energy (ΔGbind = −26.33 ± 3.57 kcal/mol), followed by verbenol-1SVC (ΔGbind = −22.14 ± 3.36 kcal/mol) and myrtenol-1SVC (ΔGbind = −17.64 ± 3.65 kcal/mol). These values indicate that myrtenal forms the most stable complex with the 1SVC protein, a finding which is consistent with the lower conformational fluctuations observed in the RMSD and RMSF data, suggesting a strong interaction of this compound with the protein's interaction site.

Comparatively, parthenolide (the reference inhibitor) exhibited a binding energy of ΔGbind = −15.47 ± 2.25 kcal/mol, which is superior in stability compared to that of myrtenol but inferior to that of myrtenal and verbenol. This difference suggests that, while parthenolide interacts effectively with the protein, the compounds myrtenal and verbenol exhibited stronger and more stable binding affinities.

The analysis of the energy components revealed that, in all complexes, electrostatic energy (ΔEele) played a predominant role in stabilizing ligand–protein interactions, especially in the case of myrtenal-1SVC, which showed the most negative ΔEele value (−98.53 ± 8.44 kcal/mol). However, this strong electrostatic contribution was partially counterbalanced by polar solvation energy (ΔGGB), which was higher for myrtenal, indicating that the electrostatic interactions were strongly solvated.

The MM-GBSA analysis results reinforce the observations from the RMSD and RMSF analyses. Myrtenal, which showed the most negative free binding energy

(−26.33 ± 3.57 kcal/mol), also induced the lowest structural fluctuations, suggesting a combination of strong interactions and dynamic conformational fit. Verbenol, with a free binding energy of −22.14 ± 3.36 kcal/mol, provided a better conformational stability than myrtenol, as observed in the RMSD and RMSF analyses, indicating that, while its binding affinity is lower than that of myrtenal, it still presents a good potential for protein modulation.

These results indicate that both myrtenal and verbenol stand out as compounds with a stronger inhibition potential relative to NF-κB compared to parthenolide, with myrtenal showing the highest potential, followed by verbenol, while myrtenol exhibited a less stable interaction profile.

Discussion

The essential oil obtained from *T. polium* was subjected to GC-MS analysis, revealing the major constituents as fenchone (31.25%), 3-carene (15.77%), limonene oxide, cis- (9.77%), and myrcene (9.15%). When comparing these results to other studies, it is observed that other metabolites such as β-caryophyllene [3], limonene [10], ledene oxide II [11], α-cardinol [51], carvacrol [6], and β-pinene were the major constituents [52]. Studies on the environmental impact on the composition of *T. polium* oil are still scarce; however, it is known that factors such as altitude, water availability, macro and micronutrients in the soil, relative air temperature, and soil pH directly affect the chemical profile of plants [53].

Myrcene was reported in previous studies as the major component of the essential oil of *T. polium* [54–58]. Myrcene was found to be the major compound in our study, too. However, the main constituents of the essential oils of the aerial parts were oxygenated monoterpenes and monoterpene hydrocarbons, findings which are in good agreement with the previous reports [54,59–62].

On the other hand, germacrene D was detected as a major compound in the essential oil of *T. polium* samples from different

regions [58,60,63–65]. Similarly, germacrene D was detected as the main compound in our study. While fenchone, 3-carene, limonene oxide, and cis- were found to be the main compounds in our study, they were minor or absent in essential oils of *Teucrium* [10,63,66]. Therefore, environmental factors, the plant part used in the extraction process, and the collection time can influence the chemical composition of the essential oil.

All selected molecules adhered to Lipinski's rule and appeared to exhibit high intestinal absorption. However, only molecules 2, 4, 5, 6, 8–14 were distributed to the CNS. Adhering to Lipinski's rule is crucial for drug candidates, as it indicates that the drug will be well absorbed in the gastrointestinal tract and adequately distributed throughout the body, allowing for oral administration [24,32,67].

All molecules seemed to be metabolized by CYP3A4, but they inhibited CYP and, sometimes, more than one CYP. Molecules that inhibit CYP can interfere with the metabolism of other drugs, necessitating dose adjustments. Another evaluated parameter was toxicity, with 8, 10, 11, 12, 13 not being mutagenic, while 7, 9, and 14 were not carcinogenic. Unfortunately, no compound was devoid of toxicity; however, all compounds had an LD50 > 1400 mg/kg. Therefore, repeated-dose toxicity studies, in vivo genotoxicity, and in vivo carcinogenicity studies are important for understanding toxic effects and potential mechanisms.

After analyzing the pharmacokinetic studies and toxicities, molecules without carcinogenic potential were selected (7—myrtenal; 9—myrtenol; 14—verbenol). Myrtenal exhibited antihyperglycemic effects, reducing blood glucose levels and hemoglobin A1C and aiding in weight recovery [68]. Derivatives of myrtenal have shown activity against various cell lines [68–71].

Other activities related to myrtenal derivatives include anxiolytic [72], antiviral [72], antifungal [73], and analgesic [74]. Another selected molecule was myrtenol, which inhibits biofilm formation and virulence in the drug-resistant *Acinetobacter baumannii*. Myrtenol improves the susceptibility of BP-AB to the antibiotic's

amikacin, piperacillin/tazobactam, cefoperazone/sulbactam, and ceftazidime. This molecule regulates the expression of biofilm-associated genes in the BP-AB strain, and qPCR analysis has been shown to reduce the expression levels of bfmR, bap, csuA/B, and ompA in groups D, E, and F compared to groups A, B, and C. A non-significant reduction in bfmR, bap, csuA/B, and ompA levels has also been found in groups A, B, and C. The genes bfmR, bap, csuA/B, and ompA are key regulators of the transition from biofilm formation to maturation in the BP-AB strain [75]. Myrtenol protects against myocardial ischemia–reperfusion injury through antioxidant and anti-apoptotic mechanisms [76], while verbenol exhibits anti-ischemic and anti-inflammatory properties [77].

To identify the potential target involved in the biological activity of myrtenal, myrtenol, and verbenol, prediction studies have been conducted, suggesting that all three bind to the nuclear factor NF-kappa-B, a family of transcription factors involved in inflammation, immunity, cell proliferation, differentiation, and survival [78]. In recent years, the presence and activation of the nuclear factor NF-kappa-B in different types of cancer have been highlighted, as well as the importance of developing inhibitors that act directly on the nuclear factor NF-kappa-B [79]. The possibility of therapeutically targeting this factor allows for a significant advance in tumor destruction during treatment, thereby enhancing antitumor activity [80].

It is worth highlighting the medicinal importance of *Teucrium* species, which have been used since ancient times in the Mediterranean region for treating gastrointestinal issues and maintaining healthy endocrine gland functions, as well as treating malaria and severe dermatological disorders. However, studies evaluating their activity are scarce. Evaluations of the essential oils and ethanolic extracts of *Teucrium polium* and *Teucrium parviflorum* have shown that the extracts exhibit antioxidant, anti-butyrylcholinesterase, anti-tyrosinase, and anti-urease activities

through in vitro and in silico assays [81]. It is noteworthy that *T. polium* oil demonstrates a moderate antioxidant potential [82].

An in vivo study with the ethanolic extract of *T. polium* demonstrated the plant's antiinflammatory potential at concentrations of 50 mg/kg, 100 mg/kg, and 150 mg/kg, leading to a reduction in paw edema in rats [83]. When correlating this result with prediction studies, the regulation of NF-κB activity is crucial to prevent chronic inflammation, meaning that substances with anti-inflammatory activity can suppress NF-κB activation or interfere with its translocation to the nucleus, reducing the expression of inflammatory genes [79]. In addition to its involvement in the inflammatory process, NF-kappa-B (NF-κB) is involved in cell proliferation, apoptosis (programmed cell death), stress response, and other aspects relevant to cancer development and progression [80].

It should be noted that the chronic inflammation process favors mutations, uncontrolled cell proliferation, and resistance to apoptosis, all of which are processes that can facilitate carcinogenesis [84]. Furthermore, NF-κB induces the production of the vascular endothelial growth factor (VEGF) and regulates molecules involved in cell mobility and tissue invasion, such as matrix metalloproteinases (MMPs) [85,86]. Considering this, it can be suggested that these molecules hold promise as antitumor and anti-inflammatory agents, and in vitro and in vivo studies are necessary to determine the best therapeutic use for these molecules.

The results obtained in the present study demonstrate that the compounds myrtenal, myrtenol, and verbenol exhibit significant interactions with the active site residues of the NF-κB protein, with binding patterns comparable to those of the reference inhibitor parthenolide. These interactions are particularly relevant, considering that the NF-κB protein plays a central role in regulating inflammatory responses and is associated with various pathologies such as cancer, autoimmune diseases, and chronic inflammation

[87]. The presence of strong interactions with critical residues in the active site suggests that the tested compounds have the potential to modulate NF-κB activity, influencing the transcription of genes involved in inflammation and disease development.

Previous docking studies of the DNA-NF-κB protein have revealed that the compounds myrtenal, myrtenol, and verbenol bind to the same pocket where the DNA interacts, a crucial point for stabilizing the ligand–protein complex. This binding at the DNA interaction site is fundamental, as it blocks the nuclear translocation of the NF-κB transcription factor, preventing its activation and subsequent expression of inflammatory genes. These findings are consistent with results described in the literature, indicating that compounds with interaction patterns similar to those of parthenolide have a greater potential as NF-κB inhibitors [36]. The similarity of the interactions with key residues at the protein's active site and the ability to block its nuclear translocation reinforce the idea that the studied compounds may represent promising strategies for developing new therapeutic agents targeting inflammatory diseases and other conditions associated with exacerbated NF-κB activation.

The results highlight myrtenal as the most promising compound among those tested, with interactions similar to those of parthenolide, including critical residues at the active site of the NF-κB protein. This underscores its potential as an effective and stable ligand, potentially contributing to the functional inhibition of NF-κB.

Conclusions

Based on the results of the molecular docking, molecular dynamics, and free energy calculations, this study suggests that the most promising compounds for modulating the NF-κB protein are myrtenal and verbenol, with myrtenal standing out due to its high stability and binding affinity to the protein's active site. Myrtenal exhibited the most negative binding energy value (ΔGbind = −26.33 ± 3.57 kcal/mol), indicating a strong and stable interaction with the

protein which was corroborated by molecular dynamics simulations revealing lower structural fluctuations (RMSD and RMSF) compared to other compounds, including parthenolide, the reference inhibitor.

Furthermore, the docking data and molecular interaction analysis indicated that myrtenal and verbenol exhibit robust binding patterns, with critical interactions with key residues of the NF-κB protein. These compounds demonstrated not only significant inhibition potential against NF-κB, but also lower conformational instability, suggesting they are viable alternatives for the development of anti-inflammatory and antitumor therapies.

Based on these results, additional chemical studies will be conducted to isolate the priority molecules from the essential oil of *T. polium*. After isolation, in vitro assays will be planned, including evaluations of cytotoxicity, genotoxicity, mutagenicity, and mechanisms of cell death. The active compound with the lowest toxic potential will be subjected to studies to assess its mechanisms of action, followed by structural modifications to optimize its inhibitory potential and reduce toxicity.

The final phase of pharmacological studies will involve in vivo testing (toxicity and activity) to establish dose–response correlations. If the pharmacological potential is confirmed, it will be possible to move forward with product development. In summary, the essential oil of *T. polium*, due to its composition, shows great promise as an anti-inflammatory and antitumor agent, with the potential for new treatments based on the compounds myrtenal and erbenol.

Supplementary Materials: The following supporting information can be downloaded at: https://www.mdpi.com/article/10.3390/cimb47010048/s1.

Author Contributions: B.B.: Investigation, writing—review and editing. F.B.: supervision, writing—review and editing. M.F.D.: methodology, supervision, writing—review and editing, funding acquisition. N.G.: methodology, writing—review and editing. O.E.: methodology, writing—review and editing. V.R.S.M.: methodology, writing—review and editing. R.A.d.C.: formal analysis, methodology, software, writing—review and editing. R.C.d.B.: formal analysis,

investigation, methodology, software, writing—original draft, writing—review and editing. S.D.P.F.: data curation, writing—review and editing. All authors have read and agreed to the published version of the manuscript.

Funding: The authors declare that financial support was received for the research, authorship, and/or publication of this article. The Dean of Research and Postgraduate Studies at the State University of Pará provided payment for the processing and publication of this article—Notice 01/2025—PAPQ/PROPESP.

Institutional Review Board Statement: Not applicable.

Informed Consent Statement: Not applicable.

Data Availability Statement: Data is contained within the article and Supplementary Materials.

Acknowledgments: The authors thank PAPQ/PROPESP/UFPA. Additionally, FAPESPA/CAPES which supports the first author as a FAPESPA/CAPES-BRAZIL Fellow.

Conflicts of Interest: The authors declare no conflicts of interest.

References

1. Abdollahi, M.; Karimpour, H.; Monsef-Esfehani, H.R. Antinociceptive Effects of *Teucrium polium* L. Total Extract and Essential Oil in Mouse Writhing Test. *Pharmacol. Res.* **2003**, *48*, 31–35. [CrossRef]
2. Bahramikia, S.; Yazdanparast, R. Phytochemistry and Medicinal Properties of *Teucrium polium* L. (Lamiaceae). *Phytother. Res.* **2012**, *26*, 1581–1593. [CrossRef] [PubMed]
3. Bahramikia, S.; Gavyar, P.H.H.; Yazdanparast, R. *Teucrium polium* L.: An Updated Review of Phytochemicals and Biological activities. *Avicenna J. Phytomed.* **2022**, *12*, 224–240. [CrossRef]
4. Vokou, D.; Bessiere, J.M. Volatile Constituents of *Teucrium polium*. *J. Nat. Prod.* **1985**, *48*, 498–499. [CrossRef]
5. Bezic´, N.; Vuko, E.; Dunkic´, V.; Rušcˇic´, M.; Blaževic´, I.; Burcˇul, F. Antiphytoviral Activity of Sesquiterpene-Rich Essential Oils from Four Croatian *Teucrium* Species. *Molecules* **2011**, *16*, 8119–8129. [CrossRef]
6. Essid, R.; Rahali, F.Z.; Msaada, K.; Sghair, I.; Hammami, M.; Bouratbine, A.; Aoun, K.; Limam, F. Antileishmanial and Cytotoxic Potential of Essential Oils from Medicinal Plants in Northern Tunisia. *Ind. Crop. Prod.* **2015**, *77*, 795–802. [CrossRef]
7. Sayyad, R.; Farahmandfar, R. Influence of *Teucrium polium* L. Essential Oil on the Oxidative Stability of Canola Oil During Storage. *J. Food Sci. Technol.* **2017**, *54*, 3073–3081. [CrossRef] [PubMed]
8. Masoudi, S. Volatile Constituents from Different Parts of Three Lamiacea Herbs from Iran. *Iran J. Pharm. Res.* **2018**, *17*, 365–376. [PubMed]
9. Vahdani, M.; Faridi, P.; Zarshenas, M.M.; Javadpour, S.; Abolhassanzadeh, Z.; Moradi, N.; Bakzadeh, Z.; Karmostaji, A.;
   Mohagheghzadeh, A.; Ghasemi, Y. Major Compounds and Antimicrobial Activity of Essential Oils from Five Iranian Endemic Medicinal Plants. *Pharmacogn. J.* **2011**, *3*, 48–53. [CrossRef]
10. Djabou, N.; Lorenzi, V.; Guinoiseau, E.; Andreani, S.; Giuliani, M.-C.; Desjobert, J.-M.; Bolla, J.-M.; Costa, J.; Berti, L.; Luciani,
    A.; et al. Phytochemical Composition of Corsican Teucrium Essential Oils and Antibacterial Activity Against Foodborne or Toxi-Infectious Pathogens. *Food Control.* **2013**, *30*, 354–363. [CrossRef]
11. Hussain, J.; Rehman, N.U.; Al-Harrasi, A.; Ali, L.; Khan, A.L.; Albroumi, M.A. Essential Oil Composition and Nutrient Analysis of Selected Medicinal Plants in Sultanate of Oman. *Asian Pac. J. Trop. Dis.* **2013**, *3*, 421–428. [CrossRef]
12. El Atki, Y.; Aouam, I.; El Kamari, F.; Taroq, A.; Lyoussi, B.; Taleb, M.; Abdellaoui, A. Total Phenolic and Flavonoid Contents and
    Antioxidant Activities of Extracts from *Teucrium polium* Growing Wild in Morocco. *Mater. Today Proc.* **2019**, *13*, 777–783. [CrossRef]
13. Fitsiou, E.; Pappa, A. Anticancer Activity of Essential Oils and Other Extracts from Aromatic Plants Grown in Greece. *Antioxidants*
    2019, *8*, 290. [CrossRef]

14. Ebadollahi, A.; Taghinezhad, E. Modeling and Optimization of the Insecticidal Effects of *Teucrium polium* L. Essential Oil Against
Red Flour Beetle (*Tribolium castaneum* Herbst) Using Response Surface Methodology. *Inf. Process. Agric.* **2020**, *7*, 286–293. [CrossRef]
15. Wassel, G.M.; Ahmed, S.S. On the Essential Oil of *Teucrium polium* L. *Pharmazie* **1974**, *29*, 351–352.
16. Ghiglione, C.; Lemordant, D.; Gast, M. The Chemical Composition of *Teucrium polium* ssp. Cylindricum. Characterization of Alkanes and of Beta-Eudesmol. *Plantes Med. Phytother.* **1976**, *10*, 221–232.
17. Cozzani, S.; Muselli, A.; Desjobert, J.-M.; Bernardini, A.-F.; Tomi, F.; Casanova, J. Chemical Composition of Essential Oil of *Teucrium polium* subsp. *capitatum* (L.) from Corsica. *Flavour Fragr. J.* **2005**, *20*, 436–441. [CrossRef]
18. Moghtader, M.; Salari, H.; Farahmand, A. Anti-Bacterial Effects of the Essential Oil of *Teucrium polium* L. on Human Pathogenic Bacteria. *Iran. J. Med. Microbiol.* **2013**, *7*, 1–7.
19. Zabihi, N.A.; Mousavi, S.M.; Mahmoudabady, M.; Soukhtanloo, M.; Sohrabi, F.; Niazmand, S. *Teucrium polium* L. Improves Blood
Glucose and Lipids and Ameliorates Oxidative Stress in Heart and Aorta of Diabetic Rats. *Int. J. Prev. Med.* **2018**, *9*, 110. [PubMed]
20. Shaker, B.; Ahmad, S.; Lee, J.; Jung, C.; Na, D. In Silico Methods and Tools for Drug Discovery. *Comput. Biol. Med.* **2021**, *137*, 104851. [CrossRef] [PubMed]
21. McLafferty, F.W.; Stauffer, D.B.; Stenhagen, E.; Heller, S.R. *The Wiley/NBS Registry of Mass Spectral Data*; NDL Search: Tokyo, Japan, 1989.
22. Linstrom, P.J. NIST Standard Reference Database Number 69. In *NIST Chemistry WebBook*; NIST: Gaithersburg, MD, USA, 2003.
23. Dong, J.; Wang, N.-N.; Yao, Z.-J.; Zhang, L.; Cheng, Y.; Ouyang, D.; Lu, A.-P.; Cao, D.-S. ADMETlab: A Platform for Systematic ADMET Evaluation Based on a Comprehensively Collected ADMET Database. *J. Chemin.* **2018**, *10*, 29. [CrossRef]
24. Lipinski, C.A. Lead- and Drug-like Compounds: The Rule-of-Five Revolution. *Drug Discov. Today Technol.* **2004**, *1*, 337–341. [CrossRef]
25. Costa, C.R.; Olivi, P.; Botta, C.M.R.; Espindola, E.L.G. A Toxicidade Em Ambientes Aquáticos: Discussão e Métodos de Avaliação. *Quim. Nova.* **2008**, *31*, 1820–1830. [CrossRef]
26. Guilhermino, L.; Diamantino, T.; Silva, M.C.; Soares, A. Acute Toxicity Test with *Daphnia magna*: An Alternative to Mammals in the Prescreening of Chemical Toxicity? *Ecotoxicol. Environ. Saf.* **2000**, *46*, 357–362. [CrossRef]
27. Zucker, E. *Hazard Evaluation Division Standard Evaluation Procedure: Acute Toxicity Test for Freshwater Fish*; US Environmental Protection Agency, Office of Pesticide Programs: Washington, DC, USA, 1985.
28. Ames, B.N.; McCann, J.; Yamasaki, E. Methods for Detecting Carcinogens and Mutagens with the Salmonella/MammalianMicrosome Mutagenicity Test. *Mutat. Res.* **1975**, *31*, 347–363. [CrossRef] [PubMed]
29. Drwal, M.N.; Banerjee, P.; Dunkel, M.; Wettig, M.R.; Preissner, R. ProTox: A Web Server for the In Silico Prediction of Rodent Oral Toxicity. *Nucleic Acids Res.* **2014**, *42*, W53–W58. [CrossRef] [PubMed]
30. Associação Brasileira de Normas Técnicas. *NBR14725-2: Produtos Químicos—Informações Sobre Segurança, Saúde e Meio Ambiente. Parte 2: Sistema de Classificação de Perigo*; ABNT: São Paulo, Brazil, 2019.
31. Nickel, J.; Gohlke, B.-O.; Erehman, J.; Banerjee, P.; Rong, W.W.; Goede, A.; Dunkel, M.; Preissner, R. SuperPred: Update on Drug Classification and Target Prediction. *Nucleic Acids Res.* **2014**, *42*, W26–W31. [CrossRef]
32. de Barros, R.C.; Araujo da Costa, R.; Farias, S.D.P.; de Albuquerque, K.C.O.; Marinho, A.M.R.; Campos, M.B.; Marinho, P.S.B.; Dolabela, M.F. In Silico Studies on Leishmanicide Activity of Limonoids and Fatty Acids from Carapa Guianensis Aubl. *Front. Chem.* **2024**, *12*, 1394126. [CrossRef]
33. Gallo, K.; Goede, A.; Preissner, R.; Gohlke, B.-O. SuperPred 3.0: Drug Classification and Target Prediction—A Machine Learning Approach. *Nucleic Acids Res.* **2022**, *50*, W726–W731. [CrossRef] [PubMed]
34. Müller, C.W.; Rey, F.A.; Sodeoka, M.; Verdine, G.L.; Harrison, S.C. Structure of the NF-KB P50 Homodimer Bound to DNA. *Nature* **1995**, *373*, 311–317. [CrossRef] [PubMed]
35. Bateman, A.; Martin, M.J.; Orchard, S.; Magrane, M.; Agivetova, R.; Ahmad, S.; Alpi, E.; Bowler-Barnett, E.H.; Britto, R.; Bursteinas, B.; et al. UniProt: The Universal Protein Knowledgebase in 2021. *Nucleic Acids Res.* **2021**, *49*, D480–D489. [CrossRef]
36. Jain, P.; Sudandiradoss, C. Andrographolide-Based Potential anti-Inflammatory Transcription Inhibitors Against Nuclear Factor

NF-Kappa-B P50 Subunit (NF-KB P50): An Integrated Molecular and Quantum Mechanical Approach. *3 Biotech* **2023**, *13*, 15. [CrossRef]

37. Bitencourt-Ferreira, G.; de Azevedo, W.F. Molegro Virtual Docker for Docking. In *Docking Screens for Drug Discovery*; Springer Nature: New York, NY, USA, 2019; pp. 149–167.
38. Dai, Y.; Guzman, M.L.; Chen, S.; Wang, L.; Yeung, S.; Pei, X.; Dent, P.; Jordan, C.T.; Grant, S. The NF (Nuclear Factor)-KB Inhibitor Parthenolide Interacts with Histone Deacetylase Inhibitors to Induce MKK7/JNK1-Dependent Apoptosis in Human Acute Myeloid Leukaemia Cells. *Br. J. Haematol.* **2010**, *151*, 70–83. [CrossRef]
39. Case, D.A.; Aktulga, H.M.; Belfon, K.; Ben-Shalom, I.; Brozell, S.R.; Cerutti, D.S.; Cheatham, T.E., III; Cruzeiro, V.W.D.; Darden, T.A.; Duke, R.E. *Amber 2021*; University of California: San Francisco, CA, USA, 2021.
40. Frisch, M.; Trucks, G.W.; Schlegel, H.B.; Scuseria, G.E.; Robb, M.A.; Cheeseman, J.R.; Scalmani, G.; Barone, V.; Mennucci, B.; Petersson, G.A. *Gaussian 09*; Gaussian Inc.: Wallingford, CT, USA, 2009; Volume 121, pp. 150–166.
41. Wang, J.; Wolf, R.M.; Caldwell, J.W.; Kollman, P.A.; Case, D.A. Development and Testing of a General Amber Force Field. *J. Comput. Chem.* **2004**, *25*, 1157–1174. [CrossRef]
42. Maier, J.A.; Martinez, C.; Kasavajhala, K.; Wickstrom, L.; Hauser, K.E.; Simmerling, C. Ff14sb: Improving the Accuracy of Protein Side Chain and Backbone Parameters from Ff99sb. *J. Chem. Theory Comput.* **2015**, *11*, 3696–3713. [CrossRef] [PubMed]
43. Dolinsky, T.J.; Czodrowski, P.; Li, H.; Nielsen, J.E.; Jensen, J.H.; Klebe, G.; Baker, N.A. PDB2PQR: Expanding and Upgrading Automated Preparation of Biomolecular Structures for Molecular Simulations. *Nucleic Acids Res.* **2007**, *35*, W522–W525. [CrossRef] [PubMed]
44. Jorgensen, W.L.; Chandrasekhar, J.; Madura, J.D.; Impey, R.W.; Klein, M.L. Comparison of Simple Potential Functions for Simulating Liquid Water. *J. Chem. Phys.* **1983**, *79*, 926–935. [CrossRef]
45. Darden, T.; York, D.; Pedersen, L. Particle Mesh Ewald: An N Log (N) Method for Ewald Sums in Large Systems. *J. Chem. Phys.* **1993**, *98*, 10089–10092. [CrossRef]
46. Case, D.A.; Aktulga, H.M.; Belfon, K.; Cerutti, D.S.; Cisneros, G.A.; Cruzeiro, V.W.D.; Forouzesh, N.; Giese, T.J.; Götz, A.W.; Gohlke, H. AmberTools. *J. Chem. Inf. Model* **2023**, *63*, 6183–6191. [CrossRef] [PubMed]
47. Genheden, S.; Ryde, U. The MM/PBSA and MM/GBSA Methods to Estimate Ligand-Binding Affinities. *Expert Opin. Drug Discov.* **2015**, *10*, 449–461. [CrossRef]
48. da Costa, R.A.; da Rocha, J.A.P.; Pinheiro, A.S.; da Costa, A.d.S.S.; da Rocha, E.C.M.; Josino, L.P.C.; da Silva Gonçalves, A.; e Lima, A.H.L.; Brasil, D.S.B. In Silico Identification of Novel Allosteric Inhibitors of Dengue Virus NS2B/NS3 Serine Protease. *J. Serbian Chem. Soc.* **2022**, *87*, 693–706.
49. Adams, R.P. *Identification of Essential Oil Components by Gas Chromatography/Mass Spectrometry*, 5 Online ed.; Texensis Publishing: Gruver, TX, USA, 2017.
50. Babushok, V.I.; Linstrom, P.J.; Zenkevich, I.G. Retention Indices for Frequently Reported Compounds of Plant Essential Oils. *J. Phys. Chem. Ref. Data* **2011**, *40*, 043101. [CrossRef]
51. Khani, A.; Heydarian, M. Fumigant and Repellent Properties of Sesquiterpene-rich Essential Oil from *Teucrium polium* Subsp. *capitatum* (L.). *Asian Pac. J. Trop. Med.* **2014**, *7*, 956–961. [CrossRef] [PubMed]
52. Ben Othman, M.; Salah-Fatnassi, K.B.H.; Ncibi, S.; Elaissi, A.; Zourgui, L. Antimicrobial Activity of Essential Oil and Aqueous and Ethanol Extracts of *Teucrium polium* L. subsp. *gabesianum* (L.H.) from Tunisia. *Physiol. Mol. Biol. Plants* **2017**, *23*, 723–729. [CrossRef] [PubMed]
53. Kutchan, T.M. Ecological Arsenal and Developmental Dispatcher. The Paradigm of Secondary Metabolism. *Plant Physiol.* **2001**, *125*, 58–60. [CrossRef]
54. Cakir, A.; Duru, M.E.; Harmandar, M.; Ciriminna, R.; Passannanti, S. Volatile Constituents of *Teucrium polium* L. from Turkey. *J. Essent. Oil Res.* **1998**, *10*, 113–115. [CrossRef]
55. Maizi, Y.; Meddah, B.; Meddah, A.T.T.; Hernandez, J.A.G. Seasonal Variation in Essential Oil Content, Chemical Composition and
Antioxidant Activity of *Teucrium polium* L. Growing in Mascara (North West of Algeria). *J. Appl. Biotechnol. Rep.* **2019**, *6*, 151–157. [CrossRef]
56. Reaisi, Z.; Yadegari, M.; Shirmardia, H.A. Effects of Phenological Stage and Elevation on Phytochemical Characteristics of Essential Oil of *Teucrium polium* L. and *Teucrium orientale* L. *Int. J. Hortic. Sci. Technol.* **2019**, *6*, 89–99.
57. Sabzeghabaie, A.; Asgarpanah, J. Essential Oil Composition of *Teucrium polium* L. Fruits. *J. EssEntial Oil Res.* **2016**, *28*, 77–80. [CrossRef]
58. Boulila, A.; Béjaoui, A.; Messaoud, C.; Boussaid, M. Variation of Volatiles in Tunisian Populations of *Teucrium polium* L. (Lamiaceae). *Chem. Biodivers.* **2008**, *5*, 1389–1400. [CrossRef] [PubMed]

59. Sadeghi, H.; Jamalpoor, S.; Shirzadi, M.H. Variability in Essential Oil of *Teucrium polium* L. of Different Latitudinal Populations. *Ind. Crop. Prod.* **2014**, *54*, 130–134. [CrossRef]
60. Belmekki, N.; Bendimerad, N.; Bekhechi, C.; Fernandez, X. Chemical Analysis and Antimicrobial Activity of *Teucrium polium* L. Essential Oil from Western Algeria. *J. Med. Plants. Res.* **2013**, *7*, 897–902.
61. Toplan, G.G.; Göger, F.; Tas¸kin, T.; Ecevit-Genç, G.; Civas¸, A.; Is¸can, G.; Kürkçüog˘lu, M.; Mat, A.; Baser, K.H.C. Phytochemical
Composition and Pharmacological Activities of *Teucrium polium* L. Collected from Eastern Turkey. *Turk. J. Chem.* **2022**, *46*, 269–282. [CrossRef]
62. Ghavam, M.; Markabi, F.S. Evaluation of Yield, Chemical Profile, and Antimicrobial Activity of Teucrium polium L. Essential Oil Used in Iranian Folk Medicine. *Appl. Biochem. Biotechnol.* **2024**, *196*, 6134–6150. [CrossRef]
63. Donmez, I. Volatile Oil Composition of Teucrium Species of Natural and Cultivated Origin in the Lake District of Turkey. *Appl. Ecol. Environ. Res.* **2022**, *20*, 2235–2245. [CrossRef]
64. Aburjai, T.; Hudaib, M.; Cavrini, V. Composition of the Essential Oil from Jordanian Germander (*Teucrium polium* L.). *J. Essent. Oil Res.* **2006**, *18*, 97–99. [CrossRef]
65. Lograda, T.; Messaoud, R.; Chalard, P. Chemical Analysis and Antimicrobial Activity of *Teucrium polium* L. Essential Oil from Eastern Algeria. *Am. J. Adv. Drug Deliv.* **2014**, *2*, 697–710.
66. Catinella, G.; Badalamenti, N.; Ilardi, V.; Rosselli, S.; De Martino, L.; Bruno, M. The Essential Oil Compositions of Three *Teucrium* Taxa Growing Wild in Sicily: HCA and PCA Analyses. *Molecules* **2021**, *26*, 643. [CrossRef]
67. Dolabela, M.F.; da Silva, A.R.P.; Ohashi, L.H.; Bastos, M.L.C.; da Silva, M.C.M.; Vale, V.V. Estudo In Silico Das Atividades de Triterpenos e Iridoides Isolados de Himatanthus Articulatus (Vahl) Woodson. *Rev. Fitos* **2018**, *12*, 227–242. [CrossRef]
68. Rathinam, A.; Pari, L. Myrtenal Ameliorates Hyperglycemia by Enhancing GLUT2 Through Akt in the Skeletal Muscle and Liver of Diabetic Rats. *Chem. Biol. Interact.* **2016**, *256*, 161–166. [CrossRef]
69. Wang, J.; Sintim, H.O. Dialkylamino-2,4-dihydroxybenzoic Acids as Easily Synthesized Analogues of Platensimycin and Platencin with Comparable Antibacterial Properties. *Chem. Eur. J.* **2011**, *12*, 3352–3357. [CrossRef]
70. Suslov, E.V.; Ponomarev, K.Y.; Rogachev, A.D.; Pokrovsky, M.A.; Pokrovsky, A.G.; Pykhtina, M.B.; Beklemishev, A.B.; Korchagina,
D.V.; Volcho, K.P.; Salakhutdinov, N.F. Compounds Combining Aminoadamantane and Monoterpene Moieties: Cytotoxicity and Mutagenic Effects. *Med. Chem.* **2015**, *11*, 629–635. [CrossRef] [PubMed]
71. Luzina, O.; Filimonov, A.; Zakharenko, A.; Chepanova, A.; Zakharova, O.; Ilina, E.; Dyrkheeva, N.; Likhatskaya, G.; Salakhutdinov, N.; Lavrik, O. Usnic Acid Conjugates with Monoterpenoids as Potent Tyrosyl-DNA Phosphodiesterase 1 Inhibitors. *J. Nat. Prod.* **2020**, *83*, 2320–2329. [CrossRef] [PubMed]
72. Kapitsa, I.G.; Suslov, E.V.; Teplov, G.V.; Korchagina, D.V.; Komarova, N.I.; Volcho, K.P.; Voronina, T.A.; Shevela, A.I.; Salakhutdinov, N.F. Synthesis and Anxiolytic Activity of 2-Aminoadamantane Derivatives Containing Monoterpene Fragments. *Pharm. Chem. J.*
2012, *46*, 263–265. [CrossRef]
73. Li-Zhulanov, N.S.; Zaikova, N.P.; Sari, S.; Gülmez, D.; Sabuncuog˘lu, S.; Ozadali-Sari, K.; Arikan-Akdagli, S.; Nefedov, A.A.;
Rybalova, T.V.; Volcho, K.P.; et al. Rational Design of New Monoterpene-Containing Azoles and Their Antifungal Activity. *Antibiotics* **2023**, *12*, 818. [CrossRef]
74. Ponomarev, K.; Morozova, E.; Pavlova, A.; Suslov, E.; Korchagina, D.; Nefedov, A.; Tolstikova, T.; Volcho, K.; Salakhutdinov, N.
Synthesis and Analgesic Activity of Amines Combining Diazaadamantane and Monoterpene Fragments. *Med. Chem.* **2017**, *13*, 773–779. [CrossRef] [PubMed]
75. Liu, L.; Liu, B.; Li, L.; He, M.-X.; Zhou, X.-D.; Li, Q. Myrtenol Inhibits Biofilm Formation and Virulence in the Drug-Resistant *Acinetobacter baumannii*: Insights into the Molecular Mechanisms. *Infect. Drug Resist.* **2022**, *15*, 5137–5148. [CrossRef]
76. de Britto, R.M.; da Silva-Neto, J.A.; Mesquita, T.R.R.; de Vasconcelos, C.M.L.; de Almeida, G.K.M.; de Jesus, I.C.G.; Dos Santos, P.H.; Souza, D.S.; Miguel-dos-Santos, R.; de Sá, L.A. Myrtenol Protects against Myocardial Ischemia-Reperfusion Injury through
Antioxidant and Anti-Apoptotic Dependent Mechanisms. *Food Chem. Toxicol.* **2018**, *111*, 557–566. [CrossRef]
77. Choi, I.-Y.; Lim, J.H.; Hwang, S.; Lee, J.-C.; Cho, G.-S.; Kim, W.-K. Anti-Ischemic and Anti-Inflammatory Activity of (S)-CisVerbenol. *Free. Radic. Res.* **2010**, *44*, 541–551. [CrossRef]

78. Oeckinghaus, A.; Ghosh, S. The NF-KB Family of Transcription Factors and Its Regulation. *Cold Spring Harb. Perspect. Biol.* **2009**, *1*, a000034. [CrossRef]
79. Betzler, A.C.; Theodoraki, M.N.; Schuler, P.J.; Döscher, J.; Laban, S.; Hoffmann, T.K.; Brunner, C. NF-KB and Its Role in Checkpoint Control. *Int. J. Mol. Sci.* **2020**, *21*, 3949. [CrossRef]
80. Li, M.; Liu, P.; Wang, B.; Zhou, J.; Yang, J. Inhibition of Nuclear Factor Kappa B as a Therapeutic Target for Lung Cancer. *Altern. Ther. Health Med.* **2022**, *28*, 44–51. [PubMed]
81. Ersoy, E.; Süvari, G.; Ercan, S.; Özkan, E.E.; Karahan, S.; Tuncay, E.A.; Cantürk, Y.Y.; Kara, E.M.; Zengin, G.; Bogˇa, M. Towards a Better Understanding of Commonly Used Medicinal Plants from Turkiye: Detailed Phytochemical Screening and Biological Activity Studies of Two *Teucrium* L. Species with In Vitro and In Silico Approach. *J. Ethnopharmacol.* **2023**, *312*, 116482. [CrossRef] [PubMed]
82. Chabane, S.; Boudjelal, A.; Napoli, E.; Benkhaled, A.; Ruberto, G. Phytochemical Composition, Antioxidant and Wound Healing Activities of *Teucrium polium* subsp. *capitatum* (L.) Briq. Essential Oil. *J. Essent. Oil Res.* **2021**, *33*, 143–151. [CrossRef]
83. Al-Naemi, H.A.; Alasmar, R.M.; Al-Ghanim, K. Alcoholic Extracts of *Teucrium polium* Exhibit Remarkable Anti-Inflammatory Activity: In Vivo Study. *Biomol. Biomed.* **2024**, *24*, 82–88. [CrossRef] [PubMed]
84. Wen, Y.; Zhu, Y.; Zhang, C.; Yang, X.; Gao, Y.; Li, M.; Yang, H.; Liu, T.; Tang, H. Chronic Inflammation, Cancer Development and Immunotherapy. *Front. Pharmacol.* **2022**, *13*, 1040163. [CrossRef]
85. Kaneko, T.; Zaw, S.Y.M.; Sueyama, Y.; Katsube, K.-I.; Kaneko, R.; Nör, J.E.; Okiji, T. Inhibition of Nuclear Factor Kappa B Prevents the Development of Experimental Periapical Lesions. *J. Endod.* **2019**, *45*, 168–173. [CrossRef] [PubMed]
86. Alharbi, K.S.; Fuloria, N.K.; Fuloria, S.; Rahman, S.B.; Al-Malki, W.H.; Shaikh, M.A.J.; Thangavelu, L.; Singh, S.K.; Allam, V.S.R.R.;
Jha, N.K.; et al. Nuclear Factor-Kappa B and Its Role in Inflammatory Lung Disease. *Chem. Interact.* **2021**, *345*, 109568. [CrossRef] [PubMed]
87. Hoesel, B.; Schmid, J.A. The Complexity of NF-KB Signaling in Inflammation and Cancer. *Mol. Cancer* **2013**, *12*, 86. [CrossRef]